

Doctorate Program in Molecular Oncology
and Endocrinology
Doctorate School in Molecular Medicine

XXI cycle - 2005–2008
Coordinator: Prof. Giancarlo Vecchio

**“Control of DNA replication by NCOA4
protein in HeLa cells”**

Livia Provitera

University of Naples Federico II
Dipartimento di Biologia e Patologia Cellulare e Molecolare
“L. Califano”

Administrative Location

Dipartimento di Biologia e Patologia Cellulare e Molecolare “L. Califano”
Università degli Studi di Napoli Federico II

Partner Institutions

Italian Institutions

Università di Napoli “Federico II”, Naples, Italy
Istituto di Endocrinologia ed Oncologia Sperimentale “G. Salvatore”, CNR, Naples, Italy
Seconda Università di Napoli, Naples, Italy
Università del Sannio, Benevento, Italy
Università di Genova, Genoa, Italy
Università di Padova, Padua, Italy

Foreign Institutions

Johns Hopkins School of Medicine, Baltimore, MD, USA
Johns Hopkins Krieger School of Arts and Sciences, Baltimore, MD, USA
National Institutes of Health, Bethesda, MD, USA
Ohio State University, Columbus, OH, USA
Université Paris Sud XI, Paris, France
Universidad Autonoma de Madrid, Spain
Centro de Investigaciones Oncologicas (CNIO), Spain
Universidade Federal de Sao Paulo, Brazil
Albert Einstein College of Medicine of Yeshiwa University, USA

Supporting Institutions

Università di Napoli “Federico II”, Naples, Italy
Ministero dell’Istruzione, dell’Università e della Ricerca
Istituto Superiore di Oncologia (ISO)
Terry Fox Foundation, Canada
Istituto di Endocrinologia ed Oncologia Sperimentale “G. Salvatore”, CNR, Naples, Italy
Centro Regionale di Competenza in Genomica (GEAR)

FACULTY

ITALIAN FACULTY

Giancarlo Vecchio, MD, Co-ordinator
Salvatore Maria Aloj, MD
Francesco Beguinot, MD
Maria Teresa Berlingieri, PhD
Angelo Raffaele Bianco, MD
Bernadette Biondi, MD
Francesca Carlomagno, MD
Gabriella Castoria, MD
Angela Celetti, MD
Annamaria Cirafici, PhD
Mario Chiariello, MD
Vincenzo Ciminale, MD
Annamaria Colao, MD
Alma Contegiacomo, MD
Sabino De Placido, MD
Monica Fedele, PhD
Pietro Formisano, MD
Alfredo Fusco, MD
Fabrizio Gentile, MD, PhD
Massimo Imbriaco, MD
Paolo Laccetti, PhD
Antonio Leonardi, MD
Barbara Majello, PhD
Rosa Marina Melillo, MD
Claudia Miele, PhD
Roberto Pacelli, MD
Giuseppe Palumbo, PhD
Angelo Paradiso MD, PhD
Silvio Parodi, MD
Giuseppe Portella, MD
Giorgio Punzo, MD
Antonio Rosato, MD
Massimo Santoro, MD
Giampaolo Tortora, MD
Donatella Tramontano, PhD
Giancarlo Troncone, MD
Bianca Maria Veneziani, MD
Giuseppe Viglietto, MD
Roberta Visconti, MD

FOREIGN FACULTY

Université Libre de Bruxelles (Belgium)

Gilbert Vassart

Universidade Federal de Sao Paulo (Brazil)

Janete Maria Cerutti

Rui Maciel

University of Turku (Finland)

Mikko O. Laukkanen

Université Paris Sud XI (France)

Martin Schlumberger, MD

University of Madras (India)

A.K: Munirajan

Pavol Jozef Šafárik University (Slovakia)

Peter Fedorocko

Universidad Autonoma de Madrid (Spain)

Juan Bernal, MD, PhD

Pilar Santisteban

Centro de Investigaciones Oncologicas (Spain)

Mariano Barbacid, MD

Albert Einstein College of Medicine of Yeshiwa University (USA)

Luciano D'Adamio, MD

Nancy Carrasco

Johns Hopkins School of Medicine (USA)

Vincenzo Casolaro, MD

Pierre Coulombe, PhD

James G. Herman MD

Robert Schleimer, PhD

Johns Hopkins Krieger School of Arts and Sciences (USA)

Eaton E. Lattman, MD

National Institutes of Health (USA)

Michael M. Gottesman, MD

Silvio Gutkind, PhD

Stephen Marx, MD

Ira Pastan, MD

Phil Gorden, MD

Ohio State University, Columbus (USA)

Carlo M. Croce, MD

**“Control of DNA
replication by NCOA4
protein in HeLa cells”**

TABLE OF CONTENTS

| | |
|---|-----------|
| LIST OF PUBLICATIONS..... | 8 |
| ABSTRACT..... | 9 |
| 1. BACKGROUND..... | 10 |
| 1.1 Thyroid cancer..... | 10 |
| 1.2 RET/PTC3 oncogene..... | 11 |
| 1.3 NCOA4 (RFG/ELE1alpha/ARA70)..... | 15 |
| 1.4Minichromosome maintenance (MCM) proteins and DNA replication..... | 17 |
| 1.5 MCM proteins and cancer..... | 19 |
| 1.6 Analysis of NCOA4-MCM7 interaction and its functional role in <i>Xenopus laevis</i> egg extract | 19 |
| 2. AIMS OF THE STUDY..... | 22 |
| 3. MATERIAL AND METHODS..... | 23 |
| 3.1 Recombinant proteins..... | 23 |
| 3.2 Protein studies..... | 23 |
| 3.3 Cell fractionation and analysis of nuclear fractions..... | 23 |
| 3.4 Cell culture methods, immunofluorescence and cytofluorimetric analysis..... | 24 |
| 3.5 Chromatin immunoprecipitation (ChIP)..... | 26 |
| 4. RESULTS AND DISCUSSIONS..... | 27 |
| 4.1 NCOA4 and MCM7 interact in the nucleus in HeLa cells..... | 27 |
| 4.2 NCOA4 protein binds to DNA replication origins in HeLa cells.... | 29 |
| 4.3 NCOA4 protein levels change during the cell cycle phases in HeLa cells..... | 30 |
| 4.4 NCOA4 protein affects cell growth and DNA synthesis rate in HeLa cells..... | 31 |
| 5. CONCLUSIONS..... | 38 |
| 6. ACKNOWLEDGEMENTS..... | 39 |

7. REFERENCES.....40

LIST OF PUBLICATIONS

- 1) **Guida T, Salvatore G, Faviana P, Giannini R, Garcia-Rostan G, Provitera L, Basolo F, Fusco A, Carlomagno F and Santoro M.** Mitogenic effects of the up-regulation of minichromosome maintenance proteins in anaplastic thyroid carcinoma. *J Clin Endocrinol Metab* 2005 Aug; 90(8):4703-9.
- 2) **Guida T, Anaganti S, Provitera L, Gedrich R, Sullivan E, Wilhelm SM, Santoro M and Carlomagno F.** Sorafenib inhibits imatinib-resistant KIT and platelet-derived growth factor receptor beta gatekeeper mutants. *Clin Canc Res* 2007 Jun 1; 13(11): 3363-9.
- 3) **Carlomagno F, Guida T, Anaganti S, Provitera L, Kjaer S, Mc Donald NQ, Ryan AJ and Santoro M.** Identification of tyrosine 806 as a molecular determinant of RET kinase sensitivity to ZD6474. *Endocr Relat Cancer* 2008 Nov 24.
- 4) **Carlomagno F, Guida T, Provitera L, Vitagliano D, Dathan N, Grieco D, Costanzo V, Fusco A and Santoro M.** Protein NCOA4 inhibits initiation of eukaryotic DNA replication. (2008 submitted)
- 5) **Guida T, Provitera L** et al. RET oncogenic mutants are HSP90 client proteins whose stability is affected by 17-AAG treatment. (in preparation)
- 6) **Provitera L, Guida T, Santoro M and Carlomagno F.** Effect of NCOA4 ubiquitination on cell cycle and DNA replication. (in preparation)

ABSTRACT

This dissertation is focused on the functional characterization of NCOA4 protein, and in particular on its role in controlling DNA replication in HeLa cells.

In human papillary thyroid carcinoma the rearrangement of RET protooncogene, in particular of its tyrosine kinase domain, with the 5' portion of a number of heterologous genes, generates the RET/papillary thyroid carcinoma (PTC) oncogenes. One of the most frequent and aggressive variants of these recombination events is the fusion of the intracellular kinase-encoding domain of RET to the first 238 amino acids of a gene named NCOA4 (ELE1/ARA70/RFG), generating the RET/PTC3 oncogene.

We previously isolated the Mini-Chromosome Maintenance 7 (MCM7) protein as an interactor of NCOA4.

MCM7 is a component of an heteroexameric complex named MCM2-7, considered a master regulator of DNA replication, acting both during DNA replication origins licensing, as part of the Pre-Replication Complex (Pre-RC), and during nascent strand elongation, as the major helicase of the fork. In *Xenopus laevis* egg extracts NCOA4 blocks DNA replication. Hindrance of DNA replication is mediated by block of MCM2-7 helicase function, leaving untouched origin licensing and activation.

Here we show that NCOA4 and MCM7 proteins interact at the endogenous level in HeLa cells and this interaction is confined in the nucleus and takes place preferentially on chromatin.

Moreover, in HeLa cells, NCOA4 binds canonical DNA replication origins, such as those propicient to the c-Myc or to the Lamin B2 gene.

RNAi-mediated depletion of NCOA4 accelerates the onset of DNA replication, whereas adoptive NCOA4 overexpression decreases cell growth and DNA synthesis.

Our results suggest that NCOA4/RET rearrangement might represent a novel paradigm of a cancer-associated chromosome rearrangement that directly targets a gene that controls cell proliferation.

1. BACKGROUND

1.1 THYROID CANCER

Thyroid carcinoma are divided into well-differentiated, poorly differentiated and undifferentiated types on the basis of the histological and clinical parameters (Fig.1). Differentiated tumors (papillary and follicular) are highly treatable and usually curable. Poorly differentiated tumors (medullary and anaplastic) are much less common, more aggressive and metastatize early displaying a poorer prognosis.

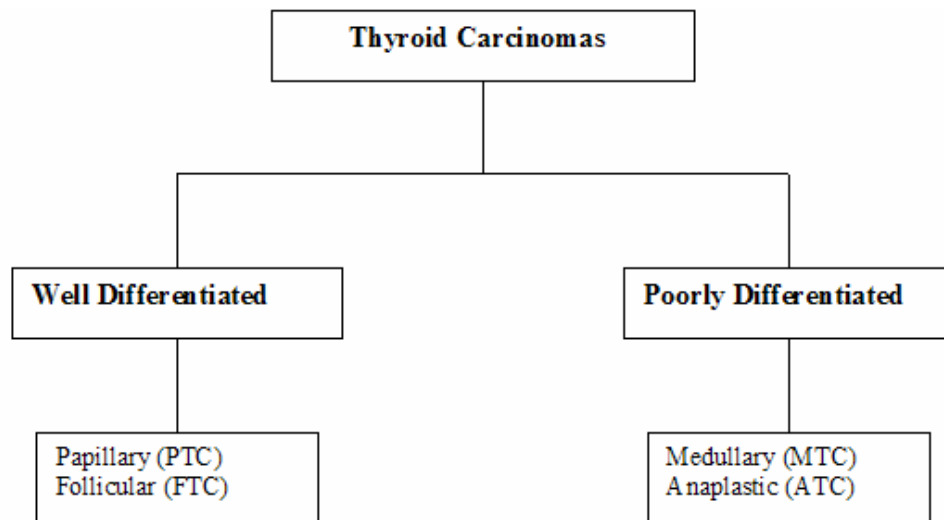


Figure 1 - Classification of thyroid carcinomas.

Papillary thyroid carcinoma (PTCs) account for around 60 to 80% of all thyroid cancers and are closely linked to exposure to ionizing irradiation (Ron et al. 1995). Young children are particularly susceptible since thyroid growth occurs primarily in childhood. A striking increase in pediatric PTC has been reported in Belarus, Ukraine, and Western regions of the Russia, following the Chernobyl disaster of 1986. The worldwide incidence of thyroid cancer in children has been estimated in the order of 1 per million children per year, while it increased by more than 30 fold after the Chernobyl disaster in the exposed areas (Williams 2002). PTC shows typically multicentricity and a tendency to spread into lymphatic vessels; regional node metastases at

presentation are found in a significant proportion of cases. There are several PTC variants including solid-follicular, follicular, tall-cell, hurthle cell variants (Ostrowski et al. 1996).

About 10 to 30% of thyroid cancers are follicular thyroid carcinomas (FTCs). FTC is linked to dietary iodine deficiency (Williams et al. 1997) and shows variable morphology ranging from well-formed colloid-containing follicles, to solid or trabecular growth pattern.

Anaplastic thyroid carcinoma (ATC) is the most aggressive type of thyroid cancer. ATC cells are extremely abnormal and spread rapidly to other parts of the body.

Medullary thyroid carcinoma (MTC) derived from neuroendocrine C cells of the thyroid, producing calcitonin (CT). About 5 to 7% of all thyroid cancers are MTC. MTC can be sporadic or familial as part of the Multiple Endocrine Neoplasia type 2 syndromes.

1.2 RET/PTC3 ONCOGENE

Papillary thyroid carcinoma (PTCs) are characterized by activating, non-overlapping events that involve the genes RET, NTRK1 (neurotrophic tyrosine kinase receptor 1), BRAF or Ras.

The *REarranged during Transfection* (RET) proto-oncogene was isolated in 1985 and was the first activated receptor-tyrosine kinase to be identified in thyroid cancer (Fusco et al. 1987; Takahashi et al. 1988). The proto-oncogene, located on chromosome 10q11.2, is composed by 21 exons and has a size of about 55 kb. It encodes a transmembrane receptor-tyrosine kinase with four cadherin-related motifs and a cysteine-rich region in the extracellular domain and an intracellular portion containing the juxtamembrane region, the tyrosine kinase domain (TK) split in two subdomains by the insertion of 27 amino acids and a COOH tail where several tyrosines function as autophosphorylation sites.

RET is normally expressed in the developing central and peripheral nervous systems and is an essential component of a signalling pathway that is required for renal organogenesis, enteric neurogenesis and spermatogenesis (Schuchardt et al. 1994). Glial-derived neurotrophic factor (GDNF)-family ligands and GDNF-family receptor alpha (GFRalpha) bind the extracellular domain of RET to induce tyrosine kinase autophosphorylation that activates several signalling pathways, including extracellular regulated kinase (ERK), phosphatidylinositol 3-kinase (PI3K), MAPK p38 and c-JUN kinase (JNK).

Gain-of-function mutations of RET are involved in sporadic and familial C-cell-derived medullary thyroid carcinoma, including multiple endocrine neoplasia 2A (MEN2A), MEN2B and familial medullary thyroid carcinoma (FMTC) (Brandi et al. 2001).

By contrast, chimeric oncogenes, designated RET/PTC, are implicated in the development of papillary carcinoma. Somatic chromosomal rearrangement leads to fusion of the 3'-terminal sequence of RET, which encodes the tyrosine kinase domain, with the 5'-terminal sequences of heterologous genes (Fig. 2).

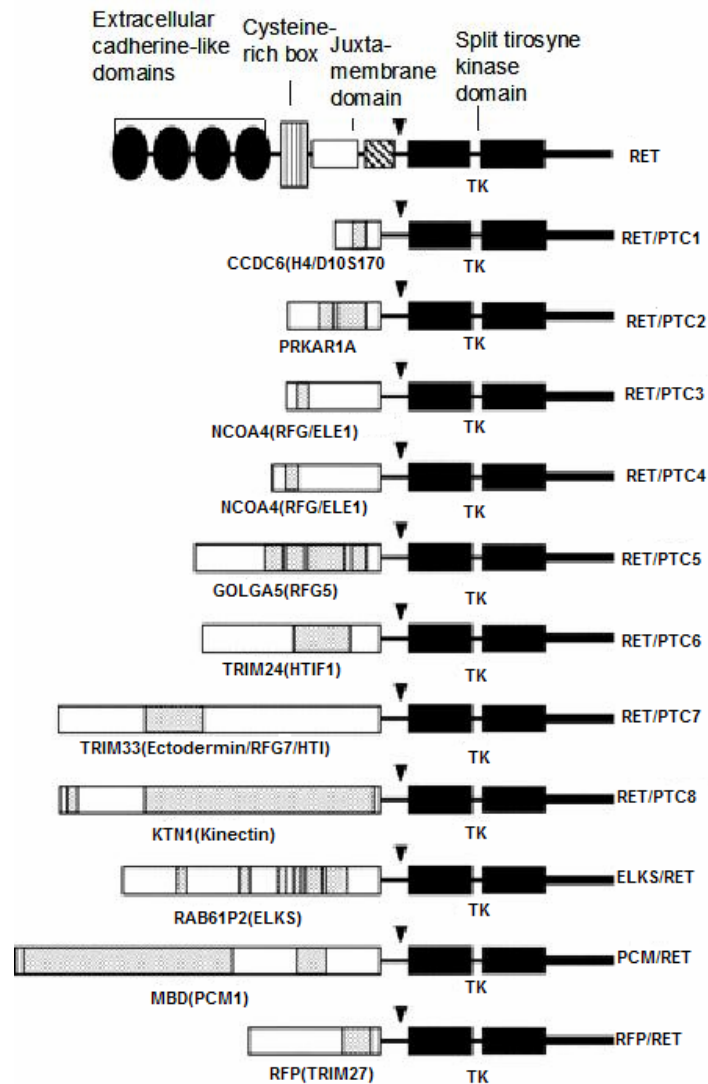


Figure 2 - RET rearrangements. Schematic drawing of the RET protein with the four extracellular cadherin-like domains, the cysteine-rich box adjacent to the plasma membrane, the juxtamembrane domain and the split tyrosine kinase domain (TK). In PTCs, RET is rearranged with diverse genes, encoding protein dimerization motifs (highlighted) that mediate ligand-independent RET dimerization. The arrowheads indicate RET and partner genes breakpoints.

Rearrangements involving the RET gene are common in radiation-associated papillary thyroid cancer (PTC) and patients with a history of

medical irradiation. Although wild-type RET is not expressed in normal follicular cells, RET/PTC chimeric oncoproteins, that lack a signal peptide and transmembrane domain, are expressed in the cytoplasm of follicular cells under the control of the newly acquired promoters. Ligand-independent tyrosine phosphorylation is induced by the constitutive activation of the fusion proteins mediated by the dimerization motifs, i.e. coiled-coil domains, of the partner sequences.

More than 10 RET/PTC rearrangements have been described in sporadic and radiation-associated papillary thyroid carcinoma. Among them the most common forms are H4(D10S170)/RET (also known as RET/PTC1) (Grieco et al. 1990) and NCOA4/RET (also known as RET/PTC3) (Santoro et al. 1994; Bongarzone et al. 1994).

In this dissertation we will focus on RET/PTC3 rearrangement which is frequent in radiation induced tumors and in the more aggressive PTC variants, like the solid follicular one.

The RET/PTC3 rearrangement results from a paracentric inversion of the long arm of chromosome 10 and is formed by fusion of the intracellular domain of RET tyrosine kinase receptor gene with the NCOA4 (ELE1/RFG/ARA70) gene (Santoro et al. 1994). Both genes are located at 10q11.2, with a minimum distance of 500 kb between them (Minoletti et al. 1994). The NCOA4 gene is expressed ubiquitously and drives the expression of the truncated RET receptor in thyroid follicular cells (Nikiforov et al. 1999) (Fig. 3).

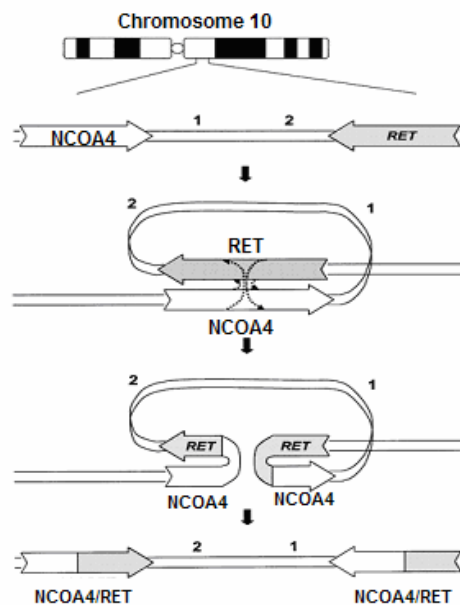


Figure 3 - Putative mechanism of RET/PTC3 rearrangement. Schematic steps of RET/PTC3 formation starting from the linear arrangement of the wild-type genes in the long arm of chromosome 10 (top), to formation of chromosomal loop juxtaposing the two genes adjacent to each other but pointed in opposite directions, to simultaneous breaks in both genes at the same

sites with reciprocal exchange via end-joining leading to inversion and gene rearrangement as demonstrated in a linear fashion (bottom). Note that as a result of this reciprocal recombination the regions 1 and 2, internal to the target genes, are also inverted.

In RET/PTC3 rearrangement, the unscheduled expression of RET tyrosine kinase (mechanism n. 1), the deletion of negative regulatory domains of the receptor (mechanism n. 2) and constitutive oligomerization of PTC3 proteins (mechanism n. 3) are responsible for PTC3-transforming activity in the thyroid (Santoro et al. 2006) (Fig. 4).

Thus, the rearrangement deletes the signal sequence, the extracellular ligand-binding domain and the intracellular juxtamembrane domains of the receptor, which negatively affect RET mitogenic signalling (Melillo et al. 2004). In addition, the amino terminal region of NCOA4 is responsible for the dimerization of the PTC3 oncoprotein in vivo. This region contains a putative coiled-coil domain, which mediates protein-protein interaction and is essential for tyrosine auto-phosphorylation and the transforming activation of PTC3 (Monaco et al. 2001).

Whereas wild-type RET is a transmembrane protein, as a further consequence of the rearrangement (mechanism n. 4), RET/PTC oncoproteins are re-localized to the cytosolic compartment. This could prevent RET/PTC from interacting with negative regulators located at the plasma membrane level, for instance, the tyrosine phosphatase protein tyrosine phosphatase receptor type-J (PTPRJ) (Iervolino et al. 2006) (Fig. 4). Finally, RET/PTC rearrangements, besides activating RET, can also alter the function of RET-fused genes, further contributing to neoplastic transformation (mechanism n. 5) (Fig. 4). Perhaps, the best example of a RET fusion partner, whose altered function may be involved in cancer development, is the regulatory subunit type 1- α of protein kinase A (PRKAR1A) that is fused to RET in RET/PTC2. PRKAR1A is, indeed, a bona fide tumor suppressor, whose germline genetic inactivation is associated to the cancer susceptibility syndrome called Carney Complex, characterized by high penetrant predisposition to thyroid cancer (Bossis and Stratakis 2004). Moreover, RI α ablation in the mouse induced the formation of thyroid tumors (Griffin et al. 2004). Also H4(D10S170) gene, RET partner in RET/PTC1, displays “tumour suppressor”-like features, acting as a proapoptotic protein involved in DNA damage response (Merolla et al. 2007) (Fig.4).

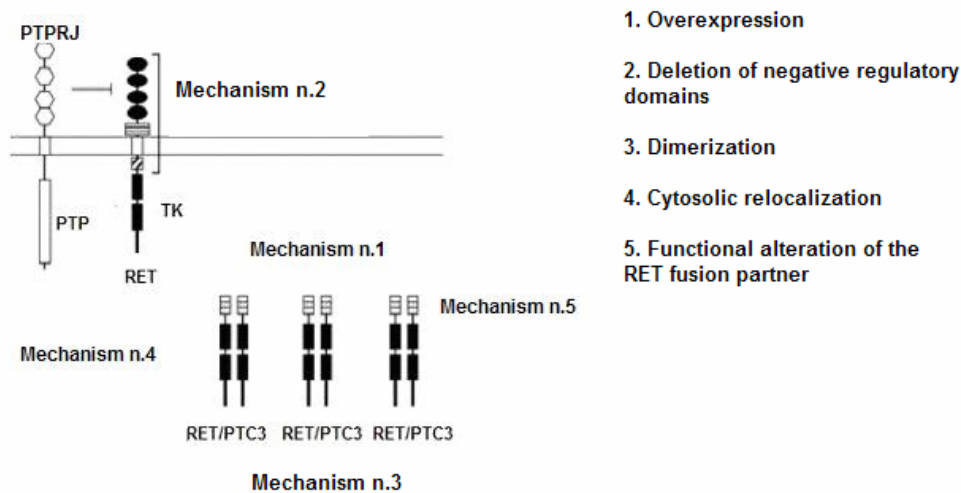


Figure 4 - Mechanisms for RET/PTC activation. The rearrangement *RET/PTC* may act at various levels. It determines the unscheduled expression of *RET* tyrosine kinase, the deletion of negative regulatory domains, the constitutive oligomerization of *PTC* proteins, mediated by the coiled coil domain. Together with the relocation and the altered function of the *RET* fusion partner, these mechanism are suspected to be responsible for the *RET/PTC3* transforming activity in the thyroid. The wild type *RET* protein, the *PTPRJ* tyrosine phosphatase and the rearranged *RET/PTC3* oncoprotein are shown.

1.3 NCOA4 (RFG/ELE1alpha/ARA70)

In the various *RET/PTC* oncoproteins, little is known about the normal role of the 5' fusion partners. As said, some common features such as constitutive expression and the presence of dimerization domains have been observed for all the *RET*-fused genes identified so far.

Although several data indicate that activation of the *RET* kinase is critical to the transforming properties, it is obscure whether disruption of the normal function of the 5' partner gene might also have an important role. To address this point, the identification of the normal physiological function of the heterologous *RET* fusion partners is required to shed light on their role in cellular homeostasis. Therefore, we have studied the product of one of the most frequently observed *RET*-fused gene, *NCOA4* (RFG/ELE1/ARA70).

The *NCOA4* gene maps on the long arm of chromosome 10 at 10q11.2 (Minoletti et al. 1994). It encodes a 1845-bp coding sequence and a 70-kDa protein. It is ubiquitously expressed, so the *RET/PTC3* activation is due to the specificity for the thyroid tissue of the somatic rearrangement of the *ret* proto-oncogene.

NCOA4 protein contains a coiled-coil domain (amino acids 17-125) that mediates protein oligomerization (Monaco et al. 2001) and two motifs,

LxxLL (aa 92-96) and FxxLF (aa 328-332), that mediate binding to *peroxisome-proliferator activated receptor gamma* (PPARgamma) and *androgen receptor* (AR), respectively (Fig. 5).

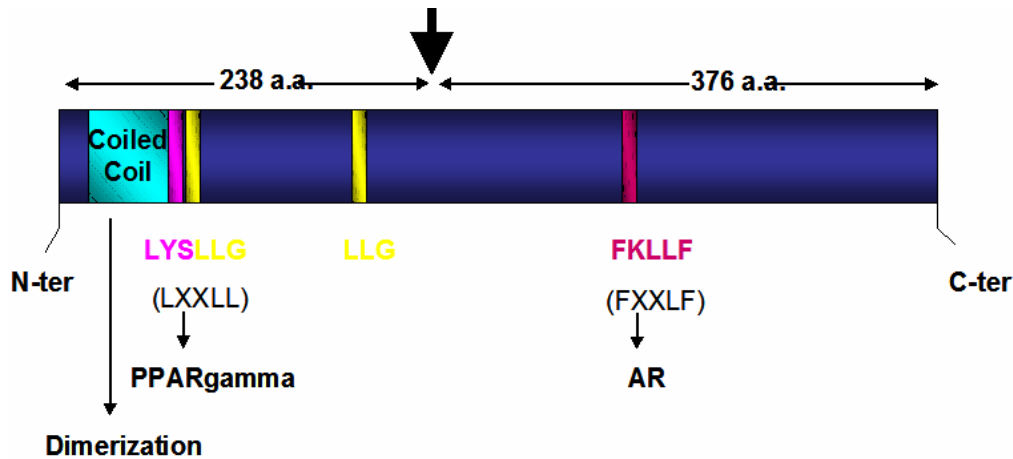


Figure 5 - RFG protein structure. The N-terminal coiled coil domain mediates dimerization. The two motifs LxxLL and FxxLF, which determine the binding, respectively, to PPARgamma and Androgen Receptor (AR) are shown. The LLG motifs which are responsible for protein-protein interaction are shown. The bold arrow indicates breakpoint in RET/PTC3.

NCOA4 functions as a co-activator of several nuclear hormone receptors transcriptional activity, including AR and PPARgamma (Yeh et al. 2002; Heinlein et al. 1999) (He 2002; Hsu 2003; Hu 2004; Miyamoto 1998; Lin 2002). It is able to support AR transcriptional activation not only by androgens but also by other ligands like antiandrogens (hydroxyflutamide, bicalutamide, cyproterone acetate, and RU58841). Proteasome function is necessary for the interaction, since the proteasome inhibitor MG132 blocks AR localization to the nucleus and interaction with NCOA4 (Lin et al. 2002).

NCOA4 protein levels have been found altered in several human tumours. Many reports have demonstrated that NCOA4 expression decreases during prostate tumorigenesis and that NCOA4 has a negative effect on growth and survival of prostate carcinoma cell lines (Tekur et al. 2001; Li et al. 2002). Moreover, it has been shown that around 50 % of invasive ductal carcinoma of the breast loses NCOA4 expression whereas the protein is present in normal mammary epithelium (Kollara et al. 2001).

In order to identify additional roles of NCOA4 protein, in our lab a yeast two-hybrid screening has been performed using the NH2 terminal portion of NCOA4, the portion fused to RET in RET/PTC3, which contains the coil coiled domain. We isolated 10 different NCOA4-encoding clones, which confirmed that NCOA4 is able to form oligomers (Monaco et al. 2001), and two cDNA clones encoding the COOH-terminal portion (aa 576-719) of the

minichromosome maintenance 7 (MCM7) protein (Carlomagno et al. submitted).

1.4 MINICHROMOSOME MAINTENANCE (MCM) PROTEINS AND DNA REPLICATION

DNA replication is tightly regulated at the initiation step by both the cell cycle machinery and checkpoint pathways (Machida et al. 2005).

In eukaryotic cells initiation of DNA synthesis occurs at defined sites (replication origins) scattered along the chromosome. Replication origins are bound by the origin recognition complex (ORC), which permits the recruitment of replication factors through a stepwise reaction leading to formation of replication forks, the functional units of DNA synthesis (Bell and Dutta 2002; Mendez and Stillman 2003; Maiorano et al. 2006).

Minichromosome maintenance proteins (MCM) were first identified in the yeast *Saccharomyces cerevisiae* as mutants defective in the maintenance of minichromosomes, suggesting a role in DNA replication.

Six of them (MCM2-7) are related to each other and interact to form a stable heteroexamer in solution (Tye 1999; Kearsy and Labib 1998).

MCM2-7 form a complex that plays a key role in licensing replication origins for DNA synthesis (Chong et al. 1995; Kubota et al. 1995; Tanaka et al. 1997; Yan et al. 1993). Several studies demonstrated that MCM proteins are able to unwind DNA, functioning as the helicase of the replication fork (Labib et al. 2000; Lee and Hurwitz 2000; You et al. 1999; Pacek et al. 2004; Labib and Diffley 2001).

They are recruited to DNA replication origins in a highly regulated reaction at mitosis exit, leading to formation of the pre-replicative complex (pre-RC) (Bell and Dutta 2002). MCM proteins bind to chromatin in a cell cycle-dependent manner, being tightly bound in late mitosis and G₁ and being removed in S- and G₂-phases (Kearsy and Labib 1998). This regulation is crucial to restrict replication of chromosomes to only one round per cell cycle (Maiorano et al. 2006).

In fact, the replication origins can switch between two chromatin states : a pre-replication state (pre-RC), when the MCM complex is localized at replication origins; and a post-replication state (post-RC), when the MCM complex is delocalized from replication origins (Diffley et al. 1994).

The pre-RC assembly starts with the binding of six-subunit origin recognition complex (ORC) to specific origin sites on DNA (Quintana and Dutta 1999). ORC binding allows the additional binding of initiation factors during a cascade of protein assembly that finally results in the formation of pre-RC (Fig. 6).

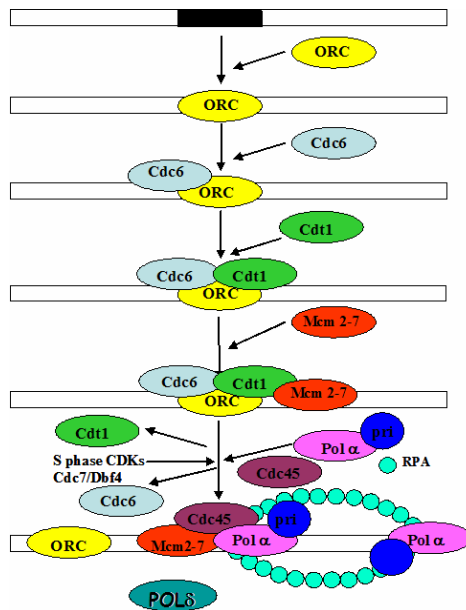


Figure 6 - Assembly of the pre-replication complex. Once ORC recognized the specific origin sites on DNA, it allows the other initiation factors to bind in highly specific manner. Cdc6 binds to ORC, then Cdt1 is recruited to the origin allowing the MCM2-7 binding. The G₁-S phase cdk phosphorylates Cdc6, which is released and Cdc45 binds to the licensed origin. Replication bubble is formed by activation of MCM2-7 helicase and recruitment of RPA and Primase-Pol α occurs.

In particular, in early G₁, the Cdc6 protein functionally interacts with ORC and loads Cdt1, which in turn recruits the MCM proteins (MCM2-7). The assembly of ORC, Cdc6, Cdt1 and MCM proteins into pre-RC makes chromatin competent or licensed for replication (Chevalier and Blow 1996). Loading of MCM2-7 complex is also regulated by the geminin protein, which binds to Cdt1 onto chromatin (Maiorano et al. 2004; Kulartz and Knippers 2004) and thereby blocks the interaction of Cdt1 with MCM2-7 (Lee et al. 2004; Saxena et al. 2004). Moreover, geminin may also contribute to pre-RC formation by stabilizing Cdt1 in G₂/M phases (Ballabeni et al. 2004). At G₁ to S phase transition, DNA replication is initiated by concerted action of S phase-promoting cyclin-dependent kinases and the Dbf4-dependent Cdc7 kinase (Pasero and Schwob 2000; Sclafani 2000). This event is referred to as “origin firing”. Cdc6 is phosphorylated and released together with Cdt1. Other replication factors as CDC45 and GINS complex bind to licensed origin. Activation of MCM2-7 helicase function is turned on by these new factors and induces opening of the replication bubble, allowing loading of the single strand binding protein RPA and Pol α -Primase, which synthesizes the RNA/DNA primer. The primer is recognized by RFC, the clamp loader, which recruits in turn PCNA, the processivity factor of DNA polymerases. PCNA allows the polymerase switching to occur and DNA pol α is replaced by DNA pol δ and DNA pol ϵ , which display greater processivity and have proofreading

exonuclease activity (Ritzi and Knippers 2000). At each replication bubble the replication starts and proceeds bidirectionally with the helicase walking ahead of the fork to generate single strand and DNA polymerases elongating the nascent DNA in 5'-3' direction. The MCM proteins gradually dissociate from chromatin as S phase proceeds (Krude et al. 1996) and replication forks merge, consistent with their predicted function as a DNA helicase (Ishimi 1997).

1.5 MCM PROTEINS AND CANCER

Because of its vital role in genome duplication in proliferating cells, deregulation of the MCM function results in chromosomal defects that may contribute to tumorigenesis. The MCM proteins are highly expressed in malignant human cancer cells and pre-cancerous cells undergoing malignant transformation. They are not expressed in differentiated somatic cells that have been withdrawn from the cell cycle. Indeed in human cells, MCM proteins have recently emerged as an important biomarker for growth and carcinogenesis. A strong correlation has been observed between entry in quiescent, differentiated or senescent state and downregulation of MCM proteins (Blow et al. 2002; Stoeber et al. 2001). In fact, deregulation of MCM2-7 appears to be an early event in tumorigenesis in a range of different tumor types and has led to recent development of human MCM antibodies as diagnostic tools for common carcinomas (Stoeber et al. 1999; Williams et al. 1998; Stoeber et al. 2002; Meng et al. 2001; Laskey 2005).

MCM proteins are overexpressed in many types of human tumour including colorectal, oesophageal, ovarian, laryngeal, urothelial, vulval and thyroid cancers (Gonzalez et al. 2005; Guida et al. 2005). A gain of the 7q chromosomal region that includes MCM7 has been observed in prostate (Ren et al. 2006) and hypopharyngeal (Cromer et al. 2004) carcinomas. Finally, targeting of MCM7 expression to the basal layer of the epidermis in transgenic mice significantly increased the incidence of tumor development after two-stage chemical carcinogenesis (Honeycutt et al. 2006). Thus, MCM proteins are believed to act as important players in the process leading to autonomous growth of neoplastic cells (Gonzalez et al. 2005).

1.6 ANALYSIS OF NCOA4-MCM7 INTERACTION AND ITS FUNCTIONAL ROLE IN *XENOPUS LAEVIS* EGG EXTRACTS

An *in vitro* pull down assay performed using two NCOA4 recombinant proteins constituted by NUS tag (NUS) fused to full length NCOA4 protein (NUS-NCOA4) or to the NH₂-terminal fragment of NCOA4 (amino acids 1-238) [NUS-NCOA4(N)] confirmed NCOA4-MCM7 interaction. Both NUS-

NCOA4 and NUS-NCOA4 (N), but not NUS moiety alone or empty beads, pulled down MCM7 protein from HeLa cells protein extracts (Fig. 7).

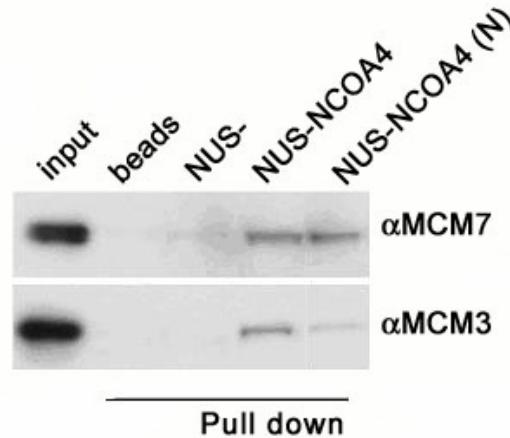


Figure 7 - HeLa cell protein extract pull down assay. *HeLa cell protein extract was subjected to an in vitro pull-down assay with the NUS, NUS-NCOA4 or NUS-NCOA4 (N) recombinant proteins in duplicate. Bound proteins were immunoblotted with anti-MCM7 and anti-MCM3 antibodies. HeLa cell total extract and the beads alone were used as a control.*

In order to investigate the functional role of NCOA4-MCM7 interaction with respect to DNA replication, we used *Xenopus laevis* cell-free DNA replication system. DNA replication can be reproduced *in vitro* using de-membranated sperm and extracts from *Xenopus laevis* eggs, containing all the components needed to replicate DNA (Murray 1991). Also in this system, we found that the recombinant protein NUS-NCOA4 (full length human NCOA4 fused to the NUS tag) was bound to the endogenous *Xenopus* MCM7 (MCM7). Exogenously added recombinant NUS-NCOA4, incubated with sperm DNA in activated *Xenopus laevis* egg extracts, inhibited DNA replication in a dose-dependent manner by interacting with MCM7 protein. Interestingly, only the full length NCOA4 protein, but neither the isolated NCOA4 NH₂-terminal fragment [NUS-NCOA4 (N)] (aa 1-238) nor the COOH-terminal fragment [NUS-NCOA4 (C)] (aa 239-614), blocked the DNA replication.

In order to understand at what level DNA replication was hindered we analyzed DNA bound proteins by chromatin pull down experiments in which DNA loaded proteins were separated from unbound fraction by centrifugation on a sucrose gradient. In the presence of NUS-NCOA4, pre-RC components (such as Cdc6 and MCM7) were not affected in their binding to DNA; neither CDC45 protein binding was decreased while PCNA binding was strongly reduced. Therefore, we hypothesized that NCOA4 might hinder late steps of DNA replication. One possibility was that NCOA4 inhibited DNA unwinding, a step secondary to CDC45 loading and preceding primer synthesis, PCNA loading and DNA elongation (Bell et al. 2002; Pacek et al. 2006; Labib et al. 2000; Takayama et al. 2003). To address this question, we measured

aphidicolin-induced hyperloading of replication protein A (RPA) in the presence of NCOA4. Aphidicolin is a DNA polymerase inhibitor that uncouples DNA unwinding from DNA polymerization, thereby generating long stretches of single-strand DNA that is rapidly covered by the single-strand binding protein RPA. Therefore, aphidicolin-induced hyperloading of RPA is a *bona fide* measurement of replicative DNA helicase activity. NUS-NCOA4 inhibited aphidicolin-induced RPA hyperloading, which indicates that it was blocking DNA unwinding. Again, NCOA4 did not affect MCM7 binding to DNA. NCOA4-induced reduction of RPA loading on chromatin was almost undetectable in the absence of aphidicolin, probably because this loading is very low during unperturbed DNA synthesis. The association of Primase/DNApol α to chromatin, which is strictly dependent on origin unwinding (Walter et al. 2000), was greatly reduced by 150 nM NUS-NCOA4. This accounts for the absence of PCNA loading. Finally, NCOA4 did not affect the replication of a circular single-strand DNA template derived from the M13 bacteriophage, a process that occurs independently of replicative DNA helicase (Cox et al. 1990; Jenkins et al. 1992; Carlomagno et al. submitted).

By generating an affinity-purified anti-XNCOA4 antibody able to immunoprecipitate *in vitro*-translated XNCOA4 and an endogenous protein from egg extracts that had the same molecular weight as *in vitro*-translated XNCOA4, we were able to demonstrate that the endogenous XNCOA4 and MCM7 proteins formed a complex in egg extracts, independently of the presence of chromatin.

Immunodepletion of endogenous XNCOA4 augmented DNA synthesis by increasing DNA unwinding, as shown by RPA increased loading. In parallel, PCNA chromatin binding was enhanced whereas MCM7 and CDC45 chromatin loading remained unchanged. As a control, the addition of exogenous NUS-NCOA4 to XNCOA4-depleted extracts restored normal levels of both DNA replication and PCNA loading (Carlomagno et al. submitted).

These data indicated that in *Xenopus laevis* egg extracts NCOA4 functions as a novel regulator of DNA replication by modulating MCM2-7 helicase activity.

2. AIMS OF THE STUDY

In papillary thyroid carcinoma (PTCs), NCOA4 is frequently targeted by chromosomal rearrangements that cause fusion of NCOA4 5' portion to the TK encoding exons of RET generating the RET/PTC3 chimeric gene. The best described role for NCOA4 in the rearrangement is to drive RET/PTC3 expression and its dimerization, activating RET enzymatic function in a constitutive manner in thyroid cells. It could not be excluded, though, that inactivation of NCOA4 function contributed to tumorigenesis as well.

We demonstrated that NCOA4 is a negative controller of DNA replication in *Xenopus laevis* egg extracts. Thus, by interacting with MCM7, NCOA4 hinders MCM2-7 helicase activity and blocks DNA unwinding which generates single strand DNA that function as template for processive DNA polymerases.

Aim of this study is to analyse the role of NCOA4 protein in mammalian cells. We used as a model system HeLa cells to:

1. investigate in which cellular compartment NCOA4 protein is located and interacts with MCM7
2. study regulation of NCOA4 protein levels in different cell cycle phases
3. investigate the role of NCOA4 in controlling DNA replication in mammalian cells by modulating its protein levels by use of TET-on inducible system and RNAi oligonucleotides.

3. MATERIALS & METHODS

3.1 RECOMBINANT PROTEINS

NUS-NCOA4 and NUS-NCOA4(N) were generated by PCR amplification of the entire NCOA4 ORF or its 5'-terminal (amino acids 2-238) portions, respectively. Fragments were then fused in-frame to the solubility tag NusA in the pET vector. The plasmids were controlled by DNA sequencing. Recombinant proteins were produced in *Escheria coli* by using standard protocols.

3.2 PROTEIN STUDIES

Proteins were extracted according to standard procedures.

Cells were lysed in a buffer containing 50 mM N-2-hydroxyethylpiperazine-N'-2-ethanesulfonic acid (HEPES; pH 7.5), 1% (vol/vol) Triton X-100, 150 mM NaCl, 5 mM EGTA, 50 mM NaF, 20 mM sodium pyrophosphate, 1 mM sodium vanadate, 2 mM phenylmethylsulphonyl fluoride (PMSF) and 1 µg/ml aprotinin. Lysates were clarified by centrifugation at 10,000 x g for 15 min. Lysates containing comparable amounts of proteins, estimated by a modified Bradford assay (Bio-Rad, Munchen, Germany), were immunoprecipitated with the required antibody or subjected to direct western blot. Immune complexes were detected with the enhanced chemiluminescence kit (Amersham Pharmacia Biotech). For binding assay (pull-down), HeLa cells lysates were incubated with 5 µg of immobilized fusion proteins. Bound proteins were detected by immunoblot analysis.

For fast protein liquid chromatography (FPLC), column was equilibrated in 50 mM sodium phosphate buffer pH 7.0 containing 0.15 M NaCl, and used at a flow rate of 0.3 ml/min. One mg of HeLa cell protein extract was loaded on the column and 30 fractions of 1 ml each were collected. The last 14 fractions were selected for TCA precipitation, re-suspended in 1X Laemmli buffer and run on a 10% SDS-PAGE. Immunoblotting was carried out with specific antibodies.

3.3 CELL FRACTIONATION AND ANALYSIS OF NUCLEAR FRACTIONS

For subcellular fractionation, cells in the mid-exponential phase of growth were collected by scraping from the culture dish after two washings

with 20 ml ice-cold 1X phosphate-buffered saline (PBS). Cell pellets were collected by centrifugation at 6,000 x g for 2 min in a refrigerated microfuge. The pellet was re-suspended in 5 packed cell volumes (PCV) of buffer A (10 mM HEPES-KOH pH 7.6, 1.5 mM MgCl₂, 10 mM KCl, 0.5 mM DTT and protease inhibitor cocktail) and swollen for 10 min. The cell suspension was transferred to a 1-ml Dounce homogeniser. Cells were broken by 40 strokes and nuclei were pelleted by centrifugation at 2,800 x g. The nuclear pellet was re-suspended in 0.9 volumes of buffer C (0.1 % Triton X-100, 20 mM HEPES-KOH pH 7.9, 25% (v/v) glycerol, 0.42 M NaCl, 1.5 mM MgCl₂, 0.2 mM EDTA, 0.5 mM DTT, protease inhibitor cocktail). The suspension was frozen and thawed three times and then nuclear debris was pelleted by centrifugation at 10,000 x g for 30 min in a cooled microfuge.

Triton X-100-extracted nuclei were prepared as follows. Cells cultured in 100-mm dishes were washed three times with ice-cold phosphate-buffered saline and divided in three aliquots. One aliquot was lysed with standard buffer (total) as described above. Two aliquots were incubated separately for 10 min on ice with 200 µl of ice-cold CSK buffer (10 mM PIPES, pH 6.8, 100mM NaCl, 300 mM sucrose, 1mM MgCl₂, 1 mM EGTA, 1 mM DTT, 1 mM phenylmethylsulfonyl fluoride, 10 mg/ml aprotinin) containing 0.5% Triton X-100 (Pierce Biotechnology, Rockford, IL). Chromatin bound proteins were separated from unbound proteins by low speed centrifugation (3,000 rpm, 3 min at 4°C). One of the two pellets was further digested with 1,000 units/ml DNase I (10 units/ml, RNase-free, Boehringer Mannheim, Germany) in 100 µl of 0.5% Triton X-100 containing CSK supplemented with 1mM ATP at 25° C for 30 min. Samples were analysed by SDS-PAGE upon loading equivalent amounts for each fraction (Fujita et al. 1997).

3.4 CELL CULTURE METHODS, IMMUNOFLUORESCENCE AND CYTOFLUORIMETRIC ANALYSIS

HeLa cells were grown in Dulbecco's modified Eagle's medium (DMEM) supplemented with 10% fetal calf serum (Invitrogen Groningen, The Netherlands).

The human NCOA4 full-length cDNA was cloned in pcDNA/TO/myc-HIS (Invitrogen) and stably transfected in HeLa T-Rex cells containing the Tet repressor under the control of the CMV promoter (Invitrogen). Marker-selected cell clones were isolated and characterized for NCOA4 expression by immunoblot. Two clones (clone 23 and 24) were selected for further studies.

Anti-NCOA4 si RNAs were designed with a program available online (<http://jura.wi.mit.edu/siRNAext>) and synthesized by Prologo (Boulder, CO). Primers sense strands were:

NCOA4 1i: 5'-UAUCUCCAUGCCAGAGCAGAA-3'

NCOA4 2i: 5'-AAGAUUCAACUGUCCUGCUCUUU-3'

NCOA4 3i: 5'-GGCCCAGGAAGUAUUACUU-3'

Scrambled: 5'-ACCGUCGAUUUCACCCGGUU-3'

Transfection was performed with 100 nM of siRNA using the oligofectamine reagent (Invitrogen).

For the double-thymidine block, cells were treated for 12-14 h with complete medium containing 2 mM thymidine, released in 24 μ M cytidine for 9 hours and retreated with 2 mM thymidine for a further 12-14 h. Upon thymidine wash-out, cells were harvested at different time points and processed for flow cytometry or immunoblot. Nocodazole arrest was performed by treating cells with 200 ng/ml nocodazole for 16 h. MG132 was used at a 50 μ M final concentration starting from a 50 mM stock solution. Thymidine, Cytidine and Nocodazole were from Sigma Chemical Co.; MG132 was from Calbiochem.

For DNA synthesis measurements, cells were seeded on glass coverslips. Bromodeoxyuridine (BrdU; Sigma Chemical Co.) was added to the cell culture medium at a final concentration of 100 μ g/ml for 1 h before harvest. Cells were fixed with paraformaldehyde (4%) and permeabilized with Triton X-100 (0.2%) before staining. Coverslips were incubated with anti-BrdU mouse monoclonal antibody and then with a Texas red-conjugated anti-mouse antibody (Boehringer Mannheim, Germany). All coverslips were counterstained in PBS containing Hoechst 33258 (final concentration, 1 μ g/ml; Sigma Chemical Co.), rinsed in PBS and mounted in Moviol on glass slides. The fluorescent signal was visualized with an epifluorescent microscope (Axiovert 2, Carl Zeiss, Göttingen, Germany) interfaced with the image analyzer software KS300 (Carl Zeiss). For PCNA foci detection, HeLa cells were seeded on glass coverslips, fixed in 4% paraformaldehyde in PBS and blocked in PBS containing 1% BSA, 0.1% Triton X-100 and 0.02% SDS. Primary and secondary antibodies were diluted in the same blocking buffer. Anti-PCNA antibody was PC-10 from Calbiochem. FITC-stained secondary anti-mouse antibody was from Molecular Probes (Invitrogen). Stained cells were observed with a Zeiss LSM 510 META confocal microscope (Zeiss, Göttingen, Germany). For cytofluorimetric analysis, cells were harvested when subconfluent, fixed in 80% ethanol for 1 h at -20°C, rehydrated in PBS, and then treated with RNase A (100U/ml) for 30 min.

Propidium iodide (50 μ g/ml) was added to the cells for 30 minutes in the dark. Samples were analysed with a CYAN flow cytometer (Dako Corporation, San Jose, CA, USA) using an argon-ion laser tuned to 488nm measuring forward and orthogonal light scatter, and red fluorescence measuring area and either peak of the fluorescent signal. Data were acquired using SUMMIT® software and analysed with Modfit® software.

For PCNA foci detection, HeLa cells were seeded on glass coverslips, fixed in 4% paraformaldehyde in PBS and blocked in PBS containing 1% BSA, 0.1% Triton X-100 and 0.02% SDS. Primary and secondary antibodies were diluted in the same blocking buffer. Anti-PCNA antibody was PC-10 from Calbiochem. FITC-stained secondary anti-mouse antibody was from

Molecular Probes (Invitrogen). Stained cells were observed with a Zeiss LSM 510 META confocal microscope (Zeiss, Gottingen, Germany). For cytofluorimetric analysis, cells were harvested when subconfluent, fixed in 80% ethanol for 1 h at -20°C, rehydrated in PBS, and then treated with RNase A (100U/ml) for 30 min.

3.5 CHROMATIN IMMUNOPRECIPITATION

Chromatin immunoprecipitation was performed from exponentially growing HeLa cells using preimmune serum and purified anti-NCOA4 and anti-RPA antibodies, using ChIP assay Kit (Upstate Biotechnology, Millipore Corporate).

Primers for PCR we as follows:

Lamin B2 origin:

Forward 5'-GGCTGGCATGGACTTTCATTTTCAG-3'

Reverse 5'-GTGGAGGGATCTTTCTTAGACATC-3'

Control region:

Forward 5'-CTGCCGCAGTCATAGAACCT-3'

Reverse 5'-ATGGTCCCCAGGATACACAA-3'

c-Myc origin:

Forward 5'-TATCTACTAACATCCCACGCTCTG-3'

Reverse 5'-CATCCTTGTCCTGTGAGTATAAATCATCG-3'

Control region:

Forward 5'-TTCTCAACCTCAGCACTGGTGACA-3'

Reverse 5'-GACTTTGCTGTTTGCTGTCAGGCT-3'

4. RESULTS AND DISCUSSION

4.1 NCOA4 AND MCM7 INTERACT IN THE NUCLEUS IN HeLa CELLS

Initially, we analysed in which cellular compartment NCOA4 protein was located in HeLa cells. MCM7 is prevalently a nuclear chromatin bound protein, even if its overexpression in cancer cells often causes an accumulation of the protein also in the cytosolic compartment.

In sub-cellular fractionation experiments, NCOA4 and MCM7 appeared in both the cytoplasmic and nuclear compartments (Fig. 8).

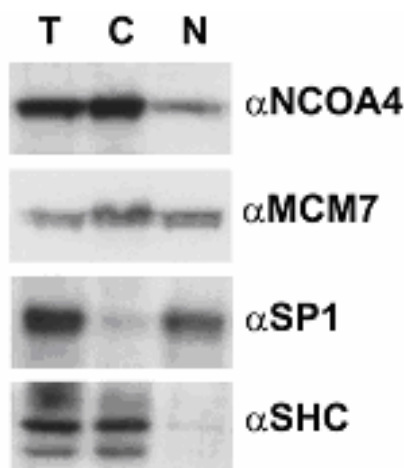


Figure 8 - NCOA4 cellular localization. *NCOA4* cytosolic (C) and nuclear (N) fractions of HeLa cells were immunoblotted with anti-NCOA4 and anti-MCM7 antibodies. Total (T) protein extract was loaded as a control. Anti SP1 (nuclear) and anti SHC (cytosolic) antibodies served to verify the purity of the fractions.

Moreover, like MCM7 (Bell et al. 2002), NCOA4 was present in the chromatin bound Triton X-100 (0.5%) insoluble fraction, and DNase treatment was able to solubilize both NCOA4 and MCM7 from chromatin (Fig. 9).

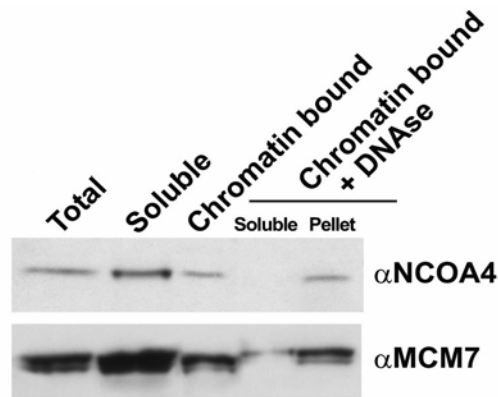


Figure 9 - NCOA4 is bound to chromatin. 0.5% Triton X-100 soluble (S) and insoluble (P) fractions, and proteins solubilized upon DNase treatment from HeLa cells were immunoblotted with anti-MCM7 and anti-NCOA4 antibodies.

Anti-NCOA4 antibody was able to co-immunoprecipitate MCM7 protein, indicating interaction of the two proteins at the endogenous level. MCM6 and MCM5 proteins were also present in the complex (data not shown), suggesting that NCOA4 interacts with MCM7 in the context of the entire MCM2-7 complex. This was also confirmed by a gel-filtration experiment, in which NCOA4 co-eluted with the MCM2-7 protein complex in a fraction whose apparent molecular mass was ~600 kDa, confirming that the protein was interacting with the entire complex (Fig. 10).

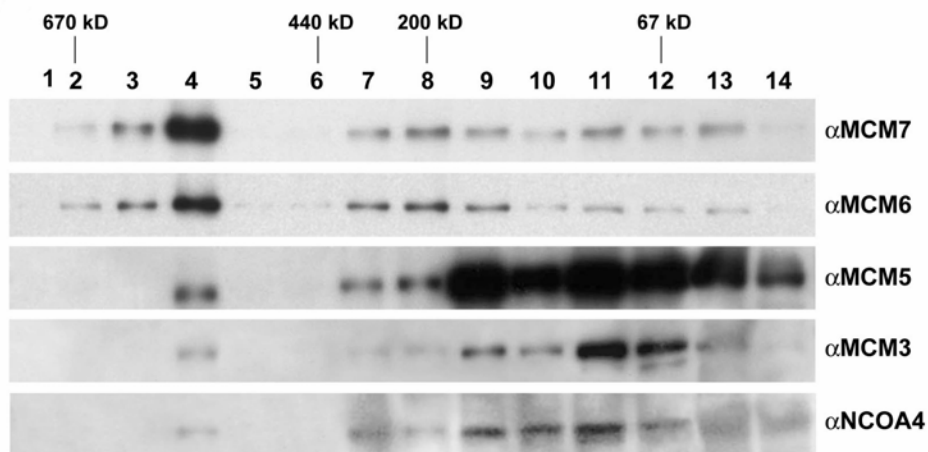


Figure 10 – NCOA4 interacts with the entire complex MCM2-7. HeLa protein extract was loaded on a fast protein liquid chromatography column and 14 sequential fractions (1-14) were collected. Western blotting of each fraction was performed with the indicated antibody. The calibration molecular mass curve is indicated.

Using HeLa sub-cellular fractions, we observed that NCOA4–MCM7 interactions was confined to the nucleus and occurred preferentially on chromatin (Fig. 11), even if the amount of NCOA4 in the nucleus is lower than in the cytosol.

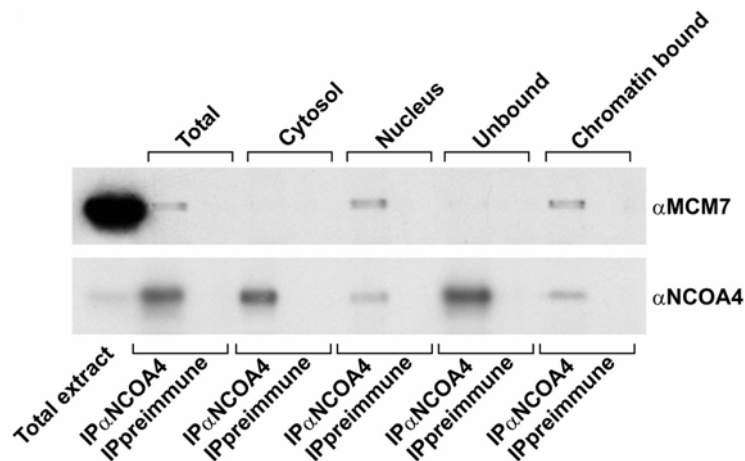


Figure 11 - NCOA4 and MCM7 interaction takes place in the nucleus and on chromatin. Cellular fractions of HeLa cells were immunoprecipitated with anti-NCOA4 antibody, in order to identify where the NCOA4-MCM7 interaction takes place. Immunoblot with anti MCM7 and anti-NCOA4 was performed. Total protein extract was loaded as control.

4.2 NCOA4 PROTEIN BINDS TO DNA REPLICATION ORIGINS IN HeLa CELLS

NCOA4 was already known to bind chromatin, functioning as a coactivator of nuclear receptor (Yeh et al. 2002; Heinlein et al. 1999) (He 2002; Hsu 2003; Hu 2004; Miyamoto 1998; Lin 2002). We ought to investigate whether the protein was loaded on DNA replication origins as well by Chromatin Immunoprecipitation assay (ChIP). We chose two canonical replication origins, Lamin B2 and c-Myc.

NCOA4 was present at both Lamin B2 (Fig. 12A) and c-Myc (Fig. 12B) origins. RPA protein was located at the same origins while neither proteins binding occurred on control region located several kb far apart (Dominguez-Sola et al. 2007) (Fig. 12).

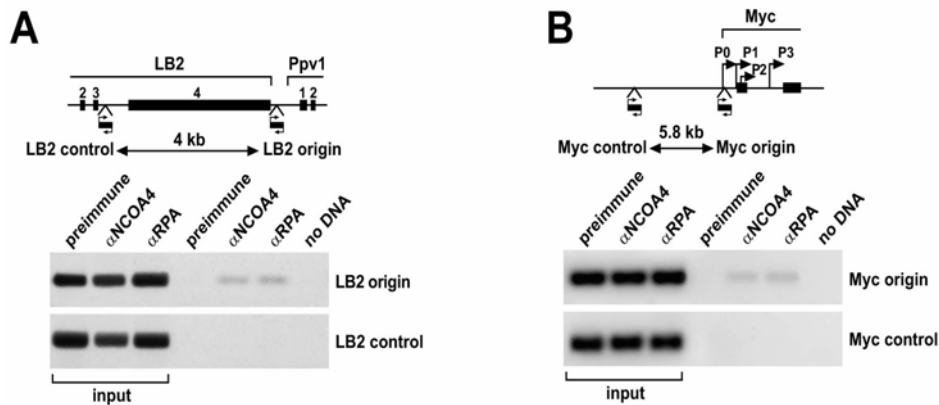


Figure 12 - Chromatin immunoprecipitation at DNA replication origins located on human Lamin B2 (LB2) (A) and c-Myc (B) loci. Immunoprecipitation was performed using preimmune serum or anti NCOA4 and anti-RPA antibodies. *Upper*: maps depicting the location of relevant regions of the two loci. PCR fragments at origins and control regions are indicated. *Lower*: ethidium bromide staining of PCR products.

4.3 NCOA4 PROTEIN LEVELS CHANGE DURING CELL CYCLE PHASES IN HeLa CELLS

Proteins exerting functions associated to specific phases of cell cycle, such as control of DNA synthesis, often display fluctuation of protein levels along cell cycle progression. The classic example is represented by the negative regulator of pre-RC assembly, Geminin, whose concentration is high in S, G2 and early M phase in order to prevent re-licensing and re-replication but decreases at the beginning of G1 phase.

To investigate whether NCOA4 protein levels were regulated during cell cycle, we arrested HeLa cells in phase G1/S (double-thymidine block) or M (nocodazole block). Cells were released from the block, proteins were harvested at different time points and NCOA4 protein levels measured by immunoblot. Geminin and cyclin B1 were used as a control of proteins whose levels change during cell cycle while tubulin was used for normalization. Cell cycle progression was monitored with cytofluorimetric analysis.

NCOA4 protein levels were low in late G1 and in S, progressively increased in G2 and peaked at the M to G1 transition (Fig. 13A, B).

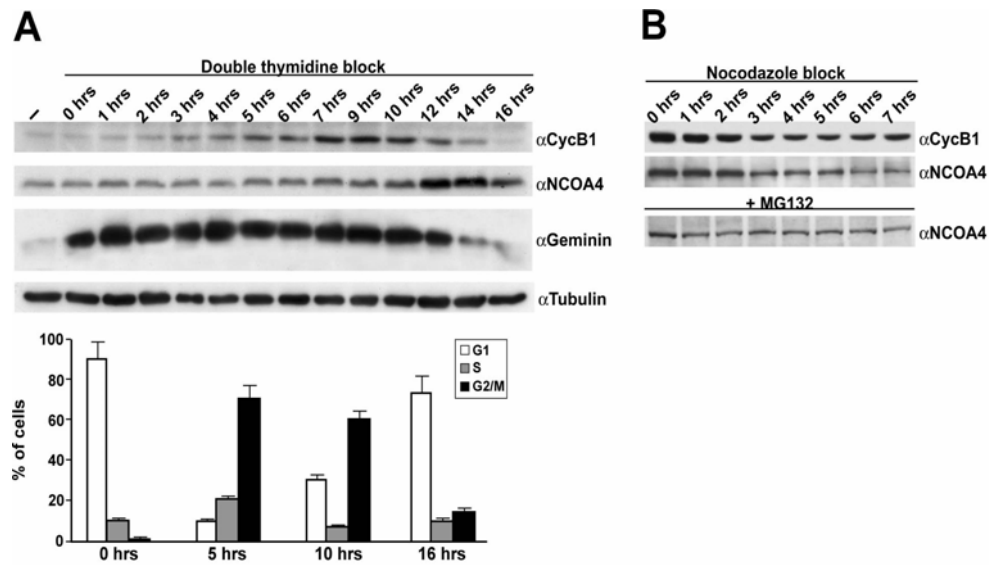


Figure 13 - NCOA4 protein levels during cell cycle phases. Upon release from double-thymidine (A) or a nocodazole (B) block, NCOA4 protein levels were measured at the indicated time points by immunoblot. Flow cytometry and immunoblotting for Cyclin B1 (*cycB1*) and Geminin were used to monitor cell cycle progression; tubulin was used for normalization.

Consistently, also in *Xenopus laevis* egg extracts, endogenous XNCOA4 levels decreased upon initiation of DNA synthesis (data not shown). The decrease of NCOA4 levels during G1 phase of HeLa cells was caused by proteasome-mediated proteolysis being prevented by the proteasome proteases inhibitor, MG132 (Fig. 13B).

4.4 NCOA4 PROTEIN AFFECTS CELL GROWTH AND DNA SYNTHESIS RATE IN HeLa CELLS

In order to investigate the role played by NCOA4 protein in mammalian cells, we investigated the effect of modulating protein levels in HeLa cells.

HeLa cells were transiently transfected with three different NCOA4 small inhibitory duplex RNAs (NCOA4 1i, 2i and 3i) and DNA synthesis was measured by Bromodeoxyuridine (BrdU) incorporation.

NCOA4 siRNAs, but not the scrambled control, increased DNA synthesis, measured as incorporation of BrdU, at both 48 and 72 hours.

This effect was more pronounced with NCOA4 2i, than with NCOA4 1i and 3i, which is in line with its stronger capacity to knock down NCOA4 protein levels (Fig. 14A and C).

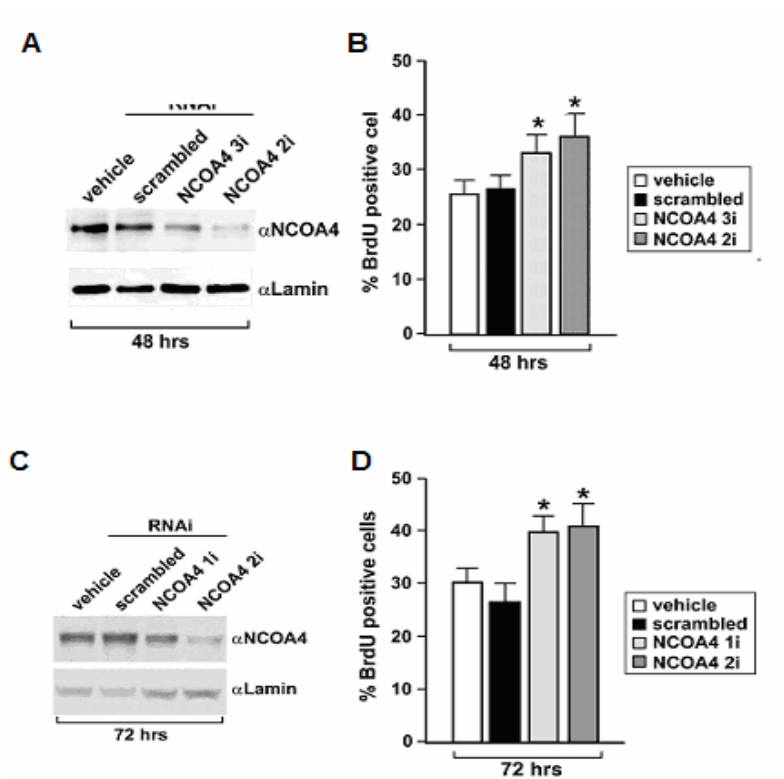


Figure 14 – Interference with NCOA4 protein increases DNA replication. *HeLa* cells were mock-transfected (-) or transfected with NCOA4 2i or NCOA4 3i siRNAs or scrambled siRNA. After 48 and 72 hour. NCOA4 protein levels were measured by immunoblotting. Anti lamin antibody was used for normalization (A and C). DNA synthesis was measured by anti-BrdU immunofluorescence (B and D). The average results \pm SD of three independent experiments made in duplicate are reported.

Moreover, in a G1/S synchronized cell population (double-thymidine block), NCOA4 2i siRNA increased DNA synthesis rate by accelerating entry in S phase. As shown in fig. 15, scrambled transfected cells, once released from the block, took one hour to enter in S phase, whereas NCOA4 2i cells moved in S phase in 20 min. The increased rate of DNA synthesis (amount of synthesized DNA in a time lapse) suggests that NCOA4 might be involved in a locking mechanism to keep either extra or late firing origins blocked so that, when decreased, the cell activates more origins simultaneously.

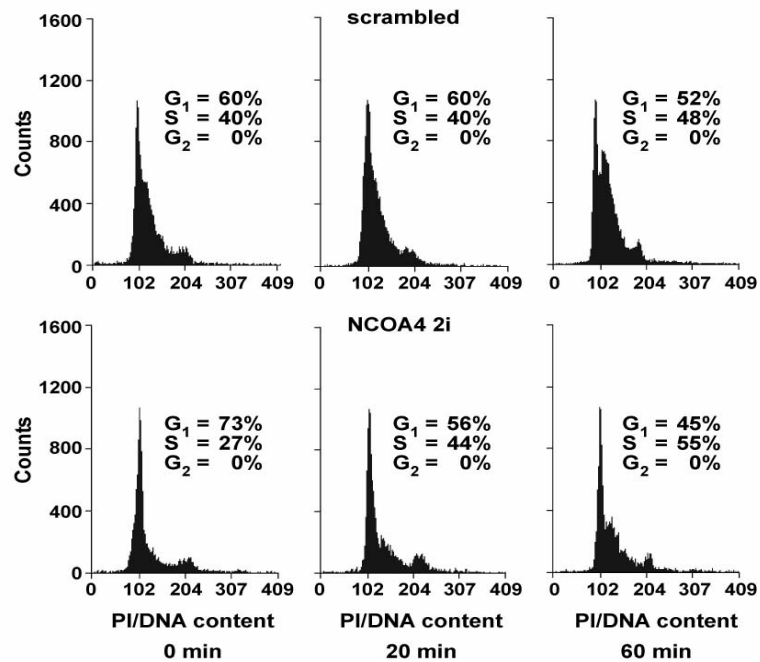


Figure 15 - Cytofluorimetric analysis of synchronized HeLa cells. *Scrambled or NCOA4 2i transfected cells were released from double-thymidine block for the indicated time points and subjected to cytometry. Percentage of cells in G₁, S and G₂ phases is indicated.*

Therefore to exclude that NCOA4 interfered cells increased DNA replication rate was due to increased licensing of origins but rather to increased activity of the fork in later steps of DNA replication, we analyzed MCM7 and PCNA loading onto chromatin. As already discussed MCM7 binding to DNA is a measure of the number of licensed origins while PCNA loading depends on the quantity of activated origins upon firing.

In NCOA4-interfered HeLa cells, the increased DNA synthesis was paralleled by augmented recruitment of PCNA to chromatin whereas the chromatin-bound fraction of MCM7 protein remained unchanged (Fig. 16).

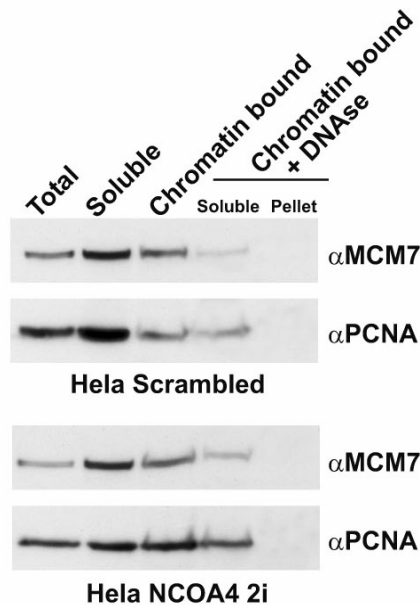


Figure 16 - MCM7 and PCNA chromatin binding in NCOA4 interfered HeLa cells. *Total, 0.5% Triton X-100 soluble and insoluble fractions, as well as soluble and insoluble fractions of the DNase-extracted insoluble aliquots (P+DNase) from scrambled RNAi or NCOA4 2i transfected cells were immunoblotted with anti MCM7 and anti-PCNA antibodies*

These data were consistent with our findings obtained in the *Xenopus laevis* model system (Carlomagno et al. submitted), where increased DNA synthesis was paralleled by augmented recruitment of PCNA to chromatin whereas the chromatin-bound fraction of MCM7 protein remained unchanged, and confirmed that, also in HeLa cells, NCOA4 does not control origin licensing but later steps of origin activation (Fig. 16).

Lastly, we investigated the effects of adoptive NCOA4 overexpression. Cells were engineered to express NCOA4 under the control of a doxycycline-inducible promoter. We were able to obtain a 1-fold induction of protein expression in two different clones, clone 23 and clone 24 (Fig. 17).

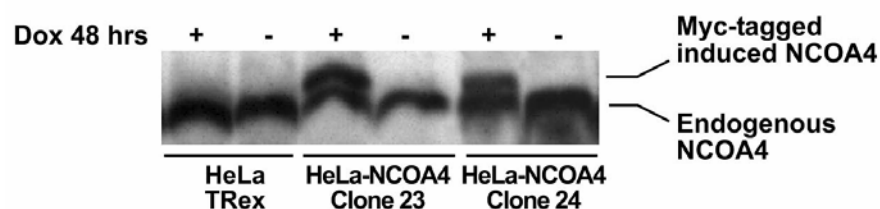


Figure 17 - NCOA4 doxycycline-induced expression. *Immunoblot detection of Myc-tagged NCOA4 protein upon doxycycline (Dox) (48 hours) induction in two independent HeLa-NCOA4 clones (clones 23 and 24).*

Induction of NCOA4 protein decreased cell growth, as shown in Fig. 18, more efficiently in clone 24 than in clone 23.

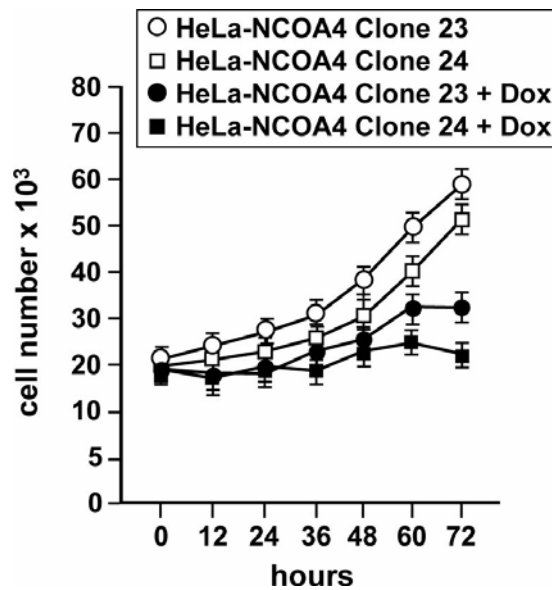


Figure 18 - NCOA4 negatively affects cell growth. *HeLa-NCOA4 (clones 23 and 24) cell growth with and without Doxycycline; the average results \pm SD of three independent experiments performed in triplicate are reported.*

In order to understand the mechanism lying behind such arrest, we measured DNA synthesis as incorporation of BrdU (Bromodeoxyuridine) measured by immunofluorescence staining with an anti-BrdU antibody. NCOA4 doxycycline-induction determined a reduced BrdU incorporation. It also caused cells to accumulate in S phase probably consequent to a reduced rate of DNA synthesis, as shown in fig. 19.

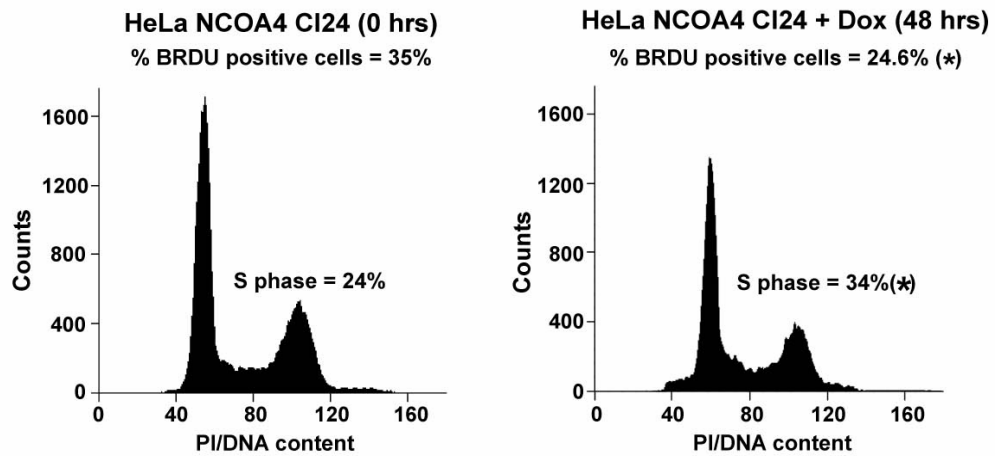


Figure 19 - HeLa-NCOA4 cells flow cytometry and anti-BrdU immunofluorescence upon Doxycycline treatment (48 hours). The average results \pm SD of three independent experiments made in duplicate are reported. * $P < 0.02$ (two-side paired Student's *t*-test). The same results were obtained with HeLa-NCOA4 clone 23 (not shown).

Decrease in BrdU incorporation with an increase in S-phase cells in an asynchronous cell population indicated that cells were able to enter S phase but were slowed down due to a hindrance of DNA synthesis, consistently with data obtained in *Xenopus laevis* egg extracts and in NCOA4 interfered cells.

Finally, we analyzed MCM7, RPA and PCNA chromatin binding to chromatin upon induction of NCOA4 protein. NCOA4 overexpression determined a reduced RPA and PCNA loading onto chromatin, while MCM7 binding remained unchanged. These data confirmed the hypothesis that DNA replication origins licensing was not affected by increased levels of NCOA4 protein, while DNA unwinding and therefore synthesis was strongly decreased (Fig. 20).

5. CONCLUSIONS

Here we identified a novel protein network involving NCOA4 (a gene fused to the RET tyrosine kinase receptor in papillary thyroid carcinoma) and MCM7 (a component of the MCM complex essential for DNA synthesis). Based on our findings, we propose NCOA4 as a novel DNA replication inhibitor. Indeed NCOA4 interacts with MCM7 at the endogenous level in HeLa cells. This interaction is localized on DNA where MCM2-7 complex is functionally active at licensing DNA replication origins and unwinding DNA. Moreover, NCOA4 protein is loaded on canonical origins such as c-Myc and Lamin B2. Modulation of NCOA4 protein levels affects both cell growth and DNA replication rate by acting on later steps of DNA replication initiation, such as DNA unwinding.

To our knowledge, this is the first example of a DNA replication controller that modulates origin unwinding, which wasn't known to be a tunable step of DNA replication associated events. Moreover, the two proteins involved in this network, MCM7 and NCOA4, are frequently deregulated in tumors by either genetic or epigenetic events that induce changes in expression levels, invoking their involvement in the process of tumorigenesis.

We postulate that chromosomal rearrangements that target the NCOA4 gene in thyroid cancer might release MCM7 mitogenic activity from the negative control exerted by NCOA4. Thus, NCOA4 N-terminal fragment is a loss of function mutant incapable of blocking DNA replication in *Xenopus laevis* egg extracts. In this context, the NCOA4 N-terminal rearrangement might represent a novel paradigm of a cancer-associated chromosome rearrangement that directly targets a gene that controls cell proliferation. Moreover we cannot exclude that the RET/PTC3 chimeric protein displays dominant negative effect on the residual NCOA4 wild type protein encoded by the NCOA4 allele that is left untouched by the rearrangement. Indeed, it was demonstrated that RET/PTC3 heterodimerizes with wt NCOA4 via its coiled-coil domain. The dominant negative role of NCOA4-RET fusion protein might be exerted by different possible mechanisms such as by localizing it to different cellular compartments or competing with MCM7 for interaction.

6. ACKNOWLEDGEMENTS

At the end of my PhD programme, I would like to acknowledge the continuous help and encouragement that I received during this period. I am thankful to Prof. Massimo Santoro, who welcomed me in his group and allowed me to carry on my research work, and to Prof. Giancarlo Vecchio, coordinator of the International Doctorate in Molecular Oncology and Endocrinology. Words of thanks would fail to express my indebtedness to Dr. Francesca Carlomagno, whose continuous support, insights and suggestions have constantly stimulated my interest for research. I would like to thank Teresa, whose kindness, experience and insights helped me during this adventure. Thanks to all the Lab 11 friends, my adventure mates. All of them have been invaluable to my activity and have contributed to my good spirit during the past three years. In particular, I want to thank Valentina and Francesco, for their smiles and their good spirit able to light my being exhausted. Recently, I spent an interesting and stimulating period in the laboratories of Dr. Vincenzo Costanzo at the LRI-Clare Hall Laboratories, South Mimms, London and I wish to thank him and all his co-workers for their kindness and hospitality. It was a very good work and life experience! Finally, I would like to say thank you to my family for the lovely, continuous encouragement and for being my best supporters, always.

7. REFERENCES

- Ballabeni A, Melixetian M, Zamponi R, Masiero L, Marinoni F, Helin K. Human geminin promotes pre-RC formation and DNA replication by stabilizing CDT1 in mitosis. *EMBO J.* 2004; 23(15):3122-32.
- Bell SP, Dutta A. DNA replication in eukaryotic cells. *Annu. Rev. Biochem.* 2002; 71: 333-374.
- Blow JJ, Hodgson B. Replication licensing--defining the proliferative state? *Trends Cell Biol.* 2002; 12(2): 72-8. Review
- Bongarzone I, Butti MG, Coronelli S, Borrello MG, Santoro M, Modellini P, Pilotti S, Fusco A, Della Porta G, Pierotti MA. Frequent activation of ret protooncogene by fusion with a new activating gene in papillary thyroid carcinomas. *Cancer Res* 1994; 54: 2979-2985.
- Bossis I, Stratakis CA. Minireview: PRKAR1A: normal and abnormal functions. *Endocrinology* 2004; 145(12):5452-8. Review
- Brandi ML, Gagel RF, Angeli A, Bilezikian JP, Beck-Peccoz P, Bordi C, Conte-Devolx B, Falchetti A, Gheri RG, Libroia A, Lips CJ, Lombardi G, Mannelli M, Pacini F, Ponder BA, Raue F, Skogseid B, Tamburrano G, Thakker RV, Thompson NW, Tomassetti P, Tonelli F, Wells SA Jr, Marx SJ. Guidelines for diagnosis and therapy of MEN type 1 and type 2. *J Clin Endocrinol Metab.* 2001; 86(12):5658-71. Review
- Chevalier S, Blow JJ. Cell cycle control of replication initiation in eukaryotes. *Curr Opin Cell Biol* 1996; 8(6):815-21. Review
- Chong J, Mahbubani HM, Khoo CY and Blow JJ. Purification of an MCM-containing complex as a component of the DNA replication licensing system. *Nature* 1995; 375: 418-421.
- Cox LS, Leno GH. Extracts from eggs and oocytes of *Xenopus laevis* differ in their capacities for nuclear assembly and DNA replication. *J Cell Sci* 1990; 97:177-184.
- Cromer A, Carles A, Millon R, Ganguli G, Chalmel F, Lemaire F, Young J, Dembele D, Thibault C, Muller D, Poch O, Abecassis J, Wasylyk B. Identification of genes associated with tumorigenesis and metastatic potential of hypopharyngeal cancer by microarray analysis. *Oncogene* 2004; 23: 2484-2498.

Diffley JF, Cocker JH, Dowell SJ, Rowley A. Two steps in the assembly of complexes at yeast replication origins in vivo. *Cell*. 1994;78(2):303-16.

Dominguez-Sola D, Ying CY, Grandori C, Ruggiero L, Chen B, Li M, Galloway DA, Gu W, Gautier J, Dalla-Favera R. Non-transcriptional control of DNA replication by c-Myc. *Nature* 2007;448: 445-451.

Fujita M, Kiyono T, Hayashi Y, Ishibashi M. In vivo interaction of human MCM heterohexameric complexes with chromatin. Possible involvement of ATP. *J Biol Chem* 1997; 272, 10928-10935.

Fusco A, Grieco M, Santoro M, Berlingieri MT, Pilotti S, Pierotti MA, Della Porta G, Vecchio G. A new oncogene in human thyroid papillary carcinomas and their lymph-nodal metastases. *Nature* 1987; 328(6126):170-2.

Gonzalez MA, Tachibana KE, Laskey RA, Coleman N. Control of DNA replication and its potential clinical exploitation. *Nat Rev Cancer* 2005; 5:135-141.

Grieco M, Santoro M, Berlingieri MT, Melillo RM, Donghi R, Bongarzone I, Pierotti MA, Della Porta G, Fusco A, Vecchio G. PTC is a novel rearranged form of the ret proto-oncogene and is frequently detected in vivo in human thyroid papillary carcinomas. *Cell* 1990; 60: 557-563.

Griffin KJ, Kirschner LS, Matyakhina L, Stergiopoulos S, Robinson-White A, Lenherr S, Weinberg FD, Claffin E, Meoli E, Cho-Chung YS & Stratakis CA. Down-regulation of regulatory subunit type 1A of protein kinase A leads to endocrine and other tumors. *Cancer Research* 2004; 64 8811–8815.

Guida T, Salvatore G, Faviana P, Giannini R, Garcia-Rostan G, Provitera L, Basolo F, Fusco A, Carlomagno F, Santoro M. Mitogenic effects of the up-regulation of minichromosome maintenance proteins in anaplastic thyroid carcinoma. *J Clin Endocrinol Metab* 2005; 90(8):4703-9.

He B, Wilson EM. The NH(2)-terminal and carboxyl-terminal interaction in the human androgen receptor. *Mol Genet Metab* 2002; 75(4):293-8. Review

Heinlein CA, Ting HJ, Yeh S, Chang C. Identification of ARA70 as a ligand-enhanced coactivator for the peroxisome proliferator-activated receptor gamma. *J Biol Chem* 1999; 274: 16147-16152.

Honeycutt KA, Chen Z, Koster MI, Miers M, Nuchtern J, Hicks J, Roop DR, Shohet JM. Deregulated minichromosomal maintenance protein MCM7 contributes to oncogene driven tumorigenesis. *Oncogene* 2006; 2: 4027-4032.

Hsu CL, Chen YL, Yeh S, Ting HJ, Hu YC, Lin H, Wang X, Chang C. The use of phage display technique for the isolation of androgen receptor interacting peptides with (F/W)XXL(F/W) and FXXLY new signature motifs. *J Biol Chem* 2003; 278(26):23691-8.

Hsu CL, Chen YL, Ting HJ, Lin WJ, Yang Z, Zhang Y, Wang L, Wu CT, Chang HC, Yeh S, Pimplikar SW, Chang C. Androgen receptor (AR) NH₂- and COOH-terminal interactions result in the differential influences on the AR-mediated transactivation and cell growth. *Mol Endocrinol* 2005; 19(2):350-61.

Hu YC, Yeh S, Yeh SD, Sampson ER, Huang J, Li P, Hsu CL, Ting HJ, Lin HK, Wang L, Kim E, Ni J, Chang C. Functional domain and motif analyses of androgen receptor coregulator ARA70 and its differential expression in prostate cancer. *J Biol Chem* 2004; 279(32):33438-46.

Iervolino A, Iuliano R, Trapasso F, Viglietto G, Melillo RM, Carlomagno F, Santoro M, Fusco A. The receptor-type protein tyrosine phosphatase J antagonizes the biochemical and biological effects of RET-derived oncoproteins. *Cancer Res* 2006; 66(12):6280-7.

Ishimi Y. A DNA helicase activity is associated with an MCM4, -6, and -7 protein complex. *J Biol Chem*. 1997;272(39):24508-13. Erratum in: *J Biol Chem* 1998; 273(36):23616.

Jenkins, TM, Saxena, JK, Kumar, A, Wilson, SH, Ackerman, EJ. DNA polymerase beta and DNA synthesis in *Xenopus* oocytes and in a nuclear extract. *Science* 1992; 258: 475-478.

Kearsey SE, Labib K. MCM proteins: evolution, properties, and role in DNA replication. *Biochim Biophys Acta* 1998; 1398(2):113-36. Review

Kollara A, Kahn HJ, Marks A, Brown TJ. Loss of androgen receptor associated protein 70 (ARA70) expression in a subset of HER2-positive breast cancers. *Breast Cancer Res Treat* 2001; 67: 245-53.

Krude T, Musahl C, Laskey RA, Knippers R. Human replication proteins hCdc21, hCdc46 and P1Mcm3 bind chromatin uniformly before S-phase and are displaced locally during DNA replication. *J Cell Sci* 1996; 109 (Pt 2):309-18.

Kubota Y, Mimura S, Nishimoto SL, Takisawa H and Nojima H. Identification of the yeast MCM3-related protein as a component of *Xenopus* DNA replication licensing factor. *Cell* 1995; 81: 601-610.

- Kulartz M, Knippers R. The replicative regulator protein geminin on chromatin in the HeLa cell cycle. *J Biol Chem* 2004; 279(40):41686-94.
- Labib K, Diffley JF. Is the MCM2-7 complex the eukaryotic DNA replication fork helicase? *Curr Opin Genet Dev* 2001; 11(1):64-70. Review
- Labib K, Tercero JA, Diffley JF. Uninterrupted MCM2-7 function required for DNA replication fork progression. *Science* 2000; 288: 1643-1647.
- Laskey R. The Croonian Lecture 2001 hunting the antisocial cancer cell: MCM proteins and their exploitation. *Philos Trans R Soc Lond B Biol Sci* 2005; 360(1458):1119-32
- Lee C, Hong B, Choi JM, Kim Y, Watanabe S, Ishimi Y, Enomoto T, Tada S, Kim Y, Cho Y. Structural basis for inhibition of the replication licensing factor Cdt1 by geminin. *Nature* 2004; 430(7002):913-7.
- Lee JK, Hurwitz J. Isolation and characterization of various complexes of the minichromosome maintenance proteins of *Schizosaccharomyces pombe*. *J Biol Chem* 2000; 275: 18871-18878.
- Li P, Yu X, Ge K, Melamed J, Roeder RG, Wang Z. Heterogeneous expression and functions of androgen receptor co-factors in primary prostate cancer. *Am J Pathol* 2002; 161: 1467-1474.
- Lin HK, Wang L, Hu YC, Altuwaijri S, Chang C. Phosphorylation-dependent ubiquitylation and degradation of androgen receptor by Akt require Mdm2 E3 ligase. *EMBO J* 2002; 21(15):4037-48.
- Machida YJ, Hamlin JL, Dutta A. Right place, right time, and only once: replication initiation in Metazoans. *Cell* 2005; 123: 13-24. Review
- Maiorano D, Cuvier O, Danis E, Mechali M. MCM8 is an MCM2-7-related protein that functions as a DNA helicase during replication elongation and not initiation. *Cell* 2005; 120: 315-328.
- Maiorano D, Lutzmann M, Mechali M. MCM proteins and DNA replication. *Curr Opin Cell Biol* 2006; 18: 130-136.
- Maiorano D, Rul W, Méchali M. Cell cycle regulation of the licensing activity of Cdt1 in *Xenopus laevis*. *Exp Cell Res* 2004; 295(1):138-49.
- Melillo RM, Cirafici AM, De Falco V, Bellantoni M, Chiappetta G, Fusco A, Carlomagno F, Picascia A, Tramontano D, Tallini G, Santoro M. The oncogenic activity of RET point mutants for follicular thyroid cells may

account for the occurrence of papillary thyroid carcinoma in patients affected by familial medullary thyroid carcinoma. *Am J Pathol* 2004; 165(2):511-21.

Méndez J, Stillman B. Perpetuating the double helix: molecular machines at eukaryotic DNA replication origins. *Bioessays*. 2003; 25(12):1158-67. Review

Meng MV, Grossfeld GD, Williams GH, Dilworth S, Stoeber K, Mulley TW, Weinberg V, Carroll PR, Tlsty TD. Minichromosome maintenance protein 2 expression in prostate: characterization and association with outcome after therapy for cancer. *Clin Cancer Res* 2001; 7: 2712-2718.

Merolla F, Pentimalli F, Pacelli R, Vecchio G, Fusco A, Grieco M, Celetti A. Involvement of H4 (D10S170) protein in ATM-dependent response to DNA damage. *Oncogene* 2007; 26(42): 6167-75.

Miyamoto H, Yeh S, Wilding G, Chang C. Promotion of agonist activity of antiandrogens by the androgen receptor coactivator, ARA70, in human prostate cancer DU145 cells. *Proc Nat Acad Sci U.S.A.* 1998; 95: 7379–7384.

Minoletti F, Butti MG, Coronelli S, Miozzo M, Sozzi G, Pilotti S, Tunnacliffe A, Pierotti MA, Bongarzone I. The two genes generating RET/PTC3 are localized in chromosomal band 10q11.2. *Genes Chromosomes Cancer* 1994; 11(1): 51-57.

Monaco C, Visconti R, Barone MV, Pierantoni GM, Berlingieri MT, De Lorenzo C, Mineo A, Vecchio G, Fusco A, Santoro M. (2001) The RFG oligomerization domain mediates kinase activation and re-localization of the RET/PTC3 oncoprotein to the plasma membrane. *Oncogene* 2001; 20: 599-608.

Murray AW. Cell cycle extracts. *Methods Cell Biol* 1991; 36: 581-605.

Nikiforov YE, Koshoffer A, Nikiforova M, Stringer J, Fagin JA. Chromosomal breakpoint positions suggest a direct role for radiation in inducing illegitimate recombination between the ELE1 and RET genes in radiation-induced thyroid carcinomas. *Oncogene* 1999; 18(46):6330-4.

Ostrowski ML, Merino MJ. Tall cell variant of papillary thyroid carcinoma: a reassessment and immunohistochemical study with comparison to the usual type of papillary carcinoma of the thyroid. *Am J Surg Pathol* 1996; 20(8):964-74.

Pacek M, Tutter AV, Kubota Y, Takisawa H, Walter JC. Localization of MCM2-7, Cdc45, and GINS to the site of DNA unwinding during eukaryotic DNA replication. *Mol Cell* 2006; 21: 581-587.

Pacek M, Walter JC. A requirement for MCM7 and Cdc45 in chromosome unwinding during eukaryotic DNA replication. *EMBO J* 2004; 23: 3667-3676.

Pasero P, Schwob E. Think global, act local--how to regulate S phase from individual replication origins. *Curr Opin Genet Dev* 2000; 10(2):178-86.

Quintana DG, Dutta A. The metazoan origin recognition complex. *Front Biosci* 1999; 4:D805-15. Review

Ren B, Yu G, Tseng GC, Cieply K, Gavel T, Nelson J, Michalopoulos G, Yu YP, Luo JH. MCM7 amplification and overexpression are associated with prostate cancer progression. *Oncogene* 2006; 25: 1090-1098.

Ritzi M, Knippers R. Initiation of genome replication: assembly and disassembly of replication-competent chromatin. *Gene* 2000; 245(1):13-20. Review

Ron E, Lubin JH, Shore RE, Mabuchi K, Modan B, Pottern LM. On target cell numbers in radiation-induced H4-RET mediated papillary thyroid cancer. *Radiat Res* 1995; 141(3):259-77.

Santoro M, Dathan NA, Berlingieri MT, Bongarzone I, Paulin C, Grieco M, Pierotti MA, Vecchio G, Fusco A. Molecular characterization of RET/PTC3; a novel rearranged version of the RET proto-oncogene in a human thyroid papillary carcinoma. *Oncogene* 1994; 9: 509-516.

Santoro M, Melillo RM, Fusco A. RET/PTC activation in papillary thyroid carcinoma: European Journal of Endocrinology Prize Lecture *Eur J Endocrinol* 2006; 155(5): 645-653.

Saxena S, Yuan P, Dhar SK, Senga T, Takeda D, Robinson H, Kornbluth S, Swaminathan K, Dutta A. A dimerized coiled-coil domain and an adjoining part of geminin interact with two sites on Cdt1 for replication inhibition. *Mol Cell* 2004; 15(2): 245-58.

Schuchardt A, D'Agati V, Larsson-Blomberg L, Costantini F, Pachnis V. Defects in the kidney and enteric nervous system of mice lacking the tyrosine kinase receptor Ret. *Nature* 1994; 367(6461): 380-3.

Sclafani RA. Cdc7p-Dbf4p becomes famous in the cell cycle. *J Cell Sci* 2000; 113 (Pt 12):2111-7.

Sterner JM, Dew-Knight S, Musahl C, Kornbluth S, Horowitz JM. Negative regulation of DNA replication by the retinoblastoma protein is mediated by its

association with MCM7. *Mol Cell Biol* 1998; 18: 2748-2757.

Stoeber K, Halsall I, Freeman A, Swinn R, Doble A, Morris L, Coleman N, Bullock N, Laskey RA, Hales CN, Williams GH. Immunoassay for urothelial cancers that detects DNA replication protein MCM 5 in urine. *Lancet* 1999; 354: 1524-1525

Stoeber K, Swinn R, Prevost AT, de Clive-Lowe P, Halsall I, Dilworth SM, Marr J, Turner WH, Bullock N, Doble A, Hales CN, Williams GH. Diagnosis of genito-urinary tract cancer by detection of minichromosome maintenance 5 protein in urine sediments. *J Natl Cancer Inst* 2002; 94(14):1071-9.

Stoeber K, Tlsty TD, Happerfield L, Thomas GA, Romanov S, Bobrow L, Williams ED, Williams GH. DNA replication licensing and human cell proliferation. *J Cell Sci* 2001; 114: 2027-2041.

Takahashi M, Inaguma Y, Hiai H, Hirose F. Developmentally regulated expression of a human "finger"-containing gene encoded by the 5' half of the ret transforming gene. *Mol Cell Biol* 1988; 8(4):1853-6.

Takahashi TS, Wigley DB, Walter JC. Pumps, paradoxes and ploughshares: mechanism of the MCM2-7 DNA helicase. *Trends Biochem Sci* 2005; 30: 437-444.

Takayama Y, Kamimura Y, Okawa M, Muramatsu S, Sugino A, Araki H GINS, a novel multiprotein complex required for chromosomal DNA replication in budding yeast. *Genes Dev* 2003; 17: 1153-1165.

Tanaka T, Knapp D and Nasmyth K. Loading of an MCM protein onto DNA replication origins is regulated by Cdc6p and CDKs. *Cell* 1997; 90:649-660.

Tekur S, Lau KM, Long J, Burnstein K, Ho SM. Expression of RFG/ELE1alpha/ARA70 in normal and malignant prostatic epithelial cell cultures and lines: regulation by methylation and sex steroids. *Mol Carcinog* 2001; 30(1):1-13.

Tye BK. MCM proteins in DNA replication. *Annu Rev Biochem* 1999; 68:649-86. Review

Walter J, Newport J. Initiation of eukaryotic DNA replication: origin unwinding and sequential chromatin association of Cdc45, RPA, and DNA polymerase alpha. *Mol Cell* 2000; 5: 617-627.

Williams D. Cancer after nuclear fall-out: lessons from the Chernobyl accident. *Nat Rev Cancer* 2002; 2:543-549.

Williams ED, Doniach I, Bjarnason O, Michie W. Thyroid cancer in an iodide rich area: a histopathological study. *Cancer* 1997; 39(1):215-22.

Williams GH, Romanovski P, Morris L, Madine M, Mills AD, Stoeber K, Marr J, Laskey RA, Coleman N. Improved cervical smear assessment using antibodies against proteins that regulate DNA replication. *Proc Natl Acad Sci USA* 1998; 95: 14932-14937.

Yan H, Merchant AM, Tye BK. Cell cycle regulated nuclear localization of MCM2 and MCM3, which are required for the initiation of DNA synthesis at chromosomal replication origins in yeast. *Genes Dev* 1993; 7: 2149-2160.

Yeh S, Chang C. Cloning and characterization of a specific coactivator, ARA70, for the androgen receptor in human prostate cells. *Proc Natl Acad Sci USA* 1996; 93: 5517-5521.

Yeh S, Tsai MY, Xu Q, Mu XM, Lardy H, Huang KE, Lin H, Yeh SD, Altuwaijri S, Zhou X, Xing L, Boyce BF, Hung MC, Zhang S, Gan L, Chang C. Generation and characterization of androgen receptor knockout (ARKO) mice: an in vivo model for the study of androgen functions in selective tissues. *Proc Natl Acad Sci U S A*. 2002; 99(21):13498-503.

You Z, Komamura Y, Ishimi Y. Biochemical analysis of the intrinsic Mcm4-Mcm6-mcm7 DNA helicase activity. *Mol Cell Biol* 1999; 19(12):8003-15.

Mitogenic Effects of the Up-Regulation of Minichromosome Maintenance Proteins in Anaplastic Thyroid Carcinoma

Teresa Guida, Giuliana Salvatore, Pinuccia Faviana, Riccardo Giannini, Ginesa Garcia-Rostan, Livia Provitera, Fulvio Basolo, Alfredo Fusco, Francesca Carlomagno, and Massimo Santoro

Istituto di Endocrinologia ed Oncologia Sperimentale del Consiglio Nazionale delle Ricerche, Dipartimento di Biologia e Patologia Cellulare e Molecolare L. Califano (T.G., G.S., L.P., A.F., F.C., M.S.), Università Federico II, 80131 Naples, Italy; Dipartimento di Oncologia (P.F., R.G., F.B.), Università di Pisa, 56126 Pisa, Italy; and Instituto de Patologia e Imunologia Molecular da Universidade do Porto (G.G.-R.), 4200-465 Porto, Portugal

Context: Anaplastic thyroid carcinomas (ATC) are among the most aggressive human malignancies and are characterized by high mitotic activity. Minichromosome maintenance proteins (MCM) 2–7 are required to initiate eukaryotic DNA replication, and their overexpression has been associated with dysplasia and malignancy.

Objective: In an attempt to cast light on the mechanisms governing ATC, we evaluated MCM5 and MCM7 expression in human normal, papillary (PTC), and anaplastic thyroid samples, as well as in primary culture cells and transgenic mouse models.

Results: MCM5 and MCM7 expression was high in 65% of ATC and negligible in normal thyroid tissue and papillary thyroid carcinomas. In ATC, high MCM5 and MCM7 expression was paralleled by high levels of MCM2 and MCM6. An analysis of human ATC primary cell

cultures and of a transgenic mouse model of ATC confirmed these findings. An increased transcription rate accounted for MCM7 up-regulation, because the activity of the MCM7 promoter was more than 10-fold higher in ATC cells compared with normal thyroid cells. Adoptive overexpression of wild-type p53, but not of its inactive (R248W and R273H) mutants, strongly down-regulated transcription from the MCM7 promoter, suggesting that p53 knock-out contributes to MCM7 up-regulation in ATC. Treatment with small inhibitory duplex RNAs, which decrease MCM7 protein levels, reduced the rate of DNA synthesis in ATC cells.

Conclusion: MCM proteins are overexpressed in ATC and sustain the high proliferative capacity of ATC cells. (*J Clin Endocrinol Metab* 90: 4703–4709, 2005)

WELL-DIFFERENTIATED THYROID carcinomas (WDC) account for more than 90% of all thyroid cancers and include papillary (PTC) and follicular (FTC) carcinomas (1). Undifferentiated or anaplastic thyroid carcinomas (ATC) are highly malignant tumors and account for less than 2–5% of all thyroid cancers. Despite its rarity, more than half of the deaths attributed to thyroid cancer result from ATC (2). ATC is usually seen in the sixth to seventh decades of life (2, 3). Almost all ATC patients present with a rapidly enlarging neck mass and frequently have evidence of distant metastases in lung, bone, or brain at diagnosis (2, 3). More than 25% of ATC patients show coincidentally detected WDC on histological examination, suggesting that, at least in some cases, ATC may derive from a preexisting WDC (1–3).

Differently from WDC, ATC have a high proliferation rate and marked genetic instability. This is reflected in the rapid tumor growth and dissemination that characterize the clin-

ical course of ATC. The combination of a short cell-doubling time and a low apoptotic rate results in one of the most rapid growth rates in any solid tumor, and ATC tumors may double in size within 1 wk (2, 3). The molecular mechanisms underlying the anaplastic transformation of thyroid follicular cells are largely unknown. Structural rearrangements of the receptor tyrosine kinases RET and TRKA (tyrosine kinase), which are common in PTC, and of PPAR γ (peroxisome proliferator-activated receptor γ), typical of FTC, are rarely seen in ATC (4). Point mutations in RAS small GTPases (5) and in the BRAF (BRCA2-associated factor) serine/threonine kinase have been detected in ATC (6), and, at variance with WDC, ATC is associated with a high prevalence of p53 gene mutations (7, 8). Mutations in β -catenin are also frequent in ATC (9). In general, ATC are characterized by a high degree of aneuploidy and complex chromosomal alterations (10); in particular, loss of 16p is common in ATC cell lines (11).

Minichromosome maintenance proteins (MCM2–MCM7) are required for DNA replication in eukaryotic cells. They were originally discovered in yeast and subsequently identified in *Drosophila melanogaster*, *Xenopus laevis*, mice, and humans (12). MCM proteins form a heterohexamer that is part of the prereplication complex (pre-RC). pre-RC factors bind to chromatin in a highly ordered sequence that triggers DNA synthesis. The process begins with the loading of the origin recognition complex. Cdc6 (cell division control protein 6) is then recruited to the site, and this allows loading of

First Published Online May 17, 2005

Abbreviations: ATC, Anaplastic thyroid carcinomas; BrdU, bromodeoxyuridine; FTC, follicular thyroid carcinomas; MCM, minichromosome maintenance protein; PCNA, proliferating cell nuclear antigen; pre-RC, prereplication complex; PTC, papillary thyroid carcinoma; siRNA, small inhibitory duplex RNA; WDC, well-differentiated thyroid carcinomas.

JCEM is published monthly by The Endocrine Society (<http://www.endo-society.org>), the foremost professional society serving the endocrine community.

the MCM complex. As cells enter S-phase, Cdc6 is released and other factors are loaded onto the replication origin to initiate DNA synthesis. The process requires the S-phase-specific kinases CDK2 (cyclin-dependent kinase)-cyclin E and Dbf4 (DNA binding factor)-Cdc7. Dissociation of the pre-RC from chromatin ensures that each region of DNA is replicated only once during a single cell cycle (12). Being one of the helicases involved in DNA unwinding at the replication forks, MCM proteins are required throughout DNA elongation (13, 14).

The expression of MCM proteins depends on the proliferation state of the cell. Quiescent and differentiated cells do not express MCM, whereas proliferating cells and cells with proliferation potential do (15). In normal or reactive tissues, MCM expression is restricted to proliferative compartments. In contrast, in dysplastic and malignant tissues, MCM proteins are present in most cells, and their expression level inversely correlates with the degree of tumor differentiation (15). Uterine cervix, prostate, and esophageal dysplasia are positive to anti-MCM antibodies, and staining increases in neoplastic lesions (16–19). MCM assay has a high specificity and sensitivity in detecting cancerous cells in feces (colorectal carcinoma) and urine (bladder carcinoma) (20, 21).

We have investigated the expression of MCM proteins in normal thyroid tissue, PTC, and ATC tumors in mice and humans. We show that MCM2, MCM5, MCM6, and MCM7 are expressed at a high level in ATC, and that MCM7 is involved in the proliferation of ATC cells.

Materials and Methods

Immunohistochemistry

Tumors were retrieved from the files of the Pathology Departments of the Hospital Central de Asturias (Oviedo University, Asturias, Spain) and the Hospital Clínico Universitario (Santiago de Compostela University, Galicia, Spain) and the Department of Oncology of the University of Pisa (Pisa, Italy). In all cases, the study protocols were approved by the respective institutional review boards. Cases were chosen randomly among those for whom detailed clinical and follow-up data were available. For each case, the sex and age of the patient at diagnosis, tumor size, extrathyroidal extension, vascular invasion, lymph node or distant metastases, stage, and survival were recorded. Normal thyroid tissue samples were also retrieved from the files of the Department of Oncology of the University of Pisa. Sections of paraffin-embedded samples were stained with hematoxylin and eosin for histological examination to ensure that the samples fulfilled the diagnostic criteria (22). Formalin-fixed and paraffin-embedded 3- to 5- μ m-thick tumor sections were deparaffinized, placed in a solution of absolute methanol and 0.3% hydrogen peroxide for 30 min, and treated with blocking serum for 20 min. The slides were incubated overnight with mouse monoclonal antibodies against MCM5 (MCA 1860; Serotec, Oxford, UK), MCM7 (141.2, sc-9966; Santa Cruz Biotechnology, Santa Cruz, CA), or proliferating cell nuclear antigen (PCNA) (MAB424; Chemicon, Temecula, CA). After incubation with biotinylated antimouse secondary antibody for 15 min, slides were stained with premixed avidin-biotin complex (Vectostain ABC kits; Vector Laboratories, Burlingame, CA). Sections were developed for 5 min with 0.05% 3,3'-diaminobenzidine tetrahydrochloride (Dako, Carpinteria, CA) and 0.01% hydrogen peroxide in 0.05 M Tris-HCl buffer (pH 7.6), counterstained with hematoxylin, dehydrated, and mounted. Negative controls were performed in each case by incubating tissue slides with preimmune serum.

Cell cultures

Primary cell cultures of normal thyroid (S11N and S63N), follicular adenoma (HTU31 and HTU42), PTC (HTU56 and HT59), and ATC

(HTU8 and S11T) were kindly donated by F. Curcio (University of Udine, Udine, Italy) and H. Zitzelsberger (Forschungszentrum für Umwelt und Gesundheit, Neuherberg, Germany). The ARO cell line was established from a human ATC by Guy J. Juillard (University of California, Los Angeles, Los Angeles, CA) (7). Cells were grown in RPMI supplemented with 20% fetal bovine serum (Invitrogen, Paisley, PA), 2 mM L-glutamine, and 100 U/ml penicillin-streptomycin (Invitrogen). For the measurement of MCM5 and MCM7 half-life, cells were grown to subconfluence and then treated with 10 μ g/ml cycloheximide (Sigma, St. Louis, MO) for up to 48 h. For bromodeoxyuridine (BrdU) incorporation, cells were seeded on glass coverslips. Forty-eight hours after transfection, BrdU (Sigma) was added to the cell culture media at a final concentration of 100 μ g/ml for 2 h before harvest. Cells were fixed with paraformaldehyde (4%) and permeabilized with Triton X-100 (0.2%) before staining. Coverslips were incubated with anti-BrdU mouse monoclonal antibody and then with a fluorescein isothiocyanate-conjugated antimouse antibody (Roche Molecular Biochemicals, Mannheim, Germany). Coverslips were counterstained in PBS containing Hoechst 33258 (final concentration, 1 μ g/ml; Sigma), rinsed in PBS, and mounted in Moviol on glass slides. The fluorescent signal was visualized with an epifluorescent microscope (Axiovert 2; Zeiss, Oberkochen, Germany) interfaced with the KS300 image analyzer software (Zeiss).

Protein analyses

Protein lysates were prepared according to standard procedures. Briefly, cells or tumor tissues were lysed in a buffer containing 50 mM HEPES (pH 7.5), 1% (vol/vol) Triton X-100, 50 mM NaCl, 5 mM EGTA, 50 mM NaF, 20 mM sodium pyrophosphate, 1 mM sodium vanadate, 2 mM phenylmethylsulfonyl fluoride, and 1 μ g/ml aprotinin. Lysates were clarified by centrifugation at 10,000 \times g for 15 min. Lysates containing comparable amounts of proteins, estimated by a modified Bradford assay (Bio-Rad, Munich, Germany), were subjected to Western blot. Immune complexes were detected with the enhanced chemiluminescence kit (Amersham Biosciences, Little Chalfont, UK). The image was saved by the Typhoon 8600 laser scanning system (Amersham Biosciences). The density and width of each band was quantified using the ImageQuant 5.0 software (Amersham Biosciences). Anti-MCM2 (N-19; sc-9839), anti-MCM6 (C-20; sc-9843), and anti-MCM7 (141.2; sc-9966) were from Santa Cruz Biotechnology. Anti-MCM5 (MCA 1860) was from Serotec. Anti- α -tubulin was from Sigma. Secondary antibodies coupled to horseradish peroxidase were from Santa Cruz Biotechnology. Triton X-100-extracted nuclei were prepared as described previously (23). Briefly, cells were cultured in 100-mm plates; then, they were washed three times with ice-cold PBS and lysed for 10 min on ice with 1 ml ice-cold CSK buffer [10 mM 1,4-piperazinediethanesulfonic acid (pH 6.8), 100 mM NaCl, 300 mM sucrose, 1 mM MgCl₂, 1 mM EGTA, 1 mM dithiothreitol, 1 mM phenylmethylsulfonyl fluoride, and 10 μ g/ml aprotinin] containing 0.5% Triton X-100. After low-speed centrifugation (3000 rpm, 3 min at 4°C), nuclei were washed once with 1 ml ice-cold 0.5% Triton X-100 in CSK, centrifuged, and directly resuspended in 1 \times SDS sample buffer. Protein amounts of Triton X-100-soluble and -insoluble fractions deriving from comparable number of cells were loaded on SDS-PAGE and subjected to Western blotting.

Northern blot

Cells were harvested and stored frozen until RNA was extracted. Total RNA was isolated by the RNeasy Kit (QIAGEN, Crawley, West Sussex, UK) and subjected to on-column DNase digestion with the RNase-free DNase set (QIAGEN) according to the instructions of the manufacturer. RNA was analyzed by electrophoresis through 1% agarose gel and visualized with ethidium bromide. Total RNA (20 μ g) was size fractionated on a denaturing formaldehyde agarose gel and blotted onto nylon filters (Hybond-N; Amersham Biosciences). The MCM5 probe was a 503-bp RT-PCR product obtained using the following primers: forward (mcm5f), 5'-ACTCAAGCGGCATTACAACC-3'; reverse (mcm5r), 5'-GTCTGGAAGTCCACGCATTT-3'.

The MCM7 probe was a 174-bp RT-PCR product obtained using the following primers: forward (mcm7f), 5'-TGAACCTCGGGAAGAAG-CA-3'; reverse (mcm7r), 5'-TGTACGGCATCAGCAAAGAG-3'.

We used the random oligonucleotide primer kit (Amersham Biosciences) to label the probe. Hybridizations and washings were per-

formed under stringent conditions. Autoradiography was performed with Eastman Kodak (Rochester, NY) XAR films at -70°C for 7 d with intensifying screens. The image was saved by the Typhoon 8600 laser scanning system, and the density and width of each band was quantified with the ImageQuant 5.0 software.

Reporter gene assay

A 440-bp PCR fragment of the human MCM7 promoter spanning from -500 to -60 relative to the transcription start (24) was cloned into the pGL3 Basic vector (Promega, Madison, WI) carrying the luciferase reporter gene, to obtain the pGL3-MCM7LUC plasmid. PCR amplification was performed on normal human genomic DNA with the following primers: forward, 5'-TAGATCTCAGCCCCAAGGGTCTAGG-3'; reverse, 5'-TAAGCTTGGGAAGCTGAGAATCTCCG-3'.

The obtained construct was controlled by DNA sequencing. Cells were transfected by using the LipofectAMINE Reagent (Invitrogen) according to the instructions of the manufacturer. Cells were transfected with the different expression plasmids together with 500 ng of the reporter plasmid DNA and 100 ng pRL-null DNA (a plasmid expressing the enzyme *Renilla* luciferase from *Renilla reniformis*) as an internal control. In all of the cases, the total amount of transfected plasmid DNA was normalized by adding empty vector DNA. After 16 h from transfection, *Firefly* and *Renilla* luciferase activities present in cellular lysates were assayed using the Dual-Luciferase Reporter System (Promega), and light emission was quantified using the Lumat LB9507 luminometer (EG Berthold, Bundoora, Australia), as specified by the manufacturer. Each experiment was performed in triplicate. Expression vectors for wild-type p53, p53 R248W, and p53 R273H mutant cDNAs, cloned in the pCMV6 vector, have been described previously (25).

RNA silencing

Premade (Smart Pool) small inhibitory duplex RNAs (siRNA) for MCM7 were purchased from Dharmacon (Chicago, IL). Another set of anti-MCM7 siRNA was designed with a program available online (<http://jura.wi.mit.edu/siRNAext/>) and synthesized by Proligo (Boulder, CO). The sense strand of the second MCM7 siRNA duplex was 5'-AAGAUGUCCUGGACGUUUACAdTdT-3'. The anti-laminaA/C siRNA (Proligo) used as control was 5'-CUGGACUCCAGAAGAA-CAdTdT-3'. Scrambled control siRNA (Proligo) was 5'-ACCGUCGA-UUUCACCCGGdTdT-3. S11T cells were grown under standard conditions. The day before transfection, cells were plated in six-well dishes at 50–60% confluency. Transfection was performed with 5 μg siRNA and 6 μl oligofectamine reagent (Invitrogen, Groningen, The Netherlands), as described previously (26). Cells were harvested at 72 h after transfection.

Statistical analysis

Significance was determined by the two-tailed Fisher's test (Statistica 6.0; StatSoft, Tulsa OK). $P < 0.05$ was considered statistically significant.

Results

MCM proteins are highly expressed in ATC

Using immunohistochemistry with specific anti-MCM5 and anti-MCM7 monoclonal antibodies, we evaluated MCM5 and MCM7 expression levels in 30 normal thyroid samples, 20 PTC samples, and 52 ATC samples. In 65% of ATC samples, more than 10% of cells (on average, 25% of the cells) were positive for MCM5, and, in 73% of the samples, more than 10% (on average, 30% of the cells) were positive for MCM7 expression. In both cases, the signal was exclusively nuclear. Virtually no MCM5 and MCM7 expression ($<2\%$ of cells) was detected in normal and PTC samples (Fig. 1 and Table 1). Expression of PCNA, a conventional proliferation marker, was also examined. PCNA expression was significantly correlated ($P < 0.01$) with MCM5 and MCM7 expression being detected mainly in ATC samples (65%). Only two PTC samples contained a few PCNA-positive cells ($<5\%$ of cells) (Table 1). Normal tissue was invariably PCNA negative. Representative examples of the expression of MCM5, MCM7, and PCNA are shown in Fig. 1. These findings suggested that MCM5 and MCM7 overexpression may be related to the high mitotic activity of ATC. We next separated pure ATC samples from ATC samples containing well-differentiated (PTC or Hurthle-cell variant FTC) areas identified by morphological features. The expression of MCM5 and MCM7 was more prevalent in pure ATC ($P < 0.05$) and in ATC with coexisting Hurthle-cell areas than in mixed PTC-ATC samples (Table 2). In parallel, pure ATC samples were also more frequently PCNA positive than mixed PTC-ATC samples ($P = 0.054$) (Table 2). More importantly, when MCM7, MCM5, and PCNA were detected in mixed PTC-ATC tumors, their expression was invariably confined to the ATC area (data not shown).

To verify these data and to analyze other MCM proteins, we probed protein extracts from 10 thyroid samples with anti-MCM7, anti-MCM5, anti-MCM2, and anti-MCM6 antibodies. MCM proteins were expressed in ATC samples at higher levels than in normal and PTC samples (Fig. 2A and data not shown). Phosphor imaging quantitation showed that MCM5 and MCM7 were induced, on average, by 4 \pm

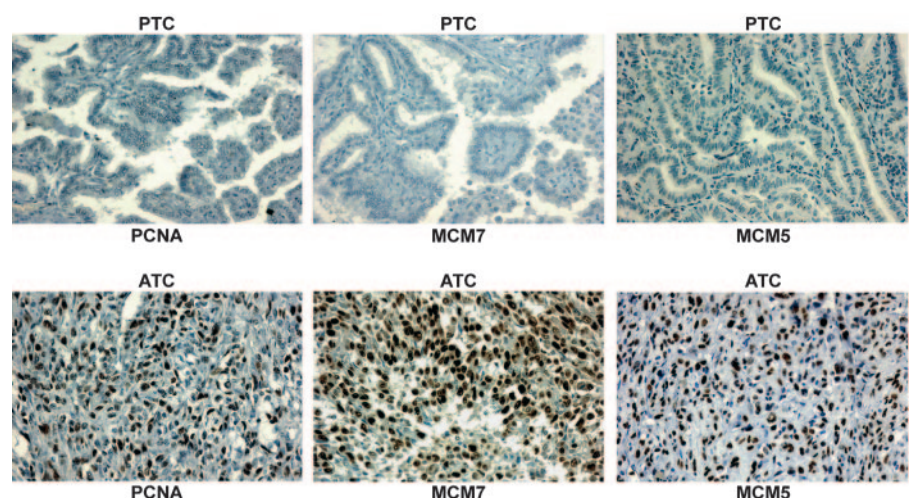


FIG. 1. Representative examples of PTC and ATC samples immunostained with PCNA, MCM5, and MCM7 antibodies. The primary antibody was omitted for a negative control (data not shown).

TABLE 1. MCM5, MCM7, and PCNA expression in thyroid samples

| Tissue | MCM5 positivity ^a | MCM7 positivity ^a | PCNA positivity ^a | MCM5/PCNA ^b | MCM7/PCNA ^b |
|--------|------------------------------|------------------------------|------------------------------|------------------------|------------------------|
| NT | 0% (0/30) | 0% (0/30) | 0% (0/30) | | |
| PTC | 0% (0/20) | 0% (0/20) | 10% (2/20) | | |
| ATC | 65% (34/52) | 73% (38/52) | 65% (34/52) | 58% (30/52) | 61% (32/52) |

NT, Normal thyroid.

^a Samples were scored positive when more than 10% of cells stained with the antibody.

^b Fraction of samples coexpressing PCNA and MCM5 or PCNA and MCM7, respectively.

1-fold and 8 ± 3 -fold, respectively, in ATC with respect to normal samples.

Transgenic mouse models of thyroid tumors generated through expression of various oncogenes under the control of the bovine thyroglobulin gene promoter have become mainstays of studies of thyroid carcinogenesis (27). RET/PTC3 (28) and TRK-T1 (29) strains develop carcinomas with cytological and histological features typical of human PTC (nuclear grooves, ground-glass nuclei, scant cytoplasm, absence of mitotic figures, and papillae containing fibrovascular stalks). Simian virus 40 large T antigen transgenic mice develop aggressive tumors with a phenotype similar to that of human ATC (27). We evaluated the expression of MCM proteins by immunoblot in representative samples of the three transgenic lines. In parallel, we verified the histologic diagnosis using hematoxylin and eosin staining. Also in the murine model, MCM protein expression was higher in ATC than in PTC or in normal thyroid (Fig. 2B). Finally, we examined primary cultures derived from two samples each of normal thyroid, follicular adenoma, PTC, and ATC. As shown in Fig. 2C, MCM protein expression was higher in ATC cells than in normal or in differentiated tumor cells.

MCM5 and MCM7 are overexpressed at mRNA level in ATC

To obtain a semiquantitative estimate of the extent of MCM5 and MCM7 overexpression, we compared protein levels in ATC cells (HTU8 and S11T) with those in normal cells (S11N) by loading increasing amounts of total protein extracts on SDS-PAGE (Fig. 3A) and compared band intensity by phosphor imaging. MCM5 and MCM7 expression was about five times greater in ATC cells than in normal cells (Fig. 3A).

To evaluate whether changes in protein turnover caused MCM5 and MCM7 up-regulation, we measured the MCM5 and MCM7 half-life in ATC and normal cells. Cells were treated with the protein synthesis inhibitor cycloheximide, and protein levels were measured at different time points (Fig. 3B). MCM5 and MCM7 had a half-life of 24 h in both

TABLE 2. MCM5, MCM7, and PCNA expression in ATC subtypes

| ATC subtype (no. of cases) ^a | MCM5 positivity | MCM7 positivity | PCNA positivity |
|---|-----------------|-----------------|-----------------|
| Pure (33) | 76% (25/33) | 82% (27/33) | 73% (24/33) |
| PTC (14) | 43% (6/14) | 50% (7/14) | 43% (6/14) |
| Hurthle-cell variant of FTC (5) | 60% (3/5) | 80% (4/5) | 80% (4/5) |

^a ATC samples were divided into those showing coexisting WDC (PTC or Hurthle-cell variant of FTC) foci and those not showing coexisting differentiated areas (pure).

ATC and normal cells, which indicates that posttranslational mechanisms were not involved in MCM protein overexpression.

We next measured MCM5 and MCM7 mRNA levels in

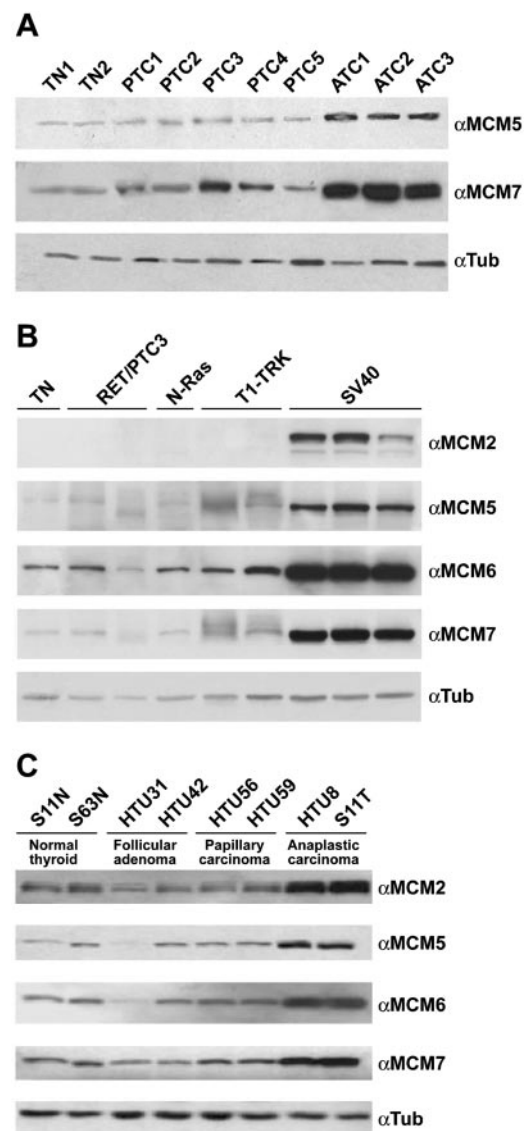


FIG. 2. Equal amounts (50 μ g) of protein extracts from normal thyroid (NT), PTC, and ATC human tissue specimens (A), from normal thyroid tissue, PTC (from RET/PTC3 and TRK-T1 transgenic mice), and ATC [from simian virus 40 (SV40) large T-transgenic mice] mouse tissue specimens (B), and from primary cultures of human thyroid cells (C) were immunoblotted with anti-MCM antibodies. The blots were reprobbed with antitubulin (α Tub) for normalization. The results are representative of at least three independent assays.

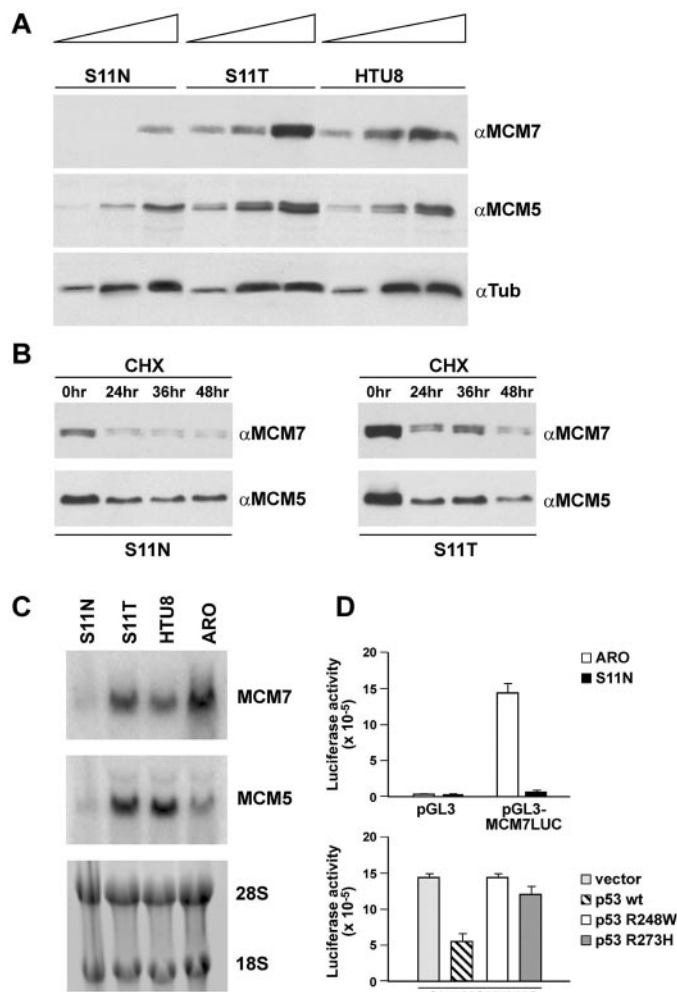


FIG. 3. A, Increasing amounts (10, 20, and 50 μ g) of protein extracts from the indicated cell lines were immunoblotted with anti-MCM7, anti-MCM5, and antitubulin (α Tub) antibodies. B, The indicated primary cell cultures were treated with cycloheximide (CHX) for different time points. Lysates (50 μ g) were run on SDS-PAGE, and MCMs expression levels were determined by immunoblot. C, MCM mRNA levels were determined by Northern blot. 28S and 18S RNA levels were used for normalization. The results are representative of at least three independent assays. D, *Top*, The indicated cell lines were transiently transfected with pGL3-MCM7LUC plasmid or the empty vector; average \pm SD levels of luciferase activity in three independent experiments are reported. *Bottom*, ARO cells were cotransfected with pGL3-MCM7LUC and the indicated plasmids. Relative luciferase activity is reported. Average \pm SD results of three independent assays are reported. wt, Wild type.

normal and ATC cells by Northern blot (Fig. 3C). MCM mRNA levels were higher in ATC than in normal cells. Importantly, the increase in mRNA (\sim 5-fold) was similar to the increase in protein, which indicates that changes at the mRNA level caused the enhanced MCM5 and MCM7 expression. Increased mRNA levels may be due to gene amplification, increased transcription, or, less frequently, an increased mRNA half-life. Amplification of MCM genes has been described in hypopharyngeal carcinomas (30). Hence, we determined the MCM2–MCM7 gene copy number by semiquantitative PCR on genomic DNA in human samples (tissue samples and primary cell cultures) listed in Fig. 2.

There was no gene amplification in any sample (data not shown), which suggests that enhanced MCM expression results from increased transcription.

The human MCM7 gene transcriptional promoter has been characterized (24). To prove our hypothesis, we cloned the MCM7 promoter (-500 to -60 relative to the transcription start site) upstream to the luciferase reporter gene (pGL3-MCM7LUC). The pGL3-MCM7LUC construct (or the empty vector) was transiently transfected in triplicate in S11N and ARO cells, and luciferase activity was measured. The MCM7 promoter displayed a significantly higher (>10 -fold) activity in anaplastic cells compared with normal ones (Fig. 3D, *top*). MCM7 expression is positively controlled by the E2F (E2 promoter binding factor) transcriptional factor (31), and the MCM7 promoter contains binding sites for E2F (24). By stimulating increased levels of the CDK inhibitor p21WAF1, p53 is able to reduce pRb phosphorylation levels and, in turn, E2F transcriptional activity, potentially keeping MCM7 expression under check (32). Thus, increased MCM7 gene transcription in ATC could be due to the inactivation of p53, a genetic hallmark of this tumor type (7, 8). We addressed this possibility by measuring p53 effects on pGL3-MCM7LUC transcription. As shown in Fig. 3D (*bottom*), adoptive overexpression of wild-type p53, but not of two inactive p53 mutants (R248W and R273H), decreased by almost 3-fold pGL3-MCM7LUC activity in ARO cells.

MCM7 overexpression is required for DNA synthesis in ATC cells

In mammalian cells, MCM proteins are present in the nuclei in two forms: one soluble form that can be extracted by non-ionic detergents and one insoluble form (23). The insoluble form is the active one, associated with prereplication chromatin as part of the pre-RC. The soluble form is considered inactive and no longer capable of binding to chromatin. We differentially extracted soluble and insoluble MCM7 from ATC and normal cell nuclei. Although the ratio chromatin-loaded/chromatin-unloaded MCM7 was slightly reduced in ATC with respect to normal cells, the absolute amount of chromatin-bound MCM7 was definitely increased in ATC cells (4-fold by phosphor imaging) (Fig. 4A).

We used two different siRNAs to interfere with MCM7 expression in anaplastic S11T cells. As controls, we used scrambled silencing RNA and siRNAs for lamin. Both MCM7 siRNAs induced a strong reduction of protein levels at 48 h after transfection, whereas control oligonucleotides had no effect (Fig. 4B). Finally, we studied the ability of MCM7-silenced cells to replicate DNA, by measuring BrdU incorporation rate. Decreased MCM7 protein levels reduced the rate of BrdU incorporation by about 50% in S11T cells, which suggests that MCM7 expression is required to sustain the proliferative capacity of ATC cells (Fig. 4B).

Discussion

MCM proteins are required for DNA replication and function (12). Their expression is restricted to proliferating and dedifferentiated tissues and is a typical feature of many malignant and premalignant diseases (16–21). ATC is a very aggressive tumor that has a high proliferation rate and a

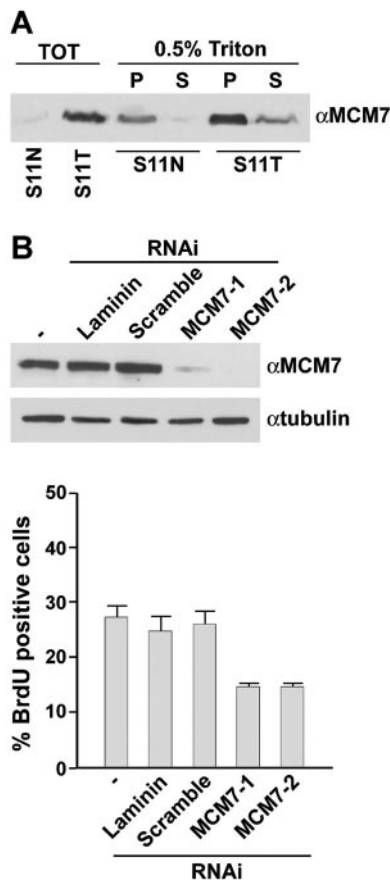


FIG. 4. A, Total (TOT) (50 μ g) and amounts of Triton X-100-soluble (S) and -insoluble (P) protein fractions from comparable cell numbers were immunoblotted with anti-MCM7 antibodies. B, *Top*, S11T cells were mock transfected (–) or transfected with two sets of MCM7 siRNAs or control laminin and scrambled siRNAs. After 48 h, MCM7 protein levels were assessed by immunoblot. Antitubulin was used for normalization. *Bottom*, Forty-eight hours after siRNA transfection, BrdU was added for 1 h, and cells were fixed and processed for immunofluorescence. Anti-BrdU, monitored by a fluorescein isothiocyanate-conjugated antimosue antibody, was used to detect the fraction of cells in S-phase. The average \pm SD results of three independent experiments in which at least 60 cells were counted are reported.

marked genetic instability. Here we show that, in thyroid tumors, MCM overexpression is present only in ATC. Accordingly, we propose that MCM protein overexpression is one of the molecular determinants of this highly mitogenic phenotype of ATC. Differently, PTC are virtually devoid of MCM expression. A corollary of these findings is that an increased mitogenic rate does not play a major role in PTC. It is also conceivable that MCM overexpression may sustain the high genetic instability of ATC. In fact, re-replication is one of the most typical mechanisms of gene copy imbalance in tumor cells, and it has been demonstrated that MCM gain-of-function in yeast promotes DNA replication reinitiation and gene amplification (33).

Our data indicate that increased gene transcription results in MCM overexpression in ATC. This fits nicely with the molecular events described in ATC. Indeed, MCM gene transcription is controlled by the E2F/pRb axis (24, 31), which, in turn, is controlled by p53. p53 stimulates increased levels of the CDK inhibitor p21WAF1, thereby inhibiting pRb phos-

phorylation and blocking E2F transcriptional activity (32). This pathway is probably disrupted in ATC because of their high prevalence of p53 mutations (7, 8). Accordingly, we have shown that the p53-null ARO ATC cells display a high rate of transcription from the MCM7 promoter compared with normal cells and that reintroduction of a wild-type p53 gene into ARO cells decreases the activity of the promoter. The mTOR (mammalian target of rapamycin) and MAPK (mitogen-activated protein kinase) pathways are also known to stimulate MCM expression (34, 35). Both pathways are probably hyperactive in ATC due to gain-of-function mutations in Ras (5), BRAF (6), and AKT/PKB (protein kinase B) (36) and might contribute to MCM up-regulation, as well.

It is the prevailing view that ATC represents a terminal dedifferentiation of a preexisting PTC or FTC. Comparison of the histology of fatal PTC with tumors of patients who survived their disease reveals a high incidence of foci of spindle and giant cell metaplasia that are indicative of transition into ATC (2, 3). Although histologic examination of different samples within the same thyroid tumor is sufficient for diagnostic identification of ATC, MCM testing could be used to identify ATC foci in otherwise well-differentiated carcinomas.

Finally, ATC is refractory to most treatment strategies and is almost always fatal. Current chemotherapeutic agents do not induce consistent beneficial therapeutic responses. Local tumor control with surgery and radiotherapy merely provides palliation and delays death. MCM proteins promote DNA synthesis thanks to their helicase function that is essential for DNA replication fork unwinding (14). Our data raise the possibility of molecular therapy of ATC based on targeting MCM proteins by interfering with their expression or blocking their helicase function with small inhibitors.

Acknowledgments

We are grateful to Dr. J. Dumont for simian virus 40 transgenics, Drs. F. Curcio and H. Zitzelsberger for cell lines, Drs. J. Cameselle-Teijeiro and A. Herrero for providing human ATC, and J. A. Gilder for text editing.

Received December 16, 2004. Accepted May 10, 2005.

Address all correspondence and requests for reprints to: Massimo Santoro, Dipartimento di Biologia e Patologia Cellulare e Molecolare L. Califano, Facoltà di Medicina e Chirurgia, via S. Pansini 5, 80131 Naples, Italy. E-mail: masantor@unina.it.

This study was supported by the Associazione Italiana per la Ricerca sul Cancro, the Progetto Strategico Oncologia of the Consiglio Nazionale delle Ricerche/Ministero dell'Istruzione, dell'Università, e della Ricerca (MIUR), the Italian Ministero per l'Istruzione, Università Ricerca Scientifica (MIUR), the BioGem scar.l. (Biotecnologia e Genetica Molecolare nel Mezzogiorno d'Italia), the Italian Ministero della Salute, and the Naples Oncogenomic Center.

References

- Sherman SI 2003 Thyroid carcinoma. *Lancet* 361:501–511
- McIver B, Hay ID, Giuffrida DF, Dvorak CE, Grant CS, Thompson GB, van Heerden JA, Goellner JR 2001 Anaplastic thyroid carcinoma: a 50-year experience at a single institution. *Surgery* 130:1028–1034
- Ain KB 1999 Anaplastic thyroid carcinoma: a therapeutic challenge. *Semin Surg Oncol* 16:64–69
- Ordóñez N, Baloch Z, Matias-Guiu X, Evans H, Farid NR, Fagin JA, Kitamura Y, Tallini G, Eng C, Haigh PI, Faquin WC, Sugitani I, Giuffrida D, Boerner S 2004 Undifferentiated (anaplastic) carcinoma. In: DeLellis RA, Lloyd RV, Heitz PU, Eng C, eds. *Pathology and genetics of tumours of endocrine organs*

- (IARC/World Health Organization classification of tumors). Lyon: International Agency for Research on Cancer; 77–80
- Garcia-Rostan G, Zhao H, Camp RL, Pollan M, Herrero A, Pardo J, Wu R, Carcangiu ML, Costa J, Tallini G 2003 ras mutations are associated with aggressive tumor phenotypes and poor prognosis in thyroid cancer. *J Clin Oncol* 21:3226–3235
 - Nikiforova MN, Kimura ET, Gandhi M, Biddinger PW, Knauf JA, Basolo F, Zhu Z, Giannini R, Salvatore G, Fusco A, Santoro M, Fagin JA, Nikiforov YE 2003 BRAF mutations in thyroid tumors are restricted to papillary carcinomas and anaplastic or poorly differentiated carcinomas arising from papillary carcinomas. *J Clin Endocrinol Metab* 88:5399–5404
 - Fagin JA, Matsuo K, Karmakar A, Chen DL, Tang SH, Koeffler HP 1993 High prevalence of mutations of the p53 gene in poorly differentiated human thyroid carcinomas. *J Clin Invest* 91:179–184
 - Donghi R, Longoni A, Pilotti S, Michieli P, Della Porta G, Pierotti MA 1993 Gene p53 mutations are restricted to poorly differentiated and undifferentiated carcinomas of the thyroid gland. *J Clin Invest* 91:1753–1760
 - Garcia-Rostan G, Tallini G, Herrero A, D'Aquila TG, Carcangiu ML, Rimm DL 1999 Frequent mutation and nuclear localization of β -catenin in anaplastic thyroid carcinoma. *Cancer Res* 59:1811–1815
 - Wreesmann VB, Ghossein RA, Patel SG, Harris CP, Schnaser EA, Shah AR, Tuttle RM, Shah JP, Rao PH, Singh B 2002 Genome-wide appraisal of thyroid cancer progression. *Am J Pathol* 161:1549–1556
 - Kadota M, Tamaki Y, Sakita I, Komoike Y, Miyazaki M, Ooka M, Masuda N, Fujiwara Y, Ohnishi T, Tomita N, Sekimoto M, Ohue M, Ikeda T, Kobayashi T, Horii A, Monden M 2000 Identification of a 7-cM region of frequent allelic loss on chromosome band 16p13.3 that is specifically associated with anaplastic thyroid carcinoma. *Oncol Rep* 7:529–533
 - Bell SP, Dutta A 2002 DNA replication in eukaryotic cells. *Annu Rev Biochem* 71:333–374
 - Labib K, Tercero JA, Diffley JF 2000 Uninterrupted MCM2–7 function required for DNA replication fork progression. *Science* 288:1643–1647
 - Pacek M, Walter JC 2004 A requirement for MCM7 and Cdc45 in chromosome unwinding during eukaryotic DNA replication. *EMBO J* 23:3667–3676
 - Stoeber K, Tlsty TD, Happerfield L, Thomas GA, Romanov S, Bobrow L, Williams ED, Williams GH 2001 DNA replication licensing and human cell proliferation. *J Cell Sci* 114:2027–2041
 - Williams GH, Romanowski P, Morris L, Madine M, Mills AD, Stoeber K, Marr J, Laskey RA, Coleman N 1998 Improved cervical smear assessment using antibodies against proteins that regulate DNA replication. *Proc Natl Acad Sci USA* 95:14932–14937
 - Freeman A, Morris LS, Mills AD, Stoeber K, Laskey RA, Williams GH, Coleman N 1999 Minichromosome maintenance proteins as biological markers of dysplasia and malignancy. *Clin Cancer Res* 5:2121–2132
 - Williams GH, Swinn R, Prevost AT, De Clive-Lowe P, Halsall I, Going JJ, Hales CN, Stoeber K, Middleton SJ 2004 Diagnosis of oesophageal cancer by detection of minichromosome maintenance 5 protein in gastric aspirates. *Br J Cancer* 91:714–719
 - Meng MV, Grossfeld GD, Williams GH, Dilworth S, Stoeber K, Mulley TW, Weinberg V, Carroll PR, Tlsty TD 2001 Minichromosome maintenance protein 2 expression in prostate: characterization and association with outcome after therapy for cancer. *Clin Cancer Res* 7:2712–2718
 - Stoeber K, Halsall I, Freeman A, Swinn R, Doble A, Morris L, Coleman N, Bullock N, Laskey RA, Hales CN, Williams GH 1999 Immunoassay for urothelial cancers that detects DNA replication protein MCM5 in urine. *Lancet* 354:1524–1525
 - Davies RJ, Freeman A, Morris LS, Bingham S, Dilworth S, Scott I, Laskey RA, Miller R, Coleman N 2002 Analysis of minichromosome maintenance proteins as a novel method for detection of colorectal cancer in stool. *Lancet* 359:1917–1919
 - Hedinger C, Williams ED, Sobin LH 1989 The WHO histological classification of thyroid tumors: a commentary on the ed. 2. *Cancer* 63:908–911
 - Fujita M, Kiyono T, Hayashi Y, Ishibashi M 1997 In vivo interaction of human MCM heterohexameric complexes with chromatin. Possible involvement of ATP. *J Biol Chem* 272:10928–10935
 - Suzuki S, Adachi A, Hiraiwa A, Ohashi M, Ishibashi M, Kiyono T 1998 Cloning and characterization of human MCM7 promoter. *Gene* 216:85–91
 - Battista S, Martelli ML, Fedele M, Chiappetta G, Trapasso F, De Vita G, Battaglia C, Santoro M, Viglietto G, Fagin JA, Fusco A 1995 A mutated p53 gene alters thyroid cell differentiation. *Oncogene* 11:2029–2037
 - Hingorani SR, Jacobetz MA, Robertson GP, Herlyn M, Tuveson DA 2003 Suppression of BRAF(V599E) in human melanoma abrogates transformation. *Cancer Res* 63:5198–5202
 - Ledent C, Dumont J, Vassart G, Parmentier M 1991 Thyroid adenocarcinomas secondary to tissue-specific expression of simian virus-40 large T-antigen in transgenic mice. *Endocrinology* 129:1391–1401
 - Powell Jr DJ, Russell J, Nibu K, Li G, Rhee E, Liao M, Goldstein M, Keane WM, Santoro M, Fusco A, Rothstein JL 1998 The RET/PTC3 oncogene: metastatic solid-type papillary carcinomas in murine thyroids. *Cancer Res* 58:5523–5528
 - Russell JP, Powell DJ, Cunnane M, Greco A, Portella G, Santoro M, Fusco A, Rothstein JL 2000 The TRK-T1 fusion protein induces neoplastic transformation of thyroid epithelium. *Oncogene* 19:5729–5735
 - Cromer A, Carles A, Millon R, Ganguli G, Chalmel F, Lemaire F, Young J, Dembele D, Thibault C, Muller D, Poch O, Abecassis J, Wasylyk B 2004 Identification of genes associated with tumorigenesis and metastatic potential of hypopharyngeal cancer by microarray analysis. *Oncogene* 23:2484–2498
 - Muller H, Bracken AP, Vernell R, Moroni MC, Christians F, Grassilli E, Prosperini E, Vigo E, Oliner JD, Helin K 2001 E2Fs regulate the expression of genes involved in differentiation, development, proliferation, and apoptosis. *Genes Dev* 15:267–285
 - Hickman ES, Moroni MC, Helin K 2002 The role of p53 and pRB in apoptosis and cancer. *Curr Opin Genet Dev* 12:60–66
 - Nguyen VQ, Co C, Li JJ 2001 Cyclin-dependent kinases prevent DNA replication through multiple mechanisms. *Nature* 411:1068–1073
 - Bruemmer D, Yin F, Liu J, Kiyono T, Fleck E, Van Herle AJ, Law RE 2003 Expression of minichromosome maintenance proteins in vascular smooth muscle cells is ERK/MAPK dependent. *Exp Cell Res* 290:28–37
 - Bruemmer D, Yin F, Liu J, Kiyono T, Fleck E, Van Herle AJ, Law RE 2003 Rapamycin inhibits E2F-dependent expression of minichromosome maintenance proteins in vascular smooth muscle cells. *Biochem Biophys Res Commun* 303:251–258
 - Vasko V, Saji M, Hardy E, Kruhlak M, Larin A, Savchenko V, Miyakawa M, Isozaki O, Murakami H, Tsushima T, Burman KD, De Micco C, Ringel MD 2004 Akt activation and localisation correlate with tumour invasion and oncogene expression in thyroid cancer. *J Med Genet* 41:161–170

JCEM is published monthly by The Endocrine Society (<http://www.endo-society.org>), the foremost professional society serving the endocrine community.

Sorafenib Inhibits Imatinib-Resistant KIT and Platelet-Derived Growth Factor Receptor β Gatekeeper Mutants

Teresa Guida,¹ Suresh Anaganti,¹ Livia Provitera,¹ Richard Gedrich,² Elizabeth Sullivan,² Scott M. Wilhelm,² Massimo Santoro,¹ and Francesca Carlomagno¹

Abstract Purpose: Targeting of KIT and platelet-derived growth factor receptor (PDGFR) tyrosine kinases by imatinib is an effective anticancer strategy. However, mutations of the gatekeeper residue (T670 in KIT and T681 in PDGFR β) render the two kinases resistant to imatinib. The aim of this study was to evaluate whether sorafenib (BAY 43-9006), a multitargeted ATP-competitive inhibitor of KIT and PDGFR, was active against imatinib-resistant KIT and PDGFR β kinases.

Experimental Design: We used *in vitro* kinase assays and immunoblot with phosphospecific antibodies to determine the activity of sorafenib on KIT and PDGFR β kinases. We also exploited reporter luciferase assays to measure the effects of sorafenib on KIT and PDGFR β downstream signaling events. The activity of sorafenib on interleukin-3-independent proliferation of Ba/F3 cells expressing oncogenic KIT or its imatinib-resistant T670I mutant was also tested.

Results: Sorafenib efficiently inhibited gatekeeper mutants of KIT and PDGFR β (IC₅₀ for KIT T670I, 60 nmol/L; IC₅₀ for PDGFR β T681I, 110 nmol/L). Instead, it was less active against activation loop mutants of the two receptors (IC₅₀ for KIT D816V, 3.8 μ mol/L; IC₅₀ for PDGFR β D850V, 1.17 μ mol/L) that are also imatinib-resistant. Sorafenib blocked receptor autophosphorylation and signaling of KIT and PDGFR β gatekeeper mutants in intact cells as well as activation of AP1-responsive and cyclin D1 gene promoters, respectively. Finally, the compound inhibited KIT-dependent proliferation of Ba/F3 cells expressing the oncogenic KIT mutant carrying the T670I mutation.

Conclusions: Sorafenib might be a promising anticancer agent for patients carrying KIT and PDGFR β gatekeeper mutations.

The KIT and platelet-derived growth factor receptors (PDGFR) are members of the type III subclass of receptor tyrosine kinases. KIT is the receptor for stem cell factors (SCF), whereas PDGFR α and PDGFR β are the receptors for platelet-derived growth factors (PDGF; ref. 1). The structure of these receptors includes an extracellular domain with five immunoglobulin-like motifs, a single membrane-spanning domain, and a cytoplasmic tyrosine kinase domain. The kinase domain is split by a kinase insert sequence into an ATP-binding region and a phosphotransferase region (1).

Authors' Affiliations: ¹Istituto di Endocrinologia ed Oncologia Sperimentale del CNR, c/o Dipartimento di Biologia e Patologia Cellulare e Molecolare, Università di Napoli Federico II, Naples, Italy and ²Bayer HealthCare Pharmaceuticals, West Haven, Connecticut

Received 11/7/06; revised 2/23/07; accepted 3/20/07.

Grant support: Associazione Italiana per la Ricerca sul Cancro, by grants from Ministero della Salute and Ministero dell'Università e della Ricerca, and by a grant from Bayer HealthCare Pharmaceuticals. S. Anaganti was a recipient of a fellowship sponsored by the Terry Fox Foundation, Naples.

The costs of publication of this article were defrayed in part by the payment of page charges. This article must therefore be hereby marked *advertisement* in accordance with 18 U.S.C. Section 1734 solely to indicate this fact.

Requests for reprints: Massimo Santoro, Dipartimento di Biologia e Patologia Cellulare e Molecolare, Università di Napoli Federico II, via S. Pansini 5, 80131 Naples, Italy. Phone: 39-81746-3056; Fax: 39-81746-3037; E-mail: masantor@unina.it.

© 2007 American Association for Cancer Research.
doi:10.1158/1078-0432.CCR-06-2667

KIT, PDGFR α , and PDGFR β are frequently activated in neoplastic diseases. More than 30 gain-of-function mutations in KIT, either single amino acid changes or small deletions/insertions, have been identified in such highly malignant human neoplastic diseases as gastrointestinal stromal tumors (GIST) and mastocytosis. GISTs are the most common type of sarcoma arising in the digestive tract and are generally distinguished from other abdominal sarcomas by the expression of KIT. Approximately 80% of these tumors show activating mutations in KIT (2). GIST mutations cluster in the KIT juxtamembrane region, whereas most mutations associated with mastocytosis target a specific aspartate residue (D816) in the kinase activation loop (3). Fusion of PDGFR α with different genes has been found in chronic myeloid leukemia and in hypereosinophilic syndrome (4). Moreover, GIST cases that are negative for KIT mutations almost invariably display activating point mutations in the juxtamembrane domain or in the activation loop of PDGFR α (5). The closely related PDGFR β receptor is often activated by rearrangements in chronic myelomonocytic leukemia (6).

Imatinib (imatinib mesylate, STI571; Gleevec or Glivec) is an ATP-competitive inhibitor that has revolutionized drug therapy of chronic myeloid leukemia. Imatinib is very effective [*in vitro* half-maximal inhibitory concentration (IC₅₀) of 25 nmol/L] against the chronic myeloid leukemia-causing kinase BCR-ABL (7). It also efficiently inhibits KIT (*in vitro* IC₅₀, 410 nmol/L) and PDGFR (*in vitro* IC₅₀, 380 nmol/L). Consequently, it has

been successful in the treatment of cancer patients carrying activating KIT or PDGFR mutations (2, 5, 7). In clinical studies, 75% to 90% of patients with advanced GISTs treated with imatinib experienced a clinical benefit (7).

However, KIT and PDGFR α variants carrying mutations in the kinase activation loop (D816 in KIT; refs. 8, 9; and D842 in PDGFR α ; ref. 5, which corresponds to D850 in PDGFR β) are refractory to imatinib. Therefore, mastocytosis (KIT) and GIST (KIT or PDGFR α) patients with these mutations respond poorly to imatinib (2, 5). X-ray analysis has shown that imatinib binds preferentially to the inactive form of the kinase. It is conceivable that these mutations disrupt the kinase structure and so disable interaction with the drug (10). Moreover, some patients who initially respond to imatinib subsequently relapse. This secondary resistance usually results from the emergence of tumor clones with mutations in the kinase domain that prevent drug binding. In particular, some mutations in KIT (T670I; refs. 11–14) or PDGFR (T674I in PDGFR α and T681I in PDGFR β) cause imatinib resistance (15–17). These mutations correspond to the Thr³¹⁵-to-isoleucine substitution (T315I) in BCR-ABL that frequently causes resistance in patients with chronic myeloid leukemia. Given its role in controlling the susceptibility of kinases to drug inhibition, this particular residue has been designated as a “gatekeeper.” The gatekeeper threonine interacts with imatinib via a hydrogen bond. It seems that its replacement with a large bulky amino acid (isoleucine) prevents the drug-kinase interaction (10). Other mutations in KIT and PDGFR have been reported to cause secondary resistance and these include mutations of D816 in KIT and D842 in PDGFR α (2).

Sorafenib, also known as BAY43-9006, is a multikinase inhibitor of the bi-aryl-urea chemical class (18). It targets the RAF family of serine/threonine kinases and the tyrosine kinase receptors VEGFR-2 (KDR), VEGFR-3 (Flt-4), Flt-3, PDGFR, and KIT (19). Sorafenib is undergoing advanced clinical trials and has been recently Food and Drug Administration–approved under the name of Nexavar for the treatment of advanced renal cell carcinoma (18). We recently showed that sorafenib is a potent inhibitor of the wild-type and mutant RET kinase. Importantly, sorafenib also inhibited RET gatekeeper mutants (V804M/L; ref. 20). Here, we have investigated the activity of sorafenib against imatinib-resistant KIT and PDGFR β mutants.

Materials and Methods

Compounds. Sorafenib [BAY 43-9006, *N*-(3-trifluoromethyl-4-chlorophenyl)-*N'*-(4-[2-methylcarbamoyl pyridin-4-yl]oxyphenyl) urea], was provided by Bayer HealthCare Pharmaceuticals. The compound was dissolved in DMSO.

Plasmids. pCMV-KIT, encoding wild-type mouse KIT, and pcDNA 3.1-PDGFR β , encoding wild-type human PDGFR β (21), were kindly donated by C. Sette (Dept. Sanita' Pubblica e Biologie Cellulare, Universita' di Roma, Rome, Italy) and C.H. Heldin (Ludwig Institute for Cancer Research, Uppsala University, Uppsala, Sweden), respectively. PDGFR β T681I and D850V mutants and KIT T670I and KIT D814V mutants were generated by site-directed mutagenesis. All the mutations were confirmed by double-strand DNA sequencing. Because the mouse KIT D814V mutation corresponds to the human KIT D816V, for the sake of clarity, this mutant is called KIT D816V throughout this article.

Antibodies. Antibodies to KIT and PDGFR β were as follows: KIT (Cell Signaling Technologies), phospho-KIT (pY721; Biosource, Invitrogen Corporation), PDGFR β (Santa Cruz Biotechnology) and phospho-

PDGFR β (pY1021; Santa Cruz Biotechnology). Antibodies to SHC were from Upstate Biotechnology, Inc., antibodies to phospho-SHC (which recognize phosphorylated SHC at Y317) were from Santa Cruz Biotechnology, antibodies to mitogen-activated protein kinases (MAPK) were from Cell Signaling Technologies, and antibodies to phospho-p44/42 MAPK (pMAPK), specific for MAPK (ERK1/2) phosphorylated at Thr²⁰²/Tyr²⁰⁴, were from Cell Signaling Technologies. Monoclonal anti- α -tubulin was from Sigma Chemical, Co. Secondary antibodies coupled to horseradish peroxidase were from Santa Cruz Biotechnology.

Cell cultures and luciferase assays. HEK293 cells were from the American Type Culture Collection and were grown in DMEM supplemented with 10% FCS, 2 mmol/L of L-glutamine, and 100 units/mL of penicillin-streptomycin (Life Technologies). NIH3T3 fibroblasts were cultured in DMEM supplemented with 10% calf serum, 2 mmol/L of L-glutamine, and 100 units/mL of penicillin-streptomycin. HeLa cells were grown in DMEM supplemented with 10% FCS, 2 mmol/L of L-glutamine, and 100 units/mL of penicillin-streptomycin.

Transient transfections were carried out with the LipofectAMINE reagent according to the manufacturer's instructions (Life Technologies). HeLa cells (1×10^6) were transiently transfected with vectors expressing KIT wt, KIT T670I and KIT D816V, and the AP1-luciferase vector (Stratagene) containing six AP1-binding sites upstream from the Firefly luciferase cDNA. Twenty-four hours after transfection, cells were serum-starved and 100 ng/mL of SCF (Prepotech) was added to the KIT wt and KIT T670I-transfected cells. NIH3T3 mouse fibroblasts (1×10^6) were transiently transfected with vectors expressing PDGFR β wt, PDGFR β T681I, or PDGFR β D850V, and with the cyclin D1-luciferase vector (22) containing -1,745 bp of the human cyclin D1 promoter upstream from the Firefly luciferase cDNA. This vector was kindly provided by S.J. Gutkind (NIH, Bethesda, MD). Twenty-four hours after transfection, cells were serum-starved and 100 ng/mL of PDGF BB (Prepotech) were added to PDGFR β wt and PDGFR β T681I-transfected cells. Ten nanograms of pRL-null (a plasmid expressing the enzyme Renilla luciferase from *Renilla reniformis*) was used as an internal control. Firefly and Renilla luciferase activities were assayed using the Dual-Luciferase Reporter System (Promega Corporation). Light emission was quantitated using a Berthold Technologies luminometer (Centro LB 960) and expressed as a percentage of residual activity compared with untreated cells. Average results of three independent assays \pm SD are indicated. Student's *t* test was used to assess statistical significance.

Stable pools of Ba/F3 cells expressing KIT Δ 557-558 or the imatinib-resistant Δ 557-558/T670I double mutant were selected for interleukin-3 (IL-3)-independent and G418-resistant growth.³ Cells were maintained in RPMI 1640 supplemented with 10% fetal bovine serum with or without IL-3 culture supplement (BD Biosciences). For cell proliferation assays, Ba/F3 cells were plated in complete medium with or without IL-3 and different doses of sorafenib. After 72 h, cell growth was evaluated by measuring luminescence with a CellTiter-Glo kit (Promega Corporation). Average IC₅₀ (nmol/L) of the compound for Ba/F3 cellular proliferation was calculated by using linear regression methods (GraphPad Software Inc.) from at least three experiments (minus IL-3: *n* > 3; plus IL-3: *n* = 3) and was reported means \pm SE.

Protein studies. Immunoblotting experiments were done according to standard procedures. Briefly, cells were harvested in lysis buffer [50 mmol/L Hepes (pH 7.5), 150 mmol/L NaCl, 10% glycerol, 1% Triton X-100, 1 mmol/L EGTA, 1.5 mmol/L MgCl₂, 10 mmol/L NaF, 10 mmol/L sodium PPi, 1 mmol/L Na₃VO₄, 10 μ g of aprotinin/mL, 10 μ g of leupeptin/mL] and clarified by centrifugation at 10,000 \times *g*. Protein concentrations were estimated with a modified Bradford assay (Bio-Rad). Antigens were revealed by an enhanced chemiluminescence detection kit (Amersham Pharmacia Biotech). Signal intensity was evaluated with the PhosphorImager (Typhoon 8600, Amersham Pharmacia Biotech) interfaced with the ImageQuant software.

For the *in vitro* KIT (23) and PDGFR β (21) kinase assays, proteins (500 μ g) were immunoprecipitated with the required antibodies.

³ Gedrich R. and Sullivan E., unpublished data.

Immunocomplexes were recovered with protein A Sepharose beads, washed five times with kinase buffer, and subjected to *in vitro* autophosphorylation by incubating (20 min at room temperature) the immunocomplex with kinase buffer, 2.5 μCi [γ - ^{32}P]ATP, unlabeled ATP (20 $\mu\text{mol/L}$), and the indicated concentrations of the compound. Samples were separated by SDS-PAGE; gels were dried and exposed to autoradiography. Signal intensity was analyzed with the PhosphorImager (Typhoon 8600) interfaced with the ImageQuant software. The average results of three experiments done in duplicate \pm SD are reported. Kinase activity curves were plotted with the curve-fitting PRISM software (GraphPad InStat Software).

Statistical analysis. Two-tailed unpaired Student's *t* test (normal distributions and equal variances) were used for statistical analysis. Differences were significant at $P < 0.02$. Statistical analyses were done using the GraphPad InStat Software program (version 3.06.3).

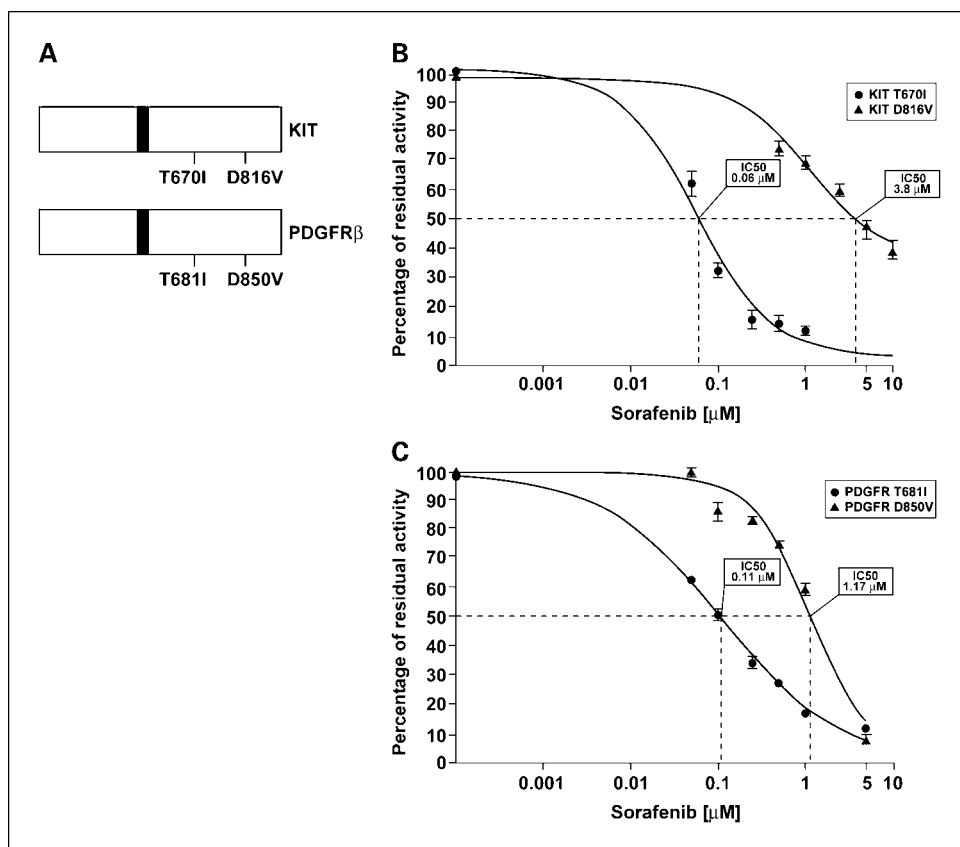
Results

Sorafenib activity on KIT and PDGFR β kinases. The IC_{50} of sorafenib for KIT and PDGFR β was 68 and 57 nmol/L, respectively (19). We tested if sorafenib inhibits imatinib-resistant KIT and PDGFR β kinases that have mutations in the gatekeeper residue (KIT T670I and PDGFR β T681I) or in the activation loop (KIT D816V and PDGFR β D850V; Fig. 1A). In an immunocomplex kinase assay, we measured KIT T670I and KIT D816V proteins' autophosphorylation *in vitro* in the presence of different sorafenib concentrations. The drug strongly inhibited the T670I KIT gatekeeper mutant (IC_{50} , 60 nmol/L), but it was less active on the D816V activation loop mutant (IC_{50} , 3.8 $\mu\text{mol/L}$; Fig. 1B). An *in vitro* kinase assay with a GST-KIT (TK) recombinant protein carrying the D816V mutation confirmed these findings (data not shown). Also, the

PDGFR β gatekeeper mutant (T681I) was potently inhibited by sorafenib *in vitro* (IC_{50} , 110 nmol/L). Similar to the D816V KIT mutant, the PDGFR β activation loop mutant (D850V) was less efficiently inhibited (IC_{50} , 1.17 $\mu\text{mol/L}$; Fig. 1C).

Next, we tested the inhibitory effects of sorafenib on KIT and PDGFR β autophosphorylation in intact cells. HEK293 cells were transiently transfected with either wild-type, gatekeeper, or activation loop mutant receptors. Transfected cells were treated with different doses (0.1, 0.5, and 1 $\mu\text{mol/L}$) of the compound for 2 h. Because they did not display detectable basal phosphorylation levels, cells expressing wild-type or gatekeeper mutant receptors were stimulated with 100 ng/mL of the specific ligand (SCF for KIT or PDGF BB for PDGFR β) for 10 min before harvesting. Consistent with their oncogenic properties, activation loop mutants displayed constitutive kinase activity and did not require ligand stimulation (1). Receptor activation was monitored by Western blotting with specific phospho-KIT (pY721) and phospho-PDGFR β (pY1021) antibodies. Relative phosphorylation levels in compound-treated compared with vehicle-treated cells were calculated with PhosphorImager. Sorafenib was very effective in blocking wild-type KIT and PDGFR β phosphorylation (Fig. 2). At the 100 nmol/L dose, the compound blocked receptor phosphorylation by >90%. Moreover, gatekeeper mutants were very sensitive to sorafenib (100 nmol/L sorafenib blocked KIT T670I and PDGFR β T681I receptor phosphorylation in intact cells by 80%; Fig. 2). Instead, the drug was clearly less active against the activation loop mutants: 1 $\mu\text{mol/L}$ of sorafenib inhibited KIT D816V and PDGFR β D850V by \sim 70%, whereas the inhibitory effect at 100 nmol/L was barely detectable.

Fig. 1. Effect of sorafenib on the *in vitro* kinase activity of KIT and PDGFR β gatekeeper and activation loop mutants. **A**, the KIT and PDGFR β mutants studied. Black bars, the transmembrane domain. **B**, HEK293 cells were transiently transfected with CMV-6 vectors expressing KIT T670I and KIT D816V mutants. KIT proteins were immunoprecipitated (500 μg) and subjected to *in vitro* autophosphorylation. Signal intensity was analyzed with PhosphorImager. The average results of three experiments done in duplicate \pm SD are plotted with the curve-fitting PRISM software. The IC_{50} for each protein is indicated. **C**, HEK293 cells were transiently transfected with pcDNA 3.1 vectors encoding PDGFR β T681I and D850V mutants. Proteins were immunoprecipitated (500 μg) and subjected to *in vitro* autophosphorylation assay. Reactions were processed as described above.



Sorafenib activity on KIT and PDGFR β signaling. Then, we investigated whether sorafenib intercepts KIT and PDGFR β downstream signaling. Ligand-stimulation of HEK293 cells adoptively expressing wild-type KIT and PDGFR β or their gatekeeper mutant-induced SHC adaptor protein and MAPK phosphorylation (ref. 24; Fig. 3). The activation loop mutants of KIT and PDGFR β also induced SHC and MAPK phosphorylation and did not require ligand triggering because of their constitutive kinase activity (Fig. 3). Treatment of cells with different doses of sorafenib strongly inhibited wild-type and gatekeeper mutant-dependent SHC and MAPK phosphorylation. In contrast, stimulation of SHC and MAPK phosphorylation by the activation loop mutants was less efficiently blocked by sorafenib; in this case, marked inhibition was seen only at a concentration of 1 μ mol/L (Fig. 3).

The effects of sorafenib on KIT and PDGFR β transcriptional activity. In a first set of experiments, we noted that KIT activation triggered the transcription of a luciferase reporter downstream from an AP1-responsive promoter in NIH3T3 murine fibroblasts and that PDGFR β was a potent activator of a cyclin D1 promoter in HeLa cells. For PDGFR β , we could not use NIH3T3 cells because fibroblasts express endogenously high levels of the receptor (data not shown). Thus, we evaluated whether sorafenib blocked receptor activity on these promoters. The AP1-luciferase reporter activity was hindered when KIT and KIT T670I cells were treated for 24 h with 0.1, 0.5, and 1 μ mol/L of sorafenib (~10-fold reduction at 1 μ mol/L; $P < 0.02$; Fig. 3C). Similarly, cyclin D1-luciferase promoter activity was inhibited when PDGFR β and PDGFR β

T681I cells were treated with 0.1, 0.5, and 1 μ mol/L of sorafenib (~40-fold reduction at 1 μ mol/L; $P < 0.02$; Fig. 3D). Although sorafenib was less active on the activation loop mutants of the two receptors, it still exerted a significant inhibitory activity at 1 μ mol/L (~2-fold reduction of KIT D816V and ~7-fold reduction of PDGFR β D850V) and some activity at 0.5 μ mol/L (1.5-fold reduction for KIT D816V and 4-fold reduction for PDGFR β D850V; $P < 0.02$; Fig. 3C and D).

The effects of sorafenib on KIT mitogenic activity. The murine pro-B cell line Ba/F3 requires the cytokine IL-3 for proliferation and survival. Expression of constitutively active KIT mutants confers IL-3-independent growth to Ba/F3 cells (25). Thus, Ba/F3 cells were transfected with plasmids expressing either the imatinib-sensitive oncogenic KIT mutant containing a deletion of residues 557 to 558 (Δ 557-558) in the juxta-membrane domain or the imatinib-insensitive KIT double mutant containing both the Δ 557-558 and the T670I mutations (3). In the absence of IL-3, sorafenib potently inhibited the growth of both the Δ 557-558 and Δ 557-558/T670I KIT-expressing cells (Table 1). The compound had virtually no effect on the proliferation of parental or Ba/F3-transfected cells grown in the presence of IL-3, indicating that the antiproliferative effects of the compound were selective and dependent on activated KIT signaling (Table 1).

Discussion

Here we show that sorafenib targets a number of mutant KIT and PDGFR β kinases. Thus, based on its advanced clinical

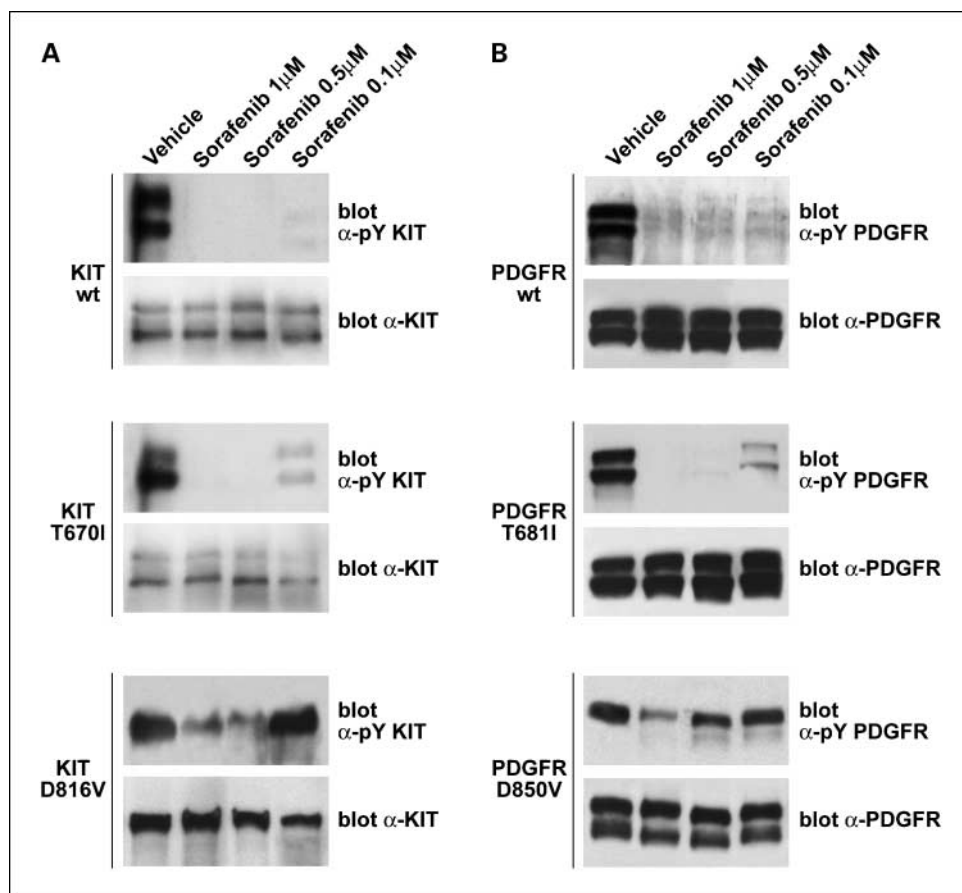


Fig. 2. Effect of sorafenib on KIT and PDGFR β gatekeeper and activation loop mutants in intact cells. HEK293 cells were transfected with vectors expressing KIT, KIT T670I, KIT D816V (A), or PDGFR β , PDGFR β T681I, and PDGFR β D850V (B). Twenty-four hours after transfection, cells were serum-starved. Two hours before being harvested, cells were treated with the indicated concentration of sorafenib. KIT wt and KIT T670I-transfected cells were stimulated with 100 ng/mL of SCF for 10 min, whereas PDGFR β wt and PDGFR β T681I-transfected cells were stimulated with 100 ng/mL of PDGF BB for 10 min. Cell lysates were analyzed by immunoblot with the antibodies to KIT, phospho-KIT (pY KIT), PDGFR β (PDGFR β) and phospho-PDGFR β (pY PDGFR β). A, proteins (0.5 mg) were immunoprecipitated with anti-KIT before being subjected to immunoblot (top and middle). Each experiment is representative of at least three independent experiments. Signal intensity was analyzed with PhosphorImager. Relative phosphorylation levels compared with vehicle-treated cells were calculated.

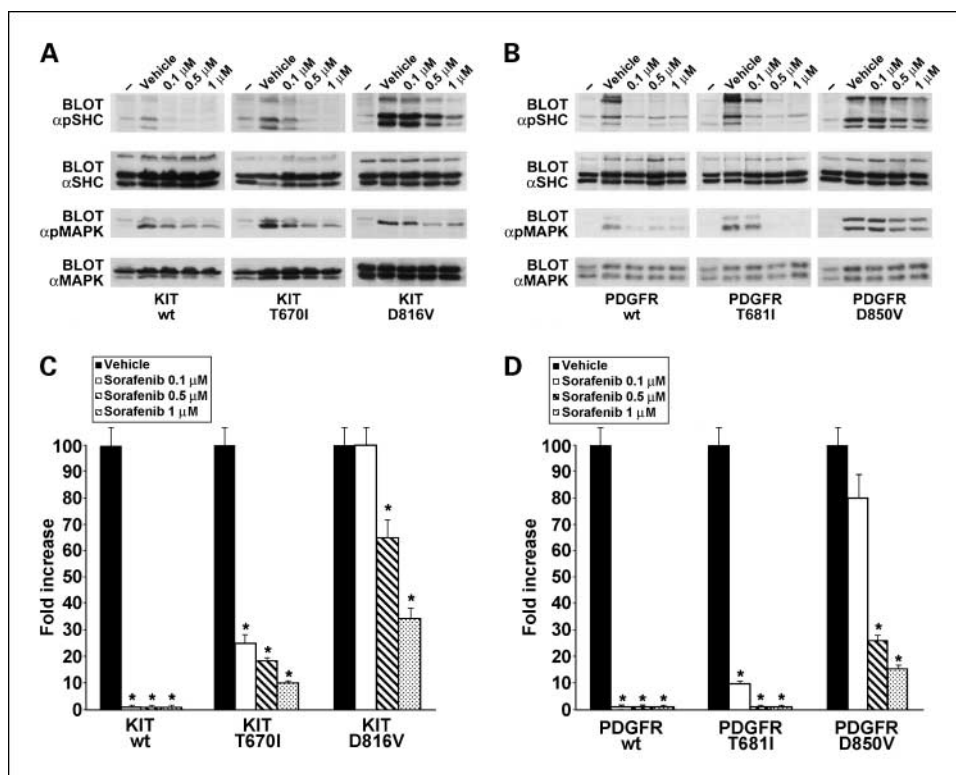


Fig. 3. Effect of sorafenib on KIT and PDGFR β intracellular signaling. HEK293 cells were transfected with vectors expressing KIT wt, KIT T670I, KIT D816V (A), PDGFR β wt, PDGFR β T681I, and PDGFR β D850V (B). Twenty-four hours after transfection, cells were serum-starved. Two hours before being harvested, cells were treated with the indicated concentration of sorafenib, and KIT wt and KIT T670I-transfected cells were then stimulated with 100 ng/mL of SCF for 10 min, whereas PDGFR β wt and PDGFR β T681I-transfected cells were stimulated with 100 ng/mL of PDGF BB for 10 min. Cell lysates were analyzed by immunoblot with antibodies to SHC, phospho-SHC (*pSHC*), MAPK, and phospho-p44/42 MAPK (*pMAPK*). Each experiment is representative of at least three experiments. C, NIH3T3 cells (1×10^6) were transiently transfected with vectors expressing KIT wt, KIT T670I, and KIT D816V, and the AP1-luciferase vector. Twenty-four hours after transfection, cells were serum-starved and 100 ng/mL of SCF was added to the KIT wt and KIT T670I-transfected cells. D, HeLa cells (1×10^6) were transiently transfected with vectors expressing PDGFR β wt, and PDGFR β T681I- and PDGFR β D850V, and with the cyclin D1-luciferase vector. Twenty-four hours after transfection, cells were serum-starved and 100 ng/mL of PDGF BB were added to PDGFR β wt and PDGFR β T681I-transfected cells. The drug was added 24 h before harvesting at the indicated concentrations. Luciferase activity is expressed as a percentage of residual activity compared with cells that had not been treated with sorafenib. Columns, average results of three independent assays; bars, SD; *, $P < 0.02$, Student's *t* test was used to assess statistical significance (vehicle versus treatment).

development, sorafenib may be effective in the treatment of cancer driven by KIT or PDGFR mutations. We also show that sorafenib is less active against the activation loop mutants of KIT and PDGFR β (D816V in KIT and D850V in PDGFR β) than against wild-type and gatekeeper mutants (T670 in KIT and T681 in PDGFR β) of the two receptors. Nevertheless, in intact cells, we observed the inhibition of activation loop mutants at concentrations between 0.5 and 1.0 $\mu\text{mol/L}$. Whatever the mechanism, such an increase in potency in cellular assays with

respect to *in vitro* kinase activity warrants further investigation to verify whether sorafenib could also be used to inhibit these mutants in a clinical setting.

Noteworthy, other compounds proved their efficacy against KIT or PDGFR activation loop mutants. These included dasatinib (BMS-354825), a small molecule inhibitor of SRC and ABL tyrosine kinases (26); PKC412, a staurosporine-derived tyrosine kinase inhibitor that targets protein kinase C; VEGFR-2, FLT-3, PDGFR and KIT (15, 27), and EXEL-0862,

Table 1. Sorafenib inhibits growth of Ba/F3 cell expressing the imatinib-resistant $\Delta 557$ -558/T670I KIT gatekeeper double mutant

| Compound | Ba/F3 cells* | | | | |
|--------------------------------|-------------------|-------------------|-------------------------|-------------------|-------------------|
| | $\Delta 557$ -558 | | $\Delta 557$ -558/T670I | | Parental |
| | -IL-3 | +IL-3 | -IL-3 | +IL-3 | +IL-3 |
| Sorafenib (IC_{50}) | 6 \pm 1 | 4,920 \pm 1,070 | 14 \pm 2 | 5,940 \pm 1,920 | 6,400 \pm 1,360 |

*Parental Ba/F3 cells or cells expressing KIT D557-558 or the imatinib-resistant D557-558/T670I double mutant were plated in complete medium with or without IL-3 and different doses of sorafenib. After 72 h, cell growth was evaluated by measuring luminescence with a CellTiter-Glo kit. Average IC_{50} (nmol/L) for Ba/F3 cellular proliferation was calculated by using linear regression method (GraphPad Software, Inc.) from at least three experiments (minus IL-3: $n > 3$; plus IL-3: $n = 3$) and is reported as means \pm SE.

Table 2. Inhibitory concentration of various TKIs against KIT and PDGFR imatinib-resistant mutants

| Mutants | Receptor | Sorafenib (nmol/L) | Dasatinib (nmol/L) | PKC412 (nmol/L) | EXEL-0862 (nmol/L) | SU-11248 (nmol/L) |
|-----------------|----------|--------------------|--------------------|-----------------|--------------------|-------------------|
| Gatekeeper | KIT | 60 | 10,000 (26) | 100 (35) | Not reported | 70 (33) |
| | PDGFR | 110 | Not reported | 50 (15) | Not reported | Not reported |
| Activation loop | KIT | 3,800 | 1-100 (26) | 44 (27) | 42 (28) | Not reported |
| | PDGFR | 1,170 | Not reported | 50 (39) | Not reported | >1,000 (34) |

a novel kinase inhibitor active against fibroblast growth factor receptors, VEGFRs, PDGFR, FLT3, and KIT (Table 2; ref. 28).

On the other hand, gatekeeper mutation induces resistance to many inhibitors, rendering the identification of second-line treatments quite difficult (29–31). Although other strategies have been envisaged to counteract the activity of these mutants, such as the use of the heat shock protein 90 inhibitor 17-allylamino-18-demethoxy-geldanamycin (32), compounds able to inhibit gatekeeper mutants are urgently needed to provide a solution to the challenge of molecular resistance due to secondary mutations at this site. Thus far, only a few compounds have been reported to be active on these mutants. SU-11248 was found to inhibit the KIT T670I kinase (33, 34) and PKC412 inhibited both KIT and PDGFR gatekeeper mutants (Table 2; refs. 15, 35). Our data indicate that sorafenib is active against KIT and PDGFR gatekeeper mutations. Indeed, these mutants were efficiently inhibited at a drug concentration (60 nmol/L for KIT T670I and 110 nmol/L for PDGFR β T681I) that is well below the average plasma concentration of the drug. Pharmacokinetic studies have shown that on multiple oral doses of 400 mg b.i.d., the C_{max} value of sorafenib was 9.35 mg/L, which corresponds to a concentration of ~ 20 μ mol/L. Up to 99% of the drug is bound to serum proteins leading to an unbound concentration of the drug of ~ 200 nmol/L (36).

Consistent with our findings, Lierman and coworkers have recently shown that FIPL1-PDGFR α , the oncogenic rearrangement of PDGFR α , another PDGFR family member, found in HES (patients with idiopathic hypereosinophilic syndrome), and its T674I gatekeeper mutant are efficiently inhibited by sorafenib (37).

In conclusion, our study suggests that sorafenib might be a useful therapeutic agent to treat tumors harboring the imatinib-resistant KIT T670I or PDGFR T681I mutants. In the chronic myeloid leukemia model, it has been reported that the combination of imatinib with an inhibitor of imatinib-resistant BCR-ABL mutants can be used to prevent the emergence of resistance (38). Similarly, the combination of sorafenib with imatinib might be envisaged to reduce the risk of the emergence of treatment-resistant neoplastic clones harboring KIT or PDGFR mutants.

Acknowledgments

We thank S.J. Gutkind for providing the CycD1-LUC reporter, C. Sette for providing pCMV-KIT, and C.H. Heldin for the PDGFR β . We also thank Ciotola Presentation for the artwork and Jean A. Gilder for text editing. R. Gedrich, E. Sullivan, and S.M. Wilhelm are employees of Bayer Health Care and own stock in Bayer.

References

- Fletcher JA. Role of KIT and platelet-derived growth factor receptors as oncoproteins. *Semin Oncol* 2004; 31:4–11.
- Heinrich MC, Corless CL, Blanke CD, et al. Molecular correlates of imatinib resistance in gastrointestinal stromal tumors. *J Clin Oncol* 2006;24:4764–74.
- Lennartsson J, Jelacic T, Linnekin D, Shivakrupa R. Normal and oncogenic forms of the receptor tyrosine kinase kit. *Stem Cells* 2005;23:16–43.
- Cools J, DeAngelo DJ, Gotlib J, et al. A tyrosine kinase created by fusion of the PDGFRA and FIP1L1 genes as a therapeutic target of imatinib in idiopathic hypereosinophilic syndrome. *N Engl J Med* 2003;348:1201–14.
- Corless CL, Schroeder A, Griffith D, et al. PDGFRA mutations in gastrointestinal stromal tumors: frequency, spectrum and *in vitro* sensitivity to imatinib. *J Clin Oncol* 2005;23:5357–64.
- Steer EJ, Cross NC. Myeloproliferative disorders with translocations of chromosome 5q31–35: role of the platelet-derived growth factor receptor β . *Acta Haematol* 2002;107:113–22.
- Druker BJ. Circumventing resistance to kinase-inhibitor therapy. *N Engl J Med* 2006;354:2594–6.
- Frost MJ, Ferrao PT, Hughes TP, Ashman LK. Juxta-membrane mutant V560GKit is more sensitive to imatinib (STI571) compared with wild-type c-kit whereas the kinase domain mutant D816VKit is resistant. *Mol Cancer Ther* 2002;1:1115–24.
- MaY, Zeng S, Metcalfe DD, et al. The c-KIT mutation causing human mastocytosis is resistant to STI571 and other KIT kinase inhibitors; kinases with enzymatic site mutations show different inhibitor sensitivity profiles than wild-type kinases and those with regulatory-type mutations. *Blood* 2002;99:1741–4.
- Schindler T, Bornmann W, Pellicena P, Miller WT, Clark B, Kuriyan J. Structural mechanism for STI-571 inhibition of Abelson tyrosine kinase. *Science* 2000;289:1938–42.
- Tamborini E, Bonadiman L, Greco A, et al. A new mutation in the KIT ATP pocket causes acquired resistance to imatinib in a gastrointestinal stromal tumor patient. *Gastroenterology* 2004;127:294–9.
- Chen LL, Sabripour M, Andtbacka RH, et al. Imatinib resistance in gastrointestinal stromal tumors. *Curr Oncol Rep* 2005;7:293–9.
- Tamborini E, Pricl S, Negri T, et al. Functional analyses and molecular modeling of two c-Kit mutations responsible for imatinib secondary resistance in GIST patients. *Oncogene* 2006;25:6140–6.
- Wardelmann E, Merkelbach-Bruse S, Pauls K, et al. Polyclonal evolution of multiple secondary KIT mutations in gastrointestinal stromal tumors under treatment with imatinib mesylate. *Clin Cancer Res* 2006; 12:1743–9.
- Cools J, Stover EH, Boulton CL, et al. PKC412 overcomes resistance to imatinib in a murine model of FIP1L1-PDGFR α -induced myeloproliferative disease. *Cancer Cell* 2003;3:459–69.
- Blencke S, Zech B, Engkvist O, et al. Characterization of a conserved structural determinant controlling protein kinase sensitivity to selective inhibitors. *Chem Biol* 2004;11:691–701.
- Bohmer FD, Karagoyozov L, Uecker A, et al. A single amino acid exchange inverts susceptibility of related receptor tyrosine kinases for the ATP site inhibitor STI-571. *J Biol Chem* 2003;278:5148–55.
- Wilhelm S, Carter C, Lynch M, et al. Discovery and development of sorafenib: a multikinase inhibitor for treating cancer. *Nat Rev Drug Discov* 2006;5:835–44.
- Wilhelm SM, Carter C, Tang L, et al. BAY 43–9006 exhibits broad spectrum oral antitumor activity and targets the RAF/MEK/ERK pathway and receptor tyrosine kinases involved in tumor progression and angiogenesis. *Cancer Res* 2004;64:7099–109.
- Carlomagno F, Anaganti S, Guida T, et al. BAY 43–9006 inhibition of oncogenic RET mutants. *J Natl Cancer Inst* 2006;98:326–34.
- Claesson-Welsh L, Eriksson A, Moren A, et al. cDNA cloning and expression of a human platelet-derived growth factor (PDGF) receptor specific for B-chain-containing PDGF molecules. *Mol Cell Biol* 1988;8:3476–86.
- Vitagliano D, Carlomagno F, Motti ML, et al. Regulation of p27Kip1 protein levels contributes to mitogenic effects of the RET/PTC kinase in thyroid carcinoma cells. *Cancer Res* 2004;64:3823–9.
- Tatton L, Morley GM, Chopra R, Khwaja A. The Src-selective kinase inhibitor PPI also inhibits Kit and Bcr-Abl tyrosine kinases. *J Biol Chem* 2003;278: 4847–53.
- Schlessinger J. Cell signaling by receptor tyrosine kinases. *Cell* 2000;103:211–25.
- Kitayama H, Kanakura Y, Furitsu T, et al. Constitutively activating mutations of c-kit receptor tyrosine kinase confer factor-independent growth and tumorigenicity

- of factor-dependent hematopoietic cell lines. *Blood* 1995;85:790–8.
26. Schittenhelm MM, Shiraga S, Schroeder A, et al. Dasatinib (BMS-354825), a dual SRC/ABL kinase inhibitor, inhibits the kinase activity of wild-type, juxta-membrane, and activation loop mutant KIT isoforms associated with human malignancies. *Cancer Res* 2006;66:473–81.
27. Growney JD, Clark JJ, Adelsperger J, et al. Activation mutations of human c-KIT resistant to imatinib mesylate are sensitive to the tyrosine kinase inhibitor PKC412. *Blood* 2005;106:721–4.
28. Pan J, Quintas-Cardama A, Kantarjian HM, et al. EXEL-0862, a novel tyrosine kinase inhibitor, induces apoptosis *in vitro* and *ex vivo* in human mast cells expressing the KIT D816V mutation. *Blood* 2007;109:315–22.
29. von Bubnoff N, Veach DR, Miller WT, et al. Inhibition of wild-type and mutant Bcr-Abl by pyridopyrimidine-type small molecule kinase inhibitors. *Cancer Res* 2003;63:6395–404.
30. Shah NP, Tran C, Lee FY, Chen P, Norris D, Sawyers CL. Overriding imatinib resistance with a novel ABL kinase inhibitor. *Science* 2004;305:399–401.
31. Daub H, Specht K, Ullrich A. Strategies to overcome resistance to targeted protein kinase inhibitors. *Nat Rev Drug Discov* 2004;3:1001–10.
32. Bauer S, Yu LK, Demetri GD, Fletcher JA. Heat shock protein 90 inhibition in imatinib-resistant gastrointestinal stromal tumor. *Cancer Res* 2006;66:9153–61.
33. Carter TA, Wodicka LM, Shah NP, et al. Inhibition of drug-resistant mutants of ABL, KIT, and EGF receptor kinases. *Proc Natl Acad Sci U S A* 2005;102:11011–6.
34. Prenen H, Cools J, Mentens N, et al. Efficacy of the kinase inhibitor SU11248 against gastrointestinal stromal tumor mutants refractory to imatinib mesylate. *Clin Cancer Res* 2006;12:2622–7.
35. Debiec-Rychter M, Cools J, Dumez H, et al. Mechanisms of resistance to imatinib mesylate in gastrointestinal stromal tumors and activity of the PKC412 inhibitor against imatinib-resistant mutants. *Gastroenterology* 2005;128:270–9.
36. Strumberg D, Richly H, Hilger RA, et al. Phase I clinical and pharmacokinetic study of the Novel Raf kinase and vascular endothelial growth factor receptor inhibitor BAY 43-9006 in patients with advanced refractory solid tumors. *J Clin Oncol* 2005;23:965–72.
37. Lierman E, Folens C, Stover EH, et al. Sorafenib is a potent inhibitor of FIP1L1-PDGFR α and the imatinib-resistant FIP1L1-PDGFR α T674I mutant. *Blood* 2006;108:1374–6.
38. O'Hare T, Walters DK, Stoffregen EP, et al. Combined Abl inhibitor therapy for minimizing drug resistance in chronic myeloid leukemia: Src/Abl inhibitors are compatible with imatinib. *Clin Cancer Res* 2005;11:6987–93.
39. Weisberg E, Wright RD, Jiang J, et al. Effects of PKC412, nilotinib, and imatinib against GIST-associated PDGFRA mutants with differential imatinib sensitivity. *Gastroenterology* 2006;131:1734–42.

1 ABSTRACT

2 ZD6474 (vandetanib, Zactima™) is an anilinoquinazoline used to target the receptor tyrosine
3 kinase RET in familial and sporadic thyroid carcinoma (IC₅₀: 100 nM). The aim of this study
4 was to identify molecular determinants of RET sensitivity to ZD6474. Here, we show that
5 mutation of RET tyrosine 806 to cysteine (Y806C) induced RET kinase resistance to ZD6474
6 (IC₅₀: 933 nM). Y806 maps close to the gate-keeper position at the RET kinase nucleotide-
7 binding pocket. Although tyrosine 806 is a RET auto-phosphorylation site, its substitution to
8 phenylalanine (Y806F) did not markedly affect RET susceptibility to ZD6474 (IC₅₀: 87 nM),
9 suggesting that phosphorylation of Y806 is not required for compound binding. Accordingly,
10 the introduction of a phosphomimetic residue (Y806E) also caused resistance to ZD6474,
11 albeit of a lesser degree (IC₅₀: 512 nM) than the cysteine mutation. Y806C/E RET mutants
12 were also resistant to ZD6474 with respect to intracellular signalling and activation of an
13 AP1-responsive promoter. We conclude that Y806 is a molecular determinant of RET
14 sensitivity to ZD6474. Y806C is a natural RET mutation identified in a patient affected by
15 multiple endocrine neoplasia type 2B. Based on its rare occurrence, it is unlikely that Y806C
16 will be a frequent cause of refractoriness to ZD6474; however, it may be envisaged that
17 mutations at this site can mediate secondary resistance formation in patients treated with the
18 compound.

1 INTRODUCTION

2 Small molecule tyrosine kinase inhibitors (TKI) are effective in a variety of human cancers
3 driven by activation of specific tyrosine kinases (Krause & Van Etten 2005; Baselga 2006). A
4 paradigmatic example is imatinib mesylate (Gleevec®, STI571), an ATP-competitive
5 inhibitor of BCR-ABL, KIT and PDGFR kinases. Imatinib is used for the treatment of
6 chronic myeloid leukaemia (CML) patients harbouring the BCR-ABL translocation and of
7 gastrointestinal stromal tumours (GIST) patients harbouring KIT or PDGFR α mutations
8 (Sherbenou & Druker 2007).

9
10 Although most CML cases initially respond to imatinib, relapses are frequent, particularly in
11 patients with advanced disease. Point mutations within the kinase domain of BCR-ABL are
12 the most frequent causes of resistance. Such mutations can either remove residues that are
13 critical for drug-kinase interaction, or create steric hindrance or display an allosteric effect,
14 preventing the kinase from adopting the correct conformation for drug binding (Daub *et al.*
15 2004; Nardi *et al.* 2004; Weisberg *et al.* 2007). The best described resistance-associated
16 mutation affects T315, the so called “gate-keeper” site. T315 is located at the base of the
17 ATP-binding pocket, where also the drug binds. Amino acid changes at the gate-keeper site
18 are able to confer resistance not only to imatinib but also to other BCR-ABL inhibitors, such
19 as dasatinib and nilotinib (Kantarjian *et al.* 2006; Talpaz *et al.* 2006). Moreover, mutation of
20 the corresponding residue has been linked to resistance of other tyrosine kinases to their
21 specific TKI (Pao *et al.* 2005).

22
23 How resistance to kinase inhibitors develops in patients is being understood. The short lag of
24 time in which resistance develops in CML patients has suggested that resistance-causing
25 mutations are present before treatment in a few tumour cells, *in cis* with the oncogenic

1 alteration, and are maintained in the tumour cell population because they increase the relative
2 fitness of the mutated cell clones. Tumour cells harbouring the resistance-causing mutation, in
3 turn, could be positively selected upon treatment with imatinib (secondary resistance)
4 (Sherbenou & Druker 2007). In other cases, the initial oncogenic mutation *per se* is refractory
5 to the drug (primary resistance). For instance, tumor-associated KIT and PDGFR α variants
6 displaying gain-of-function mutations in the kinase activation loop (D816 in KIT and D842 in
7 PDGFR α) are refractory to imatinib, and patients harbouring these mutations respond poorly
8 to imatinib (Corless *et al.* 2005). Similarly, a germline EGFR mutation (T790M) found in rare
9 families predisposed to lung cancer not only activates the oncogenic potential of EGFR but
10 also causes resistance to the EGFR TKIs gefitinib and erlotinib (Bell *et al.* 2005). An
11 understanding of the molecular basis of drug sensitivity and resistance is required to interpret
12 results of clinical trials with TKIs, to select patients for treatment and to design strategies
13 aimed at circumventing resistance formation (Kantarjian *et al.* 2006; Talpaz *et al.* 2006;
14 O'Hare *et al.* 2006; Shah *et al.* 2007).

15
16 RET receptor tyrosine kinase is frequently activated in thyroid tumours (Santoro &
17 Carlomagno 2005). Germline point mutations affecting the extracellular or kinase domains of
18 RET are associated to the autosomal dominant multiple endocrine neoplasia type 2 (MEN 2)
19 syndromes (MEN 2A, MEN 2B, familial medullary thyroid cancer), characterized by the
20 occurrence of medullary thyroid carcinoma (MTC), pheochromocytoma, parathyroid
21 adenoma, and ganglioneuromatosis of the gut. Somatic RET point mutations are found in 30-
22 40% of sporadic MTC cases (Marx 2005; Schlumberger *et al.* 2008). Most of the MEN
23 2/MTC-associated RET mutations either target extracellular cysteine residues (typically in
24 MEN 2A), or the methionine 918 (typically in MEN 2B) or few other residues (E768, L790,
25 Y791, V804, S891) in the RET kinase domain. Some patients harbour more rare mutations in

1 other codons or small insertions/deletions (Santoro & Carlomagno 2005). Moreover,
2 chromosomal rearrangements involving the RET kinase encoding domain (chimeric
3 RET/PTC oncogenes) are found in papillary thyroid carcinoma (PTC) (Santoro &
4 Carlomagno 2005). Both MEN 2/MTC-associated point mutations and RET/PTC
5 rearrangements switch on the enzymatic function of RET in a ligand-independent manner
6 (Santoro & Carlomagno 2005). Whereas adjuvant radiometabolic therapy with ^{131}I is effective
7 after surgery for PTC, MTC does not respond to conventional radiotherapy or chemotherapy,
8 and early surgery remains the only treatment for this tumour (Schlumberger *et al.* 2008).

9
10 ZD6474 (Zactima, vandetanib) is an orally bioavailable anilinoquinazoline with strong
11 inhibiting activity against VEGFR-2 ($\text{IC}_{50} = 40 \text{ nM}$) and EGFR ($\text{IC}_{50} = 500 \text{ nM}$) kinase
12 function (Ryan & Wedge 2005). ZD6474 is also a potent inhibitor of the RET kinase ($\text{IC}_{50} =$
13 100 nM) (Carlomagno *et al.* 2002). The compound could arrest the growth of human thyroid
14 cancer cell lines spontaneously harbouring RET oncogenes and was effective against a
15 *Drosophila* model of PTC and MTC (Vidal *et al.* 2005). The X-ray structure of ZD6474-
16 RET(TK) complex shows that the compound docks into the ATP-binding pocket of the RET
17 kinase (Knowles *et al.* 2006). In a phase II trial of hereditary MTC patients who had a
18 germline RET mutation, ZD6474 treatment was associated with objective tumour responses,
19 with evidence of prolonged disease stabilization and clinical benefit in up to half the patients
20 (Wells *et al.* 2006). Multicentric placebo-controlled phase II trials are in progress with this
21 drug in thyroid cancer patients (Schlumberger *et al.* 2008).

22
23 Pre-clinical *in vitro* studies have demonstrated that ZD6474 inhibited the wild-type enzyme
24 and several activated mutant forms of RET, with the notable exception of RET proteins
25 carrying mutations in residue V804 (V804L and V804M). In fact, the IC_{50} for RET kinase

1 inhibition increased by about 50-fold in the presence of V804L and V804M mutations
2 (Carlomagno *et al.* 2004). V804 in RET corresponds to the “gate-keeper” (T315) residue in
3 ABL. V804 mutations are present alone or in conjunction with other RET mutations in MEN
4 2 carriers (~4% of cases) and in sporadic MTC and could therefore cause resistance to
5 ZD6474.

6

7 Here, we screened natural RET oncogenic proteins, corresponding to BCR-ABL imatinib
8 resistant mutants, for ZD6474 response *in vitro* and in intact cells.

1 MATERIALS AND METHODS

2 Compound

3 ZD6474 (Zactima™, vandetanib) (AstraZeneca Pharmaceuticals, Macclesfield, UK) was
4 dissolved in dimethyl sulfoxide (DMSO) at a concentration of 50 mM and stored at -80° C.
5 1000X stock solution was freshly generated for each single experiment and the equivalent
6 amount of vehicle (DMSO) was used as control.

7

8 Cell culture and plasmids

9 HEK 293 and HeLa cells were from American Type Culture Collection (ATCC, Manassas,
10 VA) and were grown in Dulbecco's Modified Eagle Medium (DMEM) supplemented with
11 10% fetal calf serum, 2 mM L-glutamine, and 100 units/ml penicillin-streptomycin (GIBCO,
12 Paisley, PA). Transient transfections were carried out with the lipofectamine reagent
13 according to manufacturer's instructions (GIBCO). The alignment between RET and ABL
14 kinase domains was made with the "Lalign" tool available at the ExPASy proteomic tools
15 web site (www.expasy.ch). RET mutations V804M, E805K, Y806C, Y806E, Y806F, Y806S,
16 Y806G, E884K and D898V were generated by site-directed mutagenesis and inserted in the
17 background of an oncogenic RET C634R allele in the pcDNA 3.1 vector (Carlomagno *et al.*
18 2004). The presence of mutation was confirmed by double-strand DNA sequencing.

19

20 Protein studies

21 Protein lysates were prepared according to standard procedures. Briefly, cells were lysed in a
22 buffer containing 50 mM HEPES, pH 7.5, 1% (vol/vol) Triton X-100, 150 mM NaCl, 5 mM
23 EGTA, 50 mM NaF, 20 mM sodium pyrophosphate, 1 mM sodium vanadate, 2 mM
24 phenylmethylsulphonyl fluoride (PMSF) and 1 µg/mL aprotinin. Lysates were clarified by
25 centrifugation at 10,000 X g for 15 min. Lysates containing comparable amounts of proteins,

1 as estimated by a modified Bradford assay (Bio-Rad, Munich, Germany) were subjected to
2 direct Western blot. Immune complexes were detected with the enhanced chemiluminescence
3 kit (Amersham Pharmacia Biotech, Little Chalfort, UK). Signal intensity was analyzed using
4 a Phosphorimager (Typhoon 8600, Amersham Pharmacia Biotech) interfaced with the
5 ImageQuant software. Polyclonal anti-phospho-Shc, that recognizes phosphorylated Shc at
6 Y317, was from Upstate Biotechnology Inc. (Lake Placid, NY). Polyclonal anti-Shc was from
7 Santa Cruz Biotechnology (Santa Cruz, CA). Antibodies to MAPK were from Cell Signaling
8 Technologies (Beverly, MA, USA), and antibodies to phospho p44/42-MAPK (pMAPK),
9 specific for MAPK (ERK1/2) phosphorylated at Thr202/Tyr204, were from Cell Signaling
10 Technologies. Anti-RET is a polyclonal antibody raised against the tyrosine kinase protein
11 fragment of human RET (Santoro *et al.* 1994). Anti-phospho905 and anti-phospho1062 are
12 phospho-specific polyclonal antibodies recognizing RET proteins phosphorylated at the
13 corresponding sites (Salvatore *et al.* 2000; Carlomagno *et al.* 2003). Blots were incubated
14 with primary antibodies for 1 hour at room temperature, washed and incubated with the
15 appropriate secondary antibodies (goat anti-rabbit 1:5,000) coupled to horseradish peroxidase
16 (Santa Cruz Biotechnology). Signal intensity was evaluated with the Molecular Imager Gel
17 Doc System (Biorad) interfaced with the Quantity One software. Curves of ZD6474 inhibition
18 were plotted to identify IC₅₀ dose for each RET mutant *in vivo* autophosphorylation.

19

20 ***In vitro* kinase assay**

21 RET proteins were immunoprecipitated from HEK 293 cells transfected with different
22 mutants. Immunocomplexes were subjected to an *in vitro* kinase assay by incubation (20 min
23 at room temperature) in kinase buffer containing 200 μ M poly-(L-glutamic acid-L-tyrosine
24 [poly-GT]) (Sigma Chemical Co), 2.5 μ Ci [γ -³²P] ATP and unlabelled ATP (20 μ M) and the
25 indicated concentrations of the compound (Carlomagno *et al.* 2002). Samples were spotted on

1 Whatman 3MM paper (Springfield Mill, UK) and ^{32}P incorporation was measured with a β -
2 counter scintillator (Beckman Coulter, Unterschleissheim-Lohhof, Germany).

3

4 **Luciferase activity assay**

5 1×10^6 HeLa cells were transiently co-transfected with RET mutants and the AP1-Luc vector
6 (Stratagene, Garden Grove, CA) containing six AP1 binding sites upstream from the *Firefly*
7 luciferase cDNA. Twenty-four hours after transfection, cells were serum-starved and the
8 indicated concentration of ZD6474 or vehicle was added. Cells were harvested 48 h after
9 transfection. Ten ng of pRL-null (a plasmid expressing the enzyme *Renilla* luciferase from
10 *Renilla reniformis*) served as an internal control. *Firefly* and *Renilla* luciferase activities were
11 assayed using the Dual-Luciferase reporter system (Promega Corporation, Madison, WI) and
12 expressed as percentage of residual activity compared to cells treated with vehicle.

13

14 **Assessment of the structural impact of various Y806 mutations.**

15 The structure of the RET kinase domain in complex with ZD6474 (PDB: 2ivu) (Knowles *et al*
16 2006) was examined using the PyMOL Molecular Graphics System (<http://www.pymol.org>).
17 Tyrosine 806 was replaced with the different mutations and the structural consequences were
18 assessed.

19

20 **Statistical analysis**

21 Kinase activity curves were plotted using the curve-fitting PRIZM software (GraphPad
22 Software). The ANOVA Post-Hoc Tukey-Kramer multiple comparison test was used to
23 assess statistical significance of luciferase assay. InStat3 GraphPad Software was used.

1 **RESULTS**

2 **Identification of Y806 as a molecular determinant of RET sensitivity to ZD6474**

3 **inhibition**

4 We aligned the RET and ABL kinase domains and found that several RET residues, naturally
5 mutated in some MEN 2/MTC patients, correspond to positions in ABL whose mutation
6 causes imatinib resistance (Fig. 1A). RET changes in E768, L790 and A883 residues
7 (corresponding to E279, L301 and R372 in ABL, respectively) do not affect RET kinase
8 sensitivity to ZD6474, as previously reported (Carlomagno *et al.* 2004). Here, we evaluated
9 the effect of E805K, Y806C, E884K and D898V (corresponding to the imatinib-resistant
10 E316D, ABL F317L, E373K and L387M mutants, respectively) on RET kinase sensitivity to
11 ZD6474 (Fig. 1A). The E805K mutation was found in tandem with V804M in a patient with a
12 MEN 2B phenotype (Cranston *et al.* 2006). The adjacent Y806 residue was found mutated to
13 cysteine (Y806C) at the germline level in combination with mutation V804 in a patient with
14 MEN 2B-like clinical presentation (Miyachi *et al.* 1999; Iwashita *et al.* 2000). Notably,
15 phospho-aminoacid analysis included Y806 among RET kinase autophosphorylation sites
16 (Kawamoto *et al.* 2004). Both E805 and Y806 map in the RET catalytic domain to the same
17 loop containing the gate-keeper V804 residue (Knowles *et al.* 2006). Moreover, the E884K
18 mutation was identified in individual sporadic MTC case (Uchino *et al.* 1999). Finally,
19 residue D898 has been found deleted in a sporadic MTC patient. The same aspartic acid in
20 KIT kinase was shown to mediate resistance to imatinib when mutated to valine and ABL
21 L387 residue, located in the corresponding position, was mutated in an imatinib-resistant
22 kinase (Oriola *et al.* 2002).

23

24 Because these mutations weakly activate RET kinase (Miyachi *et al.* 1999; Iwashita *et al.*
25 2000), we introduced them in the background of a constitutively active RET allele carrying

1 the MEN 2A-associated extracellular C634R mutation. C634R strongly activates RET by
2 inducing a constitutive dimerization of the receptor through the formation of extracellular
3 disulfide bonds without affecting the natural conformation of RET kinase domain (Santoro &
4 Carlomagno 2006). Intact cells expressing RET mutants were treated with different ZD6474
5 doses and RET activity was measured by immunoblotting with anti-phospho RET antibodies
6 that recognise the Y905 and Y1062 autophosphorylation sites (Salvatore *et al.* 2000;
7 Carlomagno *et al.* 2003). When phosphorylated, Y1062 functions as multi-docking site for
8 intracellular signalling proteins, whereas Y905 resides in the activation loop and its
9 phosphorylation is necessary to maintain the kinase in an active conformation (Iwashita *et al.*
10 2000; Hayashi *et al.* 2000). As shown in Fig. 1B, ZD6474 inhibited RET proteins carrying
11 C634R/E805K (IC₅₀ = 100 nM), C634R/E884K (IC₅₀ = 200 nM) or C634R/D898V (IC₅₀ =
12 200 nM) tandem substitutions similarly to RET C634R protein (IC₅₀ = 100 nM). In contrast,
13 the RET C634R/Y806C protein was highly resistant to the drug (IC₅₀ > 1000 nM). The
14 ZD6474-resistant RET C634R/V804M mutant served as control (IC₅₀ > 1000 nM). (Fig. 1B).

15

16 **Structure-function analysis of the effect of RET Y806 mutation**

17 We generated RET mutants carrying mutations of Y806 to different amino acids, namely
18 glycine (Y806G), serine (Y806S), glutamic acid (Y806E) and phenylalanine (Y806F), in the
19 background of RET C634R. Mutations Y806G and Y806S knocked-down kinase activity (not
20 shown) and were not studied further. The substitution of tyrosine 806 with the non-
21 phosphorylatable phenylalanine (Y806F) did not significantly affect kinase activity. In
22 addition, it did not modify RET sensitivity to ZD6474, which suggested that Y806
23 phosphorylation was not necessary for ZD6474 binding (Fig. 2A). In contrast, the substitution
24 of tyrosine 806 with the phospho-mimetic glutamate (Y806E) greatly reduced RET sensitivity
25 to ZD6474, and thus had an effect comparable to the Y806C change (Fig. 2A).

1

2 Subsequently, we carried out an *in vitro* kinase assay and measured ZD6474 *in vitro* IC₅₀ for
3 the various RET Y806 mutants. As shown in Fig. 2B, ZD6474 IC₅₀ for the RET
4 C634R/Y806F protein was similar to RET C634R (87 nM vs 100 nM), whereas the IC₅₀
5 values for RET C634R/Y806E and RET C634R/Y806C were increased by 5-fold (512 nM)
6 and 10-fold (933 nM), respectively.

7

8 **Analysis of ZD6474 activity on intracellular signalling of RET Y806 mutants**

9 RET phosphorylation on Y1062 results in a docking site for Shc and other adaptor proteins
10 that, in turn, serve as anchors for Grb2/Sos and Grb2/Gab complexes thereby mediating
11 downstream RET signals (Hayashi *et al.* 2000). In turn, Grb2 containing complexes activate
12 the PI3K/AKT and RAS/MAPK pathways. ZD6474 strongly knocked-down RET C634R-
13 induced Shc and MAPK activation measured as phosphorylation of the two proteins. Once
14 again, RET C634R/Y806C and RET C634R/Y806E, as RET C634R/V804M, showed
15 resistance to ZD6474 inhibition (Fig. 3A).

16

17 Finally, we tested whether ZD6474 obstructed RET-mediated activation of an AP1-
18 responsive promoter fused to the luciferase reporter. As shown in Fig. 3B, the compound
19 reduced RET C634R activity to less than 50% at 250 nM and completely abolished promoter
20 activation at 1 µM. Instead, ZD6474, even at a concentration of 5 µM, had virtually no effect
21 on RET C634R/V804M-mediated luciferase stimulation. Compared with RET C634R, RET
22 mutants C634R/Y806C and RET C634R/Y806E were also relatively resistant to the effects of
23 ZD6474, although to a lesser extent than RET C634R/V804M.

1 **DISCUSSION**

2 The efficacy of ZD6474 in targeting RET oncogenic mutations in medullary thyroid
3 carcinoma is now being evaluated in phase II clinical trials. Although clinical benefit from
4 ZD6474 is likely to derive from inhibition of both VEGFR-2 and EGFR kinase activities in
5 addition to RET kinase, it will be necessary to identify RET mutations that respond best to the
6 compound in order to interpret the results of these trials and subsequently to select the most
7 suitable candidates for ZD6474 treatment. Here we screened natural oncogenic RET kinase
8 mutants for ZD6474 response. The majority of these mutants, although homologous to ABL
9 mutants resistant to imatinib, retains ZD6474 responsiveness. An important exception is
10 Y806C that, similar to V804M/L (Carlomagno *et al.* 2004), impairs ZD6474 efficacy.

11
12 Based on the recently resolved RET kinase X-ray structure (Knowles *et al.* 2006), tyrosine
13 806 is located between the kinase N- and C-lobes in the hinge region that forms part of the
14 nucleotide binding pocket (Fig. 4A). The Y806 side chain stacks against the aliphatic part of
15 the lysine 740 (K740) side chain and the main chain of the adjacent alanine 807 (A807) (Fig.
16 4B). The position equivalent to Y806 in other kinases is usually hydrophobic and aromatic,
17 which might explain why we found that substitution of this residue with glycine or serine
18 dramatically affects kinase function. Y806 is in direct Van der Waals contact with ATP and
19 with ZD6474. Conservative substitution of Y806 to phenylalanine (Y806F) preserves the
20 shape and hydrophobicity of this part of the nucleotide pocket. Therefore this mutated RET is
21 likely to maintain contacts with ZD6474 using Y806, which explains why the Y806F
22 mutation does not affect the sensitivity of RET towards ZD6474. On the other hand, the
23 effects of the Y806C and Y806E substitutions are subtle and unpredictable compared to the
24 V804M/L mutation, which causes a clear steric hindrance (Knowles *et al.* 2006).
25 Replacement of Y806 by a smaller cysteine will leave a cavity thereby leading to minor

1 structural alterations to the nucleotide-binding pocket, so that the kinase retains the ability to
2 bind and hydrolyse ATP. On the other hand, these changes could affect affinity for ZD6474
3 by losing direct Van der Waals interactions. Substitution of Y806 with the acidic glutamate
4 side chain introduces a negative charge into the hydrophobic environment of the inhibitor-
5 binding site. This may lead to interaction with the adjacent accessible K740 side chain and, in
6 turn, perturb the alignment of the hinge region. Differences in the hinge region are indeed
7 seen in RET structures bound to ATP compared to ZD6474 (Knowles *et al.* 2006). A possible
8 consequence of Y806E would be an altered E805 conformation. The main chain carbonyl of
9 E805 makes direct contact with ZD6474, and loss of this interaction may impact on inhibitor
10 sensitivity. This may also explain why replacing the E805 side chain by lysine (E805K)
11 appears not to affect the actions of ZD6474.

12

13 In conclusion, Y806 is involved in RET response to ZD6474. Y806 mutation may be an
14 extremely rare primary mutation causing ZD6474 refractoriness. However, mutations at Y806
15 and Y806-containing loop including V804, but not at E805, can mediate secondary resistance
16 during the treatment of thyroid cancer patients with ZD6474. This information would be
17 useful in investigating the mechanisms of lack of response to ZD6474 treatment and
18 designing second-line inhibitors to overcome resistance.

1 **DECLARATION OF INTEREST**

2 AJ Ryan is a full time employee of Astra Zeneca. M Santoro received an Astra Zeneca
3 research grant.

4

5 **FUNDING**

6 This study was supported by the Associazione Italiana per la Ricerca sul Cancro (AIRC), the
7 NOGEC (Naples OncoGENomic Center), by grants from Italian Ministero della Salute and
8 Ministero dell'Università e della Ricerca and by a research grant from Astra Zeneca. T. Guida
9 was supported by an AIRC fellowship. S. Anaganti was supported by a Terry Fox Foundation
10 fellowship.

11

12 **ACKNOWLEDGMENTS**

13 We thank Jean Ann Gilder for text editing and Ciotola Presentation for the art-work.

1 **REFERENCES**

- 2 Baselga J 2006 Targeting tyrosine kinases in cancer: the second wave. *Science* **312** 1175-
3 1178.
4
- 5 Bell DW, Gore I, Okimoto RA, Godin-Heymann N, Sordella R, Mulloy R, Sharma SV,
6 Brannigan BW, Mohapatra G, Settleman J *et al.* 2005 Inherited susceptibility to lung cancer
7 may be associated with the T790M drug resistance mutation in EGFR. *Nature Genetics* **37**
8 1315-1316.
9
- 10 Carlomagno F, Guida T, Anaganti S, Vecchio G, Fusco A, Ryan AJ, Billaud M & Santoro M
11 2004 Disease associated mutations at valine 804 in the RET receptor tyrosine kinase confer
12 resistance to selective kinase inhibitors. *Oncogene* **23** 6056-6063.
13
- 14 Carlomagno F, Vitagliano D, Guida T, Basolo F, Castellone MD, Melillo RM, Fusco A &
15 Santoro M 2003 Efficient inhibition of RET/papillary thyroid carcinoma oncogenic kinases
16 by 4-amino-5-(4-chloro-phenyl)-7-(t-butyl)pyrazolo[3,4-d]pyrimidine (PP2). *Journal of*
17 *Clinical Endocrinology and Metabolism* **88** 1897-1902.
18
- 19 Carlomagno F, Vitagliano D, Guida T, Ciardiello F, Tortora G, Vecchio G, Ryan AJ,
20 Fontanini G, Fusco A & Santoro M 2002 ZD6474, an orally available inhibitor of KDR
21 tyrosine kinase activity, efficiently blocks oncogenic RET kinases. *Cancer Research* **62** 7284-
22 7290.
23
- 24 Corless CL, Schroeder A, Griffith D, Town A, McGreevey L, Harrell P, Shiraga S,
25 Bainbridge T, Morich J & Heinrich MC 2005 PDGFRA mutations in gastrointestinal stromal

1 tumors: frequency, spectrum and in vitro sensitivity to imatinib. *Journal of Clinical Oncology*
2 **23** 5357-5364.

3

4 Cranston AN, Carniti C, Oakhill K, Radzio-Andzelm E, Stone EA, McCallion AS, Hodgson
5 S, Clarke S, Mondellini P, Leyland J, *et al* 2006 RET is constitutively activated by novel
6 tandem mutations that alter the active site resulting in multiple endocrine neoplasia type 2B.
7 *Cancer Research* **66** 10179-10187.

8

9 Daub H, Specht K & Ullrich A 2004 Strategies to overcome resistance to targeted protein
10 kinase inhibitors. *Nature Reviews Drug Discovery* **3** 1001-1010.

11

12 Hayashi H, Ichihara M, Iwashita T, Murakami H, Shimono Y, Kawai K, Kurokawa K,
13 Murakumo Y, Imai T, Funahashi H *et al.* 2000 Characterization of intracellular signals via
14 tyrosine 1062 in RET activated by glial cell line-derived neurotrophic factor. *Oncogene* **19**
15 4469-4475.

16

17 Iwashita T, Murakami H, Kurokawa K, Kawai K, Miyauchi A, Futami H, Qiao S, Ichihara M
18 & Takahashi M 2000 A two-hit model for development of multiple endocrine neoplasia type
19 2B by RET mutations. *Biochemical and Biophysical Research Communication* **268** 804-808.

20

21 Kantarjian H, Giles F, Wunderle L, Bhalla K, O'Brien S, Wassmann B, Tanaka C, Manley P,
22 Rae P, Mietlowski W, *et al* 2006 Nilotinib in Imatinib-resistant CML and Philadelphia
23 chromosome-positive ALL. *New England Journal of Medicine* **354** 2542-2551.

24

- 1 Kawamoto Y, Takeda K, Okuno Y, Yamakawa Y, Ito Y, Taguchi R, Kato M, Suzuki H,
2 Takahashi M & Nakashima I 2004 Identification of RET autophosphorylation sites by mass
3 spectrometry. *Journal of Biological Chemistry* **279** 14213-14224.
4
- 5 Knowles PP, Murray-Rust J, Kjaer S, Scott RP, Hanrahan S, Santoro M, Ibáñez CF &
6 McDonald NQ 2006 Structure and chemical inhibition of the RET tyrosine kinase domain.
7 *Journal of Biological Chemistry* **281** 33577-33587.
8
- 9 Krause DS & Van Etten RA 2005 Tyrosine kinases as targets for cancer therapy. *New*
10 *England Journal of Medicine* **353** 172-187.
11
- 12 Marx SJ 2005 Molecular genetics of multiple endocrine neoplasia types 1 and 2. *Nature*
13 *Reviews Cancer* **5** 367-375.
14
- 15 Miyauchi A, Futami H, Hai N, Yokozawa T, Kuma K, Aoki N, Kosugi S, Sugano K &
16 Yamaguchi K 1999 Two germline missense mutations at codons 804 and 806 of the RET
17 proto-oncogene in the same allele in a patient with multiple endocrine neoplasia type 2B
18 without codon 918 mutation. *Japanese Journal of Cancer Research* **90** 1-5.
19
- 20 Nardi V, Azam M & Daley GQ 2004 Mechanisms and implications of Imatinib resistance
21 mutations in BCR-ABL. *Current Opinion in Hematology* **11** 35-43.
22
- 23 O'Hare T, Corbin AS & Druker BJ 2006 Targeted CML therapy: controlling drug resistance,
24 seeking cure. *Current Opinion in Genetics and Development* **16** 92-99.
25

- 1 Oriola J, Halperin I, Rivera-Fillat F & Donis-Keller H 2002 The finding of a somatic deletion
2 in RET exon 15 clarified the sporadic nature of a medullary thyroid carcinoma suspected to
3 be familial. *Journal of Endocrinological Investigation* **25** 25-31.
- 4
- 5 Pao W, Miller VA, Politi KA, Riely GJ, Somwar R, Zakowski MF, Kris MG & Varmus H
6 2005 Acquired resistance of lung adenocarcinomas to gefitinib or erlotinib is associated with
7 a second mutation in the EGFR kinase domain. *PLoS Medicine* **2** e73.
- 8
- 9 Ryan AJ & Wedge SR 2005 ZD6474-a novel inhibitor of VEGFR and EGFR tyrosine kinase
10 activity. *British Journal of Cancer* **92** S6–S13.
- 11
- 12 Salvatore D, Barone MV, Salvatore G, Melillo RM, Chiappetta G, Mineo A, Fenzi G,
13 Vecchio G, Fusco A & Santoro M 2000 Tyrosines 1015 and 1062 are in vivo
14 autophosphorylation sites in ret and ret-derived oncoproteins. *Journal of Clinical*
15 *Endocrinology and Metabolism* **85** 3898-3907.
- 16
- 17 Santoro M & Carlomagno F 2006 Drug insight: Small-molecule inhibitors of protein kinases
18 in the treatment of thyroid cancer. *Nature Clinical Practice Endocrinology and Metabolism* **2**
19 42-52.
- 20
- 21 Santoro M, Wong WT, Aroca P, Santos E, Matoskova B, Grieco M, Fusco A & di Fiore PP
22 1994 An epidermal growth factor receptor/ret chimera generates mitogenic and transforming
23 signals: evidence for a ret-specific signaling pathway. *Molecular and Cellular Biology* **14**
24 663-675.
- 25

- 1 Schlumberger M, Carlomagno F, Baudin E, Bidart JM & Santoro M_2008 New therapeutic
2 approaches to treat medullary thyroid carcinoma. *Nature Clinical Practice Endocrinology and*
3 *Metabolism* **4** 22-32.
- 4
- 5 Shah NP, Skaggs BJ, Branford S, Hughes TP, Nicoll JM, Paquette RL & Sawyers CL 2007
6 Sequential ABL kinase inhibitor therapy selects for compound drug-resistant BCR-ABL
7 mutations with altered oncogenic potency. *Journal of Clinical Investigation* **117** 2562-2569.
- 8
- 9 Sherbenou DW & Druker BJ 2007 Applying the discovery of the Philadelphia chromosome.
10 *Journal of Clinical Investigation* **117** 2067-2074.
- 11
- 12 Talpaz M, Shah NP, Kantarjian H, Donato N, Nicoll J, Paquette R, Cortes J, O'Brien S,
13 Nicaise C, Bleickardt E *et al* 2006 Dasatinib in Imatinib-resistant Philadelphia chromosome-
14 positive leukemias. *New England Journal of Medicine* **354** 2531-2541.
- 15
- 16 Uchino S, Noguchi S, Yamashita H, Sato M, Adachi M, Yamashita H, Watanabe S, Ohshima
17 A, Mitsuyama S, Iwashita T *et al* 1999 Somatic mutations in RET exons 12 and 15 in
18 sporadic medullary thyroid carcinomas: different spectrum of mutations in sporadic type from
19 hereditary type. *Japanese Journal of Cancer Research* **90** 1231-1237.
- 20
- 21 Vidal M, Wells S, Ryan A & Cagan R 2005 ZD6474 suppresses oncogenic RET isoforms in a
22 *Drosophila* model for type 2 multiple endocrine neoplasia syndromes and papillary thyroid
23 carcinoma. *Cancer Research* **65** 3538-3541.
- 24

- 1 Weisberg E, Manley PW, Cowan-Jacob SW, Hochhaus A & Griffin JD 2007 Second
- 2 generation inhibitors of BCR-ABL for the treatment of Imatinib-resistant chronic myeloid
- 3 leukaemia. *Nature Reviews Cancer* **7** 345-356.
- 4
- 5 Wells S, You YN, Lakhani V, Hou J, Langmuir P, Headley D, Skinner M, Morse M, Burch
- 6 W & Schlumberger M 2006 A phase II trial of ZD6474 in patients with hereditary metastatic
- 7 medullary thyroid cancer. *Journal of Clinical Oncology* 2006 ASCO Annual Meeting
- 8 Proceedings Part I. **24** No. 18S (June 20 Supplement): 5533

1 LEGENDS TO FIGURES

2

3 Figure 1: Y806 residue determines RET kinase sensitivity to ZD6474

4 **A)** Alignment of ABL and RET kinase domains. P-Loop (phosphate binding-loop) and A-
5 loop (activation-loop) are indicated. Mutations that cause resistance to imatinib in ABL and
6 that correspond to naturally occurring RET mutations are highlighted in grey. For RET, the
7 position of the mutated amino acid is reported. **B)** HEK293 cells were transfected with
8 pcDNA 3.1 vectors expressing the indicated RET mutants. Twenty-four hours after
9 transfection, cells were serum-starved. Two hours before harvest, cells were treated with
10 various ZD6474 doses or vehicle. Cell lysates were immunoblotted with the indicated
11 antibodies. Each immunoblot is representative of at least three independent experiments.

12

13 Figure 2: Effect of alternative RET Y806 substitutions on sensitivity to ZD6474

14 **A)** HEK293 cells were transfected with pcDNA 3.1 vectors expressing the indicated RET
15 mutants. Twenty-four hours after transfection, cells were serum-starved and treated (2 h) with
16 ZD6474 or vehicle. Cell lysates were analyzed by immunoblot with the indicated antibodies.
17 Each immunoblot is representative of at least three independent experiments. **B)** HEK293
18 cells were transfected with RET mutants-expressing vectors. RET proteins were
19 immunoprecipitated and subjected to an *in vitro* kinase assay on a artificial substrate (poly-
20 Glu-Tyr). Each experiment was performed in triplicate and done at least three times. Results
21 from kinase assay have been plotted using a curve-fitting software. SD are indicated.

22

23 Figure 3: ZD6474 effects on RET mutants intracellular signaling

24 **A)** HEK293 cells were transfected with RET mutants expressing vectors. Twenty-four hours
25 after transfection, cells were serum-starved and treated (2 h) with the indicated concentration

1 of ZD6474. Cell lysates were analyzed by immunoblot with the indicated antibodies. Each
2 experiment is representative of at least three assays. **B)** 1×10^6 HeLa cells were transiently
3 transfected with RET mutants expressing vectors and the AP1-Luc vector pRL-null (a
4 plasmid expressing the enzyme *Renilla* luciferase from *Renilla reniformis*) served as an
5 internal control. *Firefly* and *Renilla* luciferase activities are expressed as percentage of
6 residual activity compared to cells treated with vehicle. Average results of three independent
7 assays \pm SD are indicated. The ANOVA Post-Hoc Tukey-Kramer multiple comparison test
8 was used to assess statistical significance ($P < 0.01$).

9

10 Figure 4. Structure of RET Kinase-ZD6474 complex

11 **A)** The kinase domain of RET in complex with ZD6474. ZD6474 binds in the nucleotide
12 binding pocket between the N- and C-lobes. **B)** Close-up of the nucleotide binding pocket
13 showing how the tyrosine 806 (red) interacts with the aliphatic chain of lysine 740 and the
14 main chain moiety of alanine 807, and establishes Van der Waals contacts with ZD6474.

A**P-loop**

```

-----
ABL: 241  --DITMKHKLGGGQYGEVYEGVWKK-----YSL
RET: 721  RKNLVLGKTLGEGEFGKVVKATAFHLKGRAGYT

                K                F                D
                I|L
ABL: 267  TVAVKTLKEDTM--EVEEFLKEAAVMKEIKHPNLVQLLGVCTREPPFYIITEFMTYGNLL 324
RET: 754  TVAVKMLKENASPSELRDLLSEFNVLKQVNHHPVIKLYGACSQDGPLLLIVEYAKYGSRLR 813
                768                790                804|806
                D                F                L|M|C
                805
                K
ABL: 325  DYLRECNRQE-----VNAVLLYMATQISSAMEYLEKKNFIHR 362
RET: 814  GFLRESRKVGPYLGSGGSRNSSSLDHPDERALTMGDLISFAWQISQGMQYLAEMKLVHR 873

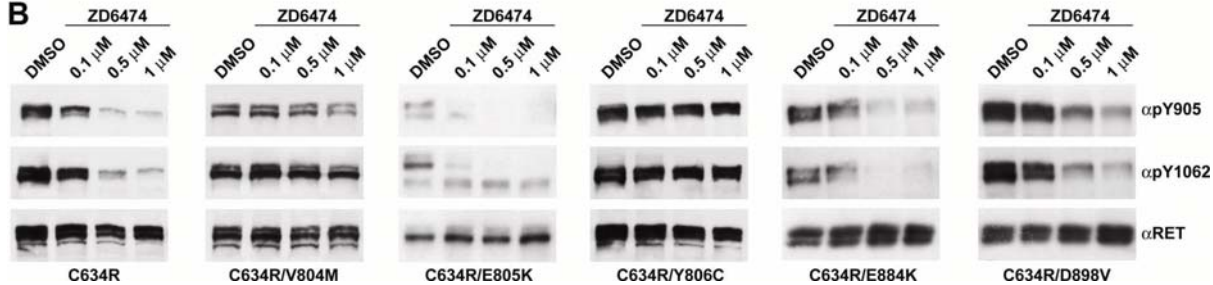
```

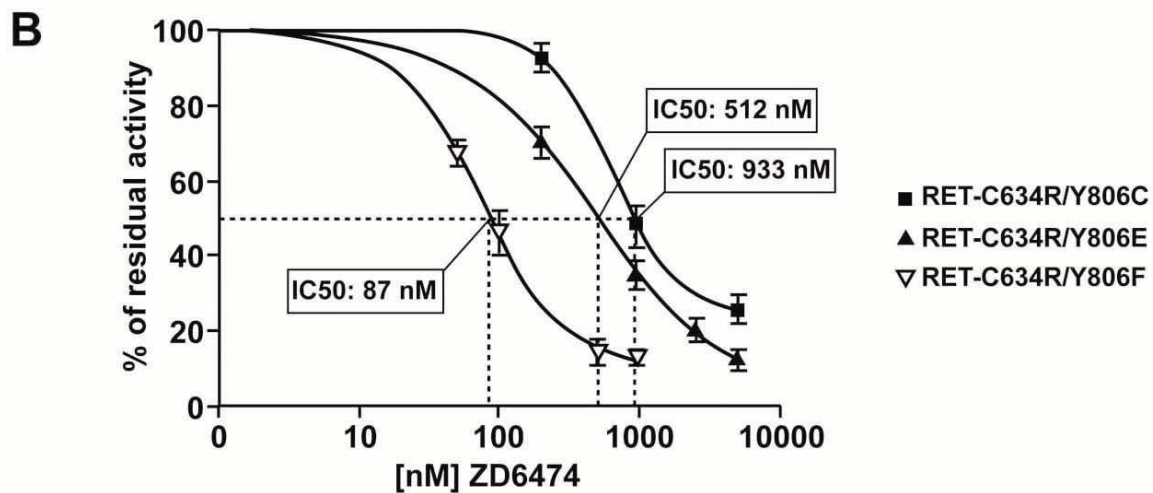
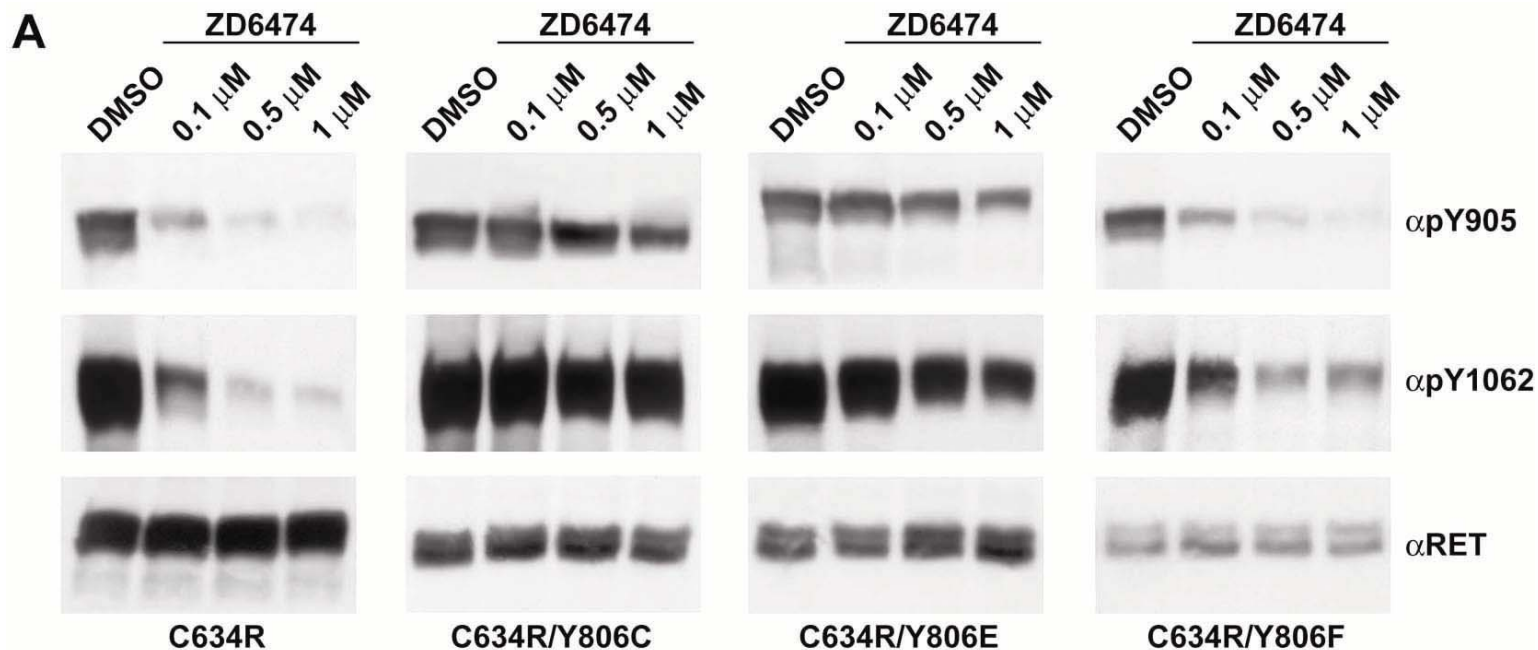
A-loop

```

-----
                RK                M
ABL: 363  DLAARNCLVGENHVLKVKVADFGLSRLMTGDTYTAH-AGAKFPIKWTAPESLAYNKFSIKSD 421
RET: 874  DLAARNILVAEGRKMKISDFGLSRDVYEEDSYVKRSQGRIPVKWMATIESLFDHIYTTQSD 933
                883 884                898
                F  K                V/(del898-902)

```

B



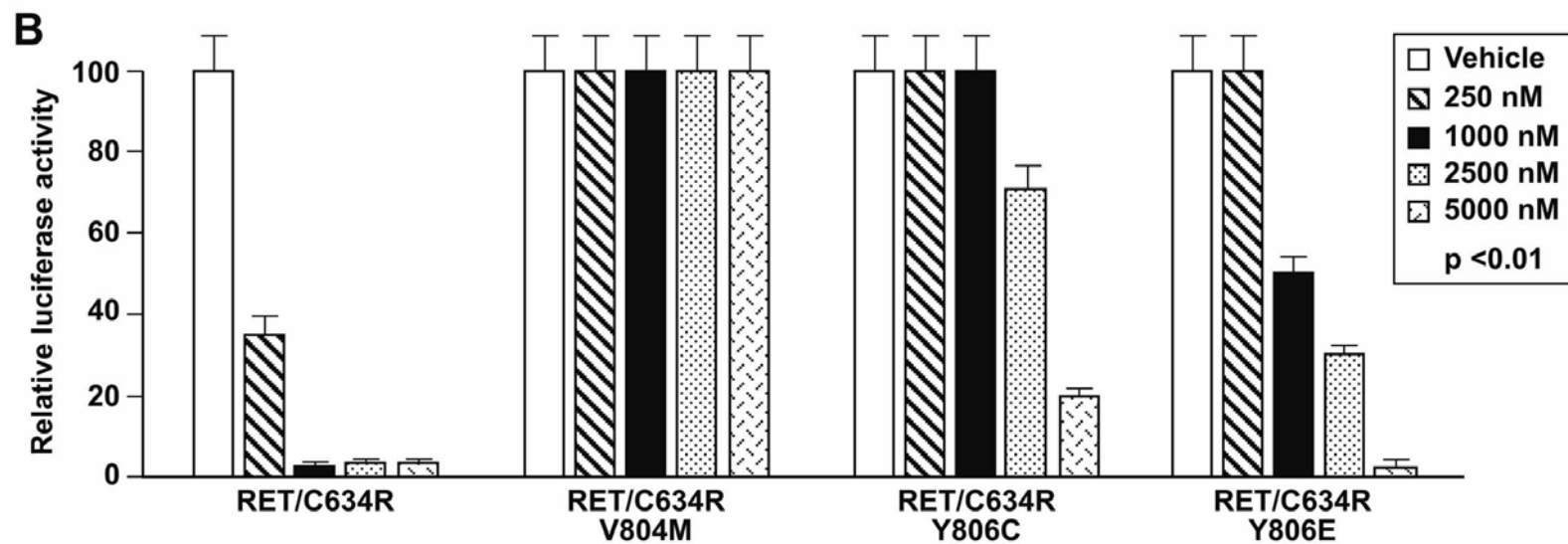
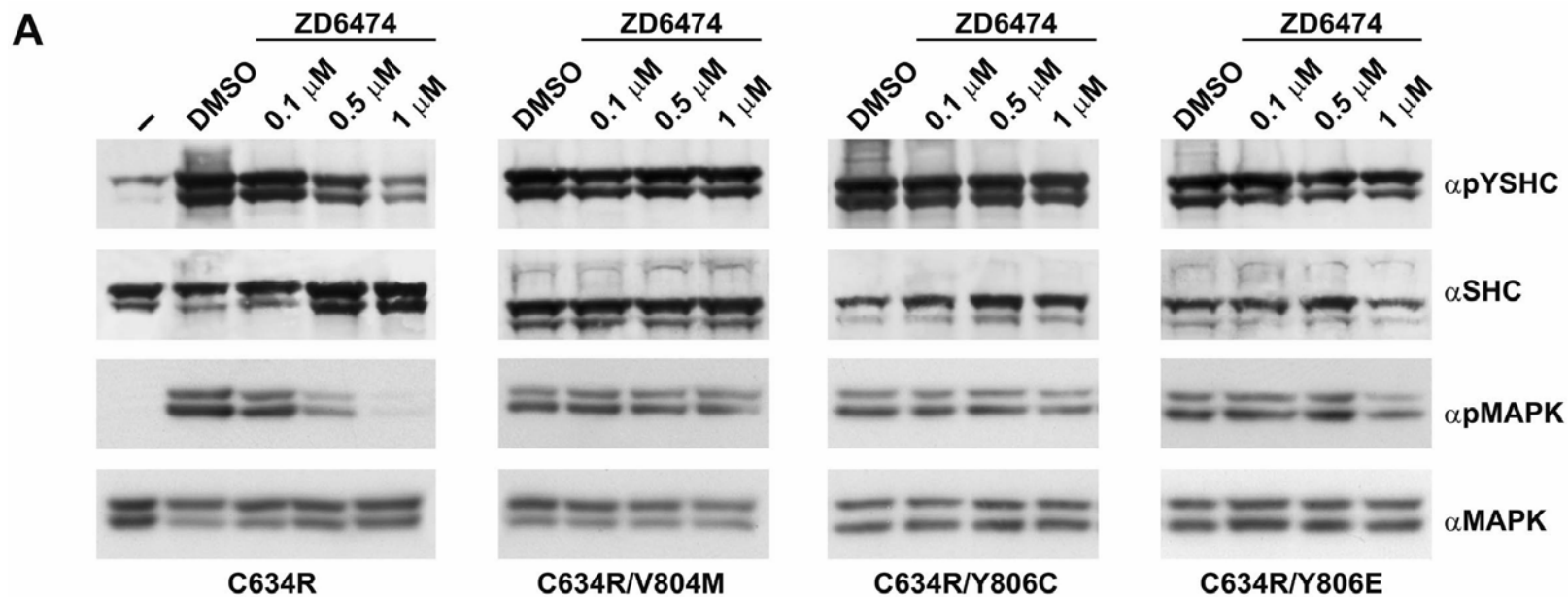
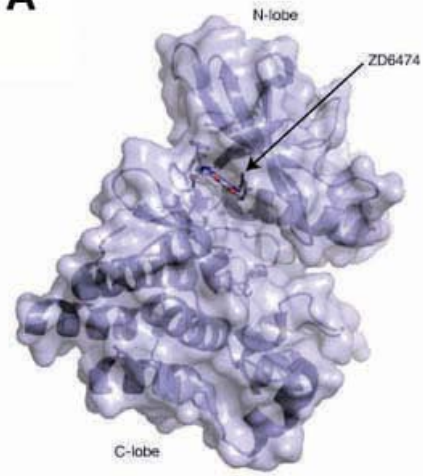


Fig. 4

A



B

